



TAMPEREEN TEKNILLINEN YLIOPISTO
TAMPERE UNIVERSITY OF TECHNOLOGY

SANKEERTH SHIVAKUMAR
MODELLING AND SIMULATION OF HYDRAULIC BOOM FOR
OFFSHORE PURPOSES

Master of Science Thesis

Examiner: prof. Kari T Koskinen
Examiner and topic approved on 29
August 2018

ABSTRACT

SANKEERTH SHIVAKUMAR: Modelling and simulation of hydraulic boom for offshore purposes

Tampere University of technology

Master of Science Thesis 63 pages, 8 Appendix pages

November 2018

Master's Degree Programme in Automation Technology

Major: Fluid power automation

Examiner: Professor Kari T Koskinen

Keywords: Hydraulic boom, Simulation, Mechanical design, Control system, Active Heave Compensation, Kinematics

Hydraulic manipulators are widely used in offshore industries to transport cargo containers. Modern-day hydraulic manipulators on board with huge cargo carrying surface vessel are built to transport heavy payloads. These hydraulic manipulators are usually controlled manually through a joystick. The combination of modern electronics and hydraulics has been an imperative tool for the inception of new applications. One such application is discussed in this thesis report. Wherein, a new generation hydraulic manipulator for a small surface vehicle is designed and modern control schemes are implemented to launch and retrieve the UAV (Unmanned Aerial Vehicle) and AUV (Autonomous Underwater Vehicle).

In this thesis, design, control, and stabilization of lightweight and corrosion resistant hydraulic boom are presented. The main features of the mechanical design are Aluminium sheet metal design of arms and an indigenous design of 6 link mechanism to convert the linear movement of the double-sided piston to the rotary movement of the second arm. A robust control system is implemented to compensate the uncertainties in the offshore environment. The hydraulic system is simulated along with the SIMSCAPE representation of the mechanical assembly. The stabilization of the hydraulic manipulator is performed by calculating the manipulator dynamics and through some motion detection sensors. The results of this thesis show a new and conceptual design of the hydraulic boom for offshore usage, provides a substantial evidence for the type of controller and feedback system to be used and presents a prospective future work required for the implementations. This research presents a profound collection of the qualitative and quantitative data to manufacture the manipulator and design a control system for launching and retrieving of the UAV and AUV.

PREFACE

The Master Thesis “Modeling and simulation of hydraulic boom for offshore purposes” was done at Mechanical Engineering and Industrial Systems (MEI) department at Tampere University of Technology (TUT). The work was done in cooperation with Alamarin Jet and aColor project. First, I would like to thank Prof. Kari T Koskinen and Dr. Jussi Aaltonen for all the guidance, feedback and opportunity to work at MEI department. It has been an amazing work experience at MEI department.

I would like to thank my mother, who has been my greatest support in each stage of my life, she has been an inspiration for me, words are not enough to express her gratefulness. It is because of her hard work I was able to live the dreams which I dreamt off. I want to thank my father for his motivation and support. I thank my girlfriend for motivating me. She has been with me through all the rough times and helped get out of it. I express my utmost gratitude for Tampere University of Technology for providing excellent facilities at the university. Mikko Heikkilä from IHA (Intelligent Hydraulic and Automation) provided an extended support to complete my thesis work. Jose, the man behind the aColor project, I thank him for his valuable suggestions. My second family, Vijendra and Sandhya, the amount of support they have given me is unexplainable. Vijendra has been an elder brother to me. My friends Madan Patnamsetty, Disheet Shah, Gaurav Mohanty, Pekka Johansson, Hanna Johansson, Raija Johansson, Marika Salo, Joe David, Palash Halder and Madhusudan Gowda. I thank them for the support they have shown all these years in Finland.

“This moment” is not an idea, it is the only reality – Sadguru.

Tampere, 15.11.2018

Sankeerth Shivakumar

CONTENTS

1	INTRODUCTION.....	1
	1.1 Research methodology and scope of thesis.....	3
2	BACKGROUND STUDY	4
3	MECHANICAL DESIGN AND ANALYSIS	6
	3.1 Approximating the angle of cylinder when boom is in transport position.....	6
	3.2 Approximating the angle of cylinder when boom reaches maximum height	8
	3.3 Mechanics of the boom	9
	3.4 Design of rack and pinion gear	10
	3.5 Sheet metal design of the manipulator components.....	13
	3.5.1 Sheet metal design of arms	13
	3.5.2 Sheet metal design of base	15
	3.6 Design of cylinder placements	17
	3.7 Design of linkages.....	17
	3.8 Mechanical assembly of the boom	18
4	MODELLING OF HYDRAULIC SYSTEM.....	22
	4.1 Modelling of 4/3 direction control valve.....	22
	4.1.1 Valve dynamics.....	24
	4.1.2 Relative openings	24
	4.1.3 Orifice modelling	25
	4.1.4 Flow paths	27
	4.1.5 Simulink block diagram representation of 4/3 valve	28
	4.2 Modelling of hydraulic cylinder.....	29
	4.3 Integration of DCV and cylinder to the hydraulic system	31
	4.4 Modelling and Simulation of a physical system of hydraulic boom.....	32
	4.5 Control System.....	34
	4.5.1 PID Controller.....	35
	4.5.2 Cylinder stroke feedback	36
	4.5.3 Boom angle feedback	37
	4.6 Controller testing.....	38
5	DYNAMIC BEHAVIOUR ANALYSIS OF THE HYDRAULIC BOOM.....	39
	5.1 Cylinder stroke feedback.....	39
	5.2 Boom angle feedback	42
	5.3 Comparison of stroke feedback and boom angle feedback.....	44
6	KINEMATICS OF THE HYDRAULIC BOOM.....	46
	6.1 Forward kinematics of the hydraulic boom.....	46
	6.2 Inverse kinematics of hydraulic boom	48
	6.2.1 Inverse kinematics of 3-DOF manipulator.....	48
	6.2.2 Inverse kinematics of 2-DOF manipulator.....	50
	6.3 Testing the inverse kinematics program.....	51
	6.4 Joint space control.....	53

6.5	Active heave compensation (Stabilization).....	56
7	CONCLUSION AND FUTURE WORK.....	59
7.1	Future work	60
	REFERENCES.....	61

APPENDIX A: Assembly drawings

APPENDIX B: Bill of materials of hydraulic boom

APPENDIX C: MATLAB code for hydraulic parameters

APPENDIX D: MATLAB code for inverse kinematics

LIST OF FIGURES

Figure 1: BlueROV (Under-water vehicle) [4]	2
Figure 2: Albatross fixed wing UAV [5]	2
Figure 3: Surface vessel	2
Figure 4: When the boom is in transport position.....	6
Figure 5: When the boom is at maximum height.....	8
Figure 6: Schematic diagram of the forces acting on the boom.....	9
Figure 7: Rack gear[20].....	12
Figure 8: Pinion gear[20]	13
Figure 9: Top view of the aColor surface vehicle showing the area where the hydraulic boom can be assembled.....	14
Figure 10: Sheetmetal design of first arm	14
Figure 11: Sheetmetal design of second arm	15
Figure 12: Sheetmetal design of the base.....	15
Figure 13: Shaft connecting the base part and pinion	16
Figure 14: Assembly of rack and pinion system.....	16
Figure 15: Placement of hydraulic cylinder for first arm	17
Figure 16: Cylinder placement for the second arm.....	17
Figure 17: Linkage design for the rotary movement of second arm	18
Figure 18: Assembly of the hydraulic boom in transport position.....	18
Figure 19: Assembly of the boom when cylinder of first arm is at full stroke.....	19
Figure 20: Working position of the boom.....	19
Figure 21: Top view of the boom.....	20
Figure 22: Isometric view of the hydraulic boom showing degrees of freedom (DOF)	20
Figure 23: Assembly of boom in the surface vessel.....	21
Figure 24: Assembly of boom and surface, when the boom is in transport position	21
Figure 25: Basic layout of hydraulic system [24]	22
Figure 26: 4/3 direction control valve (DCV) [25].....	23
Figure 27: 4/3 proportional DCV [25]	23
Figure 28: A Simulink block diagram of servo valve dynamics	24
Figure 29: A Simulink block diagram of Relative openings of the valve	24
Figure 30: Flow vs Input signal (Bosch Rexroth 4WRA) [28].....	25
Figure 31: Layout of an orifice [29].	25
Figure 32: Simulink block diagram of an orifice	26
Figure 33: Subsystem of orifice block	27
Figure 34: Flow paths in a 4/3 valve [26]	27
Figure 35: A Simulink block diagram representation of flow paths in 4/3 valve.....	28
Figure 36: A Simulink block diagram representation 4/3 valve.....	28
Figure 37: Schematic diagram of hydraulic cylinder [26]	29
Figure 38: A Simulink block diagram representation of hydraulic cylinder.....	31

Figure 39: A Simulink block diagram representation of hydraulic system	31
Figure 40: A Simulink block diagram representation of 3 cylinders and 3 DCV's connected	32
Figure 41: SIMSCAPE block diagram of Rack and Pinion	33
Figure 42: SIMSCAPE visualization of the boom	33
Figure 43: A Simulink block diagram representation of hydraulic system connect to SIMSCAPE block.....	34
Figure 44: Initial control system scheme	34
Figure 45: PID control [35]	35
Figure 46: PID controller used in simulation	35
Figure 47: A Simulink block diagram of the hydraulic system with controller.....	36
Figure 48: Hydraulic cylinder assembled with sensor [37].....	36
Figure 49: Incremental encoder from BEI sensors[40]	37
Figure 50: Closed loop system with disturbance and noise	38
Figure 51: Step response of cylinder 1,2 and 3 with cylinder stroke as feedback and disturbance (sine wave of 31rad/s frequency)	39
Figure 52: Force, Boom angle, Cylinder stroke and Piston Velocity vs Simulation time (10 seconds) for stroke feedback	40
Figure 53: Step response of cylinder 1,2 and 3 with cylinder stroke as feedback and disturbance (sine wave of 0.7 rad/s frequency)	41
Figure 54: Step response of cylinder 1,2 and 3 with cylinder boom angle as feedback and disturbance (sine wave of 31rad/s frequency).....	42
Figure 55: Force, Boom angle, Cylinder stroke and Piston Velocity vs Simulation time (10 seconds) for boom angle feedback	43
Figure 56: Step response of cylinder 1,2 and 3 with boom angle as feedback and disturbance (sine wave of 0.7 rad/s frequency).....	44
Figure 57: Schematic representation of hydraulic boom [12]	46
Figure 58: DH parameters general representation [12]	47
Figure 59: Configurations of the manipulator [12]	49
Figure 60: 2-DOF Manipulator [12]	50
Figure 61: Schematic representation of manipulator in robotics toolbox	52
Figure 62: Teaching the movements of the manipulator using the toolbox	52
Figure 63: General scheme of joint space control [12]	53
Figure 64: Joint control scheme with cylinder stroke feedback.....	53
Figure 65: Joint space control scheme with boom angle feedback.....	54
Figure 66: Joint control scheme implemented in the simulation	54
Figure 67: Loading position (x, y) = (4, 3) (mode 6)	55
Figure 68: Launching position (x, y) = (4, 5.8) (mode 5)	55
Figure 69: Extreme position (x, y) = (5.8, 5.8) (mode 4)	56
Figure 70: Location of MRU and movements of the vessel [47]	56
Figure 71: Implementation of AHC in the system [13]	58

LIST OF TABLES

<i>Table 1:</i> Parameter values to calculate F_H	10
<i>Table 2:</i> Some important quantities estimated by mechanical assembly.....	20
<i>Table 3:</i> Gain values used in the project	45
<i>Table 4:</i> DH parameter for the hydraulic boom.....	47

LIST OF SYMBOLS AND ABBREVIATIONS

Symbols

Δ	Triangle	
θ	Angle for cylinder placement	
β	Angle of the boom along the horizontal	
$^\circ$	Degree	
v_1, v_2, v_3	Joint values of the manipulator	[rad]
σ_e	Flexural endurance limit stress	[Mpa]
ρ	Fluid mass density	[N/ m ²]
π	pi	

Variables used

A	Area of cross section	[m ²]
A_A	Area of cylinder chamber A	[m ²]
A_B	Area of cylinder chamber B	[m ²]
a_2	length of link 1	[m]
a_3	length of link 2	[m]
B_H	Distance at which the cylinder is attached to the arm	[mm]
B_{cm}	Distance where the center of mass acts on the boom	[mm]
B_L	Total length of the boom	[mm]
b_1	Breadth of rectangle 1	[mm]
b_2	Breadth of rectangle 1	[mm]
C_s	Service factor of gear	
C_D	Deformation factor of gear	[N/mm]
C_q	Flow Coefficient	
D	Piston diameter of A-side chamber	[m]
d	Piston diameter of the B-side chamber	[m]
F_L	Load force at the end of the boom	[N]
F_B	Force due to the weight of the boom	[N]
F_H	Force of the hydraulic cylinder	[N]
F_{cyl}	Force generated by hydraulic cylinder	[N]
F_μ	Viscous friction force	[N]
h_1	Height of rectangle 1	[mm]
h_2	Height of rectangle 2	[mm]
I_X	Moment of inertia of rectangular cross section	[mm ⁴]
I_{X1}	Moment of inertia of rectangle 1	[mm ⁴]
I_{X2}	Moment of inertia of rectangle 2	[mm ⁴]
K_p	Proportional gain	
K_i	Integral gain	
K_d	Derivative gain.	
L_b	weight of boom	[kg]
m_p	Module	[mm]
n_p	Speed of the pinion	[rpm]
P_p	Power generated by the rack and pinion	[W]
p_c	Circular pitch	[mm]
p_A	Pressure in chamber A	[Mpa]
p_B	Pressure in chamber B	[Mpa]

p_1	Pressure before the orifice	[Mpa]
p_2	Pressure after the orifice	[Mpa]
p_{tr}	Transition pressure	[Mpa]
p_{wx}, p_{wy}, p_{wz}	Position orientation of end effector	[m]
Q	Flow rate	[m ³ /s]
q_1, q_2, q_3	Joint values of the manipulator	[rad]
r_p	Radius of the pinion	[m]
T_p	Torque generated by the rack and pinion	[Nm]
T_n	Number of teeth on gear	
U_s	Input Signal to the hydraulic system	
V_A	Volume of the chamber A of hydraulic cylinder	[m ³]
V_{0A}	Dead volume of chamber A	[m ³]
V_B	Volume of the chamber B of hydraulic cylinder	[m ³]
V_{0B}	Dead volume of chamber B	[m ³]
v_p	Pitch line velocity	[m/s]
W_T	Tangential tooth load	[N]
W_D	Dynamic tooth load	[N]
W_S	Static tooth load	[N]
W_g	Force due to weight of boom	[N]
x_{max}	Maximum stroke	[m]
x	Piston position	[m]
Y_T	Half thickness of the tooth at critical section	

Abbreviations

AUV	Autonomous Underwater Vehicle
aColor	Autonomous and Collaborative Offshore Robotics
BHN	Brinell Hardness Number
CAD	Computer Aided Design
DCV	Direction Control Valve
DLS	Damped Least Squares
DOF	Degree of Freedom
DH	Denavit-Hartenberg
FEA	Finite Element Analysis
IMU	Inertial Measurement Unit
MRU	Motion Reference Unit
MEI	Mechanical Engineering and Industrial systems
PID	Proportional Integral Derivative
TUT	Tampere University of Technology
UAV	Unmanned Aerial Vehicle
USV	Unmanned Surface Vehicle

1 INTRODUCTION

Offshore technology plays a predominant role in Finnish offshore industries. Offshore is one of the major industries in the marine industry sector. Some of the major technological developments for these industries are in the field of material handling cranes, automation and manufacturing. The revenue generated by the Finnish offshore industries is approximating to 1 billion euros and over 170 offshore companies have employed 4600 personnel in the year 2016. Over 60 % of the revenue of the Finnish offshore industries is by technological developments while the remaining is through subcontracting and engineering [1]. Therefore, the offshore industries are technologically demanding as they require robust, stable and efficient engineering solutions to work in a harsh working environment [2].

This Master's thesis is conducted as a part of aColor (Autonomous Collaborative Offshore Robotics) project at MEI (Mechanical Engineering and Industrial systems) department of Tampere University of Technology. The main objective of the aColor project is to collaborate Autonomous Underwater Vehicle (AUV) in Figure 1, fixed wing Unmanned Aerial Vehicle (UAV) in Figure 2 and the Unmanned Surface Vessel (USV) in Figure 3. The underwater and aerial vehicle is used for offshore exploration [3]. The launch and retrieving of these vehicles demand a hydraulic arm on the USV. Therefore, this thesis work focuses on the mechanical design of the hydraulic boom, control, and stabilization for the launch and retrieval of the underwater and aerial vehicle. For the rest of the thesis USV will be addressed as a surface vessel.

Most of the offshore hydraulic booms are on board with a surface vessel, the main applications of this hydraulic boom are to lift and transport the cargo. Offshore hydraulic booms are usually used in difficult working conditions which involves the disturbances from the sea waves and wind. Due to these disturbances, the hydraulic boom undergoes several problems like load sway, position inaccuracy and collision [2]. Therefore, a robust control system has to be designed in such a way that the disturbances from the waves can be compensated. Furthermore, the mechanical design of the hydraulic boom must consider the corrosion factors. The offshore corrosion might lead to damage of components which could lead to the malfunction of the hydraulic manipulator.

Modelling and simulation of offshore hydraulic manipulator involve in sophisticated and multidisciplinary tasks like the mechanical design of a hydraulic manipulator, modelling of hydraulic systems and designing the control system. Therefore, this thesis work is divided into several stages. In Section 1.1, the methodology to conduct this research is explained.



Figure 1: BlueROV (Under-water vehicle) [4]



Figure 2: Albatross fixed wing UAV [5]



Figure 3: Surface vessel

1.1 Research methodology and scope of thesis

This thesis work focuses on design and control of the offshore hydraulic manipulator for aColor project. The key aspects of this thesis work include mechanical design of the hydraulic manipulator, modelling of the hydraulic system, joint space control and Active Heave Compensation (AHC) for stabilization. There are several solutions for the design and control of the hydraulic boom, but this thesis is designed to cater to the special requirements of the aColor project.

Research methodology involves a systematic approach to discover new facts, analyze verify and validate the facts. This thesis follows qualitative and quantitative approaches to study the background data and implement that data in the simulations. Qualitative research involves finding the reason behind any decision or statements of fact whereas, quantitative data involves in strengthening these facts by numerical data or results. In this thesis, a background study and reason behind any implementation is explained along with the results from the simulations to validate those implementations. To conduct this thesis work some of the steps followed were:

1. Background Study: This study involves in a collection of all the facts and data which is required for the thesis work. Additionally, the project requirements are studied in detail.
2. Design calculations: The initial assumptions of the design can be tested and validated by performing some basic mathematical calculations to place the hydraulic cylinders and to calculate joint space requirements.
3. Mechanical design: The arms are designed using aluminium sheet metal. These arms are assembled with all the components in the hydraulic boom using SOLID-WORKS software.
4. Modelling of hydraulic system: The hydraulic system is modelled using numerical equations and then a closed loop control system is implemented. The hydraulic model is represented through Simulink block diagrams.
5. Kinematics: To check the dynamic behavior of the hydraulic boom, the kinematics programs are implemented. Additionally, these programs can be used to stabilize the offshore hydraulic boom.
6. Dynamic behavior analysis: These analysis results provide numerical facts and data to validate the thesis work.

2 BACKGROUND STUDY

Offshore hydraulic manipulators are extensively used for pick and place operations. Offshore industries use hydraulic manipulators to move the cargo from offshore to land and vice versa. The hydraulic manipulator located on the surface vessel or a ship encounters a lot of disturbances due to wind and waves in the offshore. When the manipulator is carrying some payload in the offshore, due to these disturbances the payload can swing, and it might cause some damage. In the past two decades, a lot of advancements are happening in the offshore industry. Most of the advancements involve in developing control systems, electronics on board and robotics [6]. The advancements in electronics has made way for a range of applications, wherein some applications are developed to compensate these disturbances in offshore.

The mechanical design comprises of designing a 3-dimensional model of the hydraulic boom virtually using a CAD software. The software used in this project is SOLIDWORKS. In this software, different parts of the hydraulic boom are designed and assembled in a 3-dimensional platform. The movement of the parts with respect to each other can be virtually visualized. This helps in reducing the risk while manufacturing the prototype, the lifecycle cost is reduced, provides a tool to check the inefficiency of the design and lowers the cost of manufacturing of the prototype [7]. In addition, these models can be utilized for SIMSCAPE simulation. These models are further converted to 2-dimensional drawings which are a reference to the manufacturer and they are more accurate than the hand drawings.

In the development process of any system, scientific methods involve in “real-world” and “conceptual world” implementations. Real world pertains to the physical system built in reality and conceptual world comprises of modelling and simulations which help to analyze, predict, validate and test the behavior of the system virtually. Numerical modelling involves modelling a block diagram through various mathematical equations [8]. To model a block diagram of the hydraulic valve and cylinders, some basic equations related to flow has to be used and it is explained in Chapter 4. These models benefit the simulations in real-time systems.

The term PID stands for Proportional Integral Derivative. PID control approaches are widely used for real-world problems. With the advancement in science and technology, there are wide options for control schemes. Nevertheless, most of the companies employ PID algorithms. Proportional term generates a signal proportional to the error signal through the proportional gain factor. The integral term comprises of a low-frequency integrator that helps in reducing the steady-state errors. Derivative consists of a high-frequency compensator to improve the transient response of the system. These three terms are connected in a parallel manner. By tuning the derivative gain of the system, the stability can be improved. The advantages of using PID controller are increased stability, robustness, noise attenuation and fewer uncertainties [9]. Hence, PID controller could be selected as it is generally known to be a robust controller.

In the hydraulic boom, several types of feedback systems can be employed. In this project, there are two feasible feedback systems namely boom angle feedback and cylinder stroke feedback. The main objective of a feedback control is to track the reference input. Feedback control improves the stability of the plant, improves the system performance and helps in the detection of errors[10].

The formulation of the kinematic equations of the hydraulic boom will help in determining the relations between the end effector position and joint values of the hydraulic boom. To initiate this, the DH (Denavit-Hartenberg) parameters have to be determined. Further with these parameters, the forward and inverse kinematic equations are formulated. The end-effector position can be determined through forward kinematics when the joint angle is known. The joint angles can be determined through inverse kinematics when the end effector position is defined. The angular velocity of the joints can be determined by using a transformation matrix with Jacobian matrix [11]. The initial step to conduct joint space control scheme is by formulating inverse kinematics for the hydraulic manipulator.

The joint space control is implemented in two stages. In the first stage, the inverse kinematics equations are formulated and then in the second stage, the input reference for the controller is provided by the inverse kinematics program. When a position is defined in the space, the inverse kinematics program generates the joint values corresponding to the position in the joint space [12]. These values are used as an input reference for the system.

The offshore environment is prone to a lot of disturbances due to wind and ocean waves. These disturbances can be compensated through some effective approaches like AHC (Active Heave Compensation). In this project, the heave disturbance is given a major priority because the end effector must be very stable to retrieve the UAV. If the end effector of the hydraulic boom is not in a constant position, there are chances of UAV colliding the manipulator. If the heaves in the offshore are compensated, then the end effector can be more stable. Active Heave compensation involves in an integration of IMU (Inertial Measurement Unit) or MRU (Motion Reference Unit) to detect the motion of the surface vessel in all directions [13]. Then a compensation method is applied by calculating the dynamics of the hydraulic boom. These compensation methods are studied in detail in Section 6.5.

3 MECHANICAL DESIGN AND ANALYSIS

As a first step, the mechanical design of the hydraulic boom was created using SOLIDWORKS modelling software. There are several design considerations in this project and the hydraulic arm is custom made according to the requirements of the aColor project.

The design considerations are as follows:

1. The hydraulic boom should be lightweight and corrosion resistant as it is used in the offshore, therefore aluminium was the material chosen as it is corrosion resistant and lightweight [14].
2. The hydraulic boom must be able to carry 30 kg at a span of 5.8m and 100 kg at span 3m.
3. The total span of boom should not be more than 5.8m.
4. The boom should have 2 arms.
5. The cylinder must be placed in such a way that the piston is not exposed to the atmosphere, to avoid water splashing.
6. The boom must be placed on the deck, in front of the boat mast. (Dimensional restrictions during operation)
7. The base of the boom must be attached to the base of the mast through a thick aluminium sheet-metal base.

To initiate the design process, the geometric layout of the hydraulic boom is made wherein, the angle the cylinder placement is calculated. The total length of the 2 arms cannot exceed over 5.8 meters. Therefore, the length of the first arm is considered to be 3 meters and the second arm to be 2.8 meters. The angular position of the cylinder is of utmost importance to prevent the collision of the arm with cylinder.

3.1 Approximating the angle of cylinder when boom is in transport position

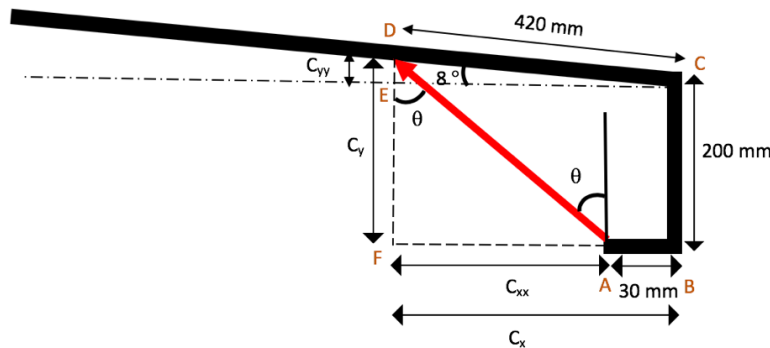


Figure 4: When the boom is in transport position

The geometric layout of the hydraulic boom would provide a range of angular values for cylinder placement.

In Figure 4, the red arrow shows the cylinder placement. The first arm is placed at an angle of 8° to avoid the collision of the second arm with the deck of the surface vessel. The angle of the cylinder to be calculated is θ .

Consider the triangle ΔDCE , the side DC is 420mm, therefore C_{xx} can be calculated as follows:

$$C_x = 420 \text{ mm} \cos (8^\circ), C_x = 415.913 \text{ mm}$$

$$C_{xx} = C_x - 30 \text{ mm}$$

$$C_{xx} = 385.913 \text{ mm}$$

Now calculating C_y . Consider the ΔDCE

$$C_{yy} = 420 \text{ mm. } \sin (8^\circ), C_{yy} = 58.453 \text{ mm}$$

$$C_y = C_{yy} + 200 \text{ mm}$$

$$C_y = 258.453 \text{ mm}$$

The length of the cylinder can be calculated as follows:

$$C_{length} = \sqrt{C_{xx}^2 + C_y^2}$$

$$C_{length} = 464.463 \text{ mm} \quad (3.1)$$

Therefore, the angle for cylinder placement in transport position is as follows:

$$\theta = \tan^{-1} (C_{xx}/C_y)$$

$$\theta = 56.189^\circ \quad (3.2)$$

3.2 Approximating the angle of cylinder when boom reaches maximum height

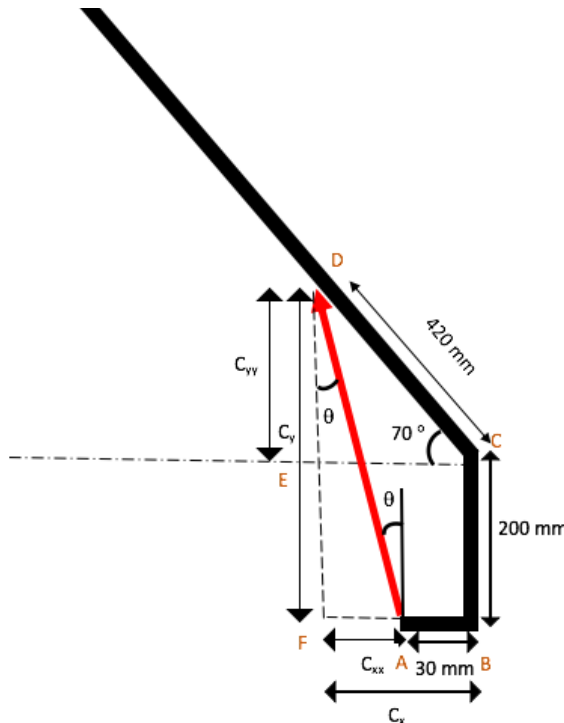


Figure 5: When the boom is at maximum height

The angle made by the boom when it attains the maximum height is assumed to be 70° along the horizontal as seen in Figure 5. The angle of the cylinder placement (θ) is calculated as follows.

Consider the triangle ΔDCE , the side DC is 420mm, therefore C_{xx} is calculated as follows:

$$C_x = 420 \text{ mm. } \cos (70^\circ), C_x = 143.648 \text{ mm}$$

$$C_{xx} = C_x - 30 \text{ mm}$$

$$C_{xx} = 113.648 \text{ mm}$$

Now calculating C_y . Consider the ΔDCE

$$C_{yy} = 420 \text{ mm. } \sin (70^\circ), C_{yy} = 394.671 \text{ mm}$$

$$C_y = C_{yy} + 200 \text{ mm}$$

$$C_y = 594.671 \text{ mm}$$

The length of the cylinder to attain the maximum height can be calculated as follows:

$$C_{length} = \sqrt{C_{xx}^2 + C_y^2}$$

$$C_{length} = 605.433 \text{ mm} \quad (3.3)$$

Therefore, the angle for cylinder placement to attain maximum height is as follows:

$$\theta = \tan^{-1}(C_{xx}/C_y)$$

$$\theta = 10.819^\circ \quad (3.4)$$

Thus, the obtained results from the geometric layout would provide an idea of the boom angle and the stroke required while assembling the cylinders to reach different positions of the boom along its operating range. The operating range here implies the values between the transport position and maximum height of the boom.

3.3 Mechanics of the boom

To analyze the design of any manipulator, forces acting on it are an important parameter. In this section, theoretical calculations are performed to understand the forces acting on the manipulator [15]. Therefore, the force required by hydraulic cylinder can be estimated by finding the rotational equilibrium [16].

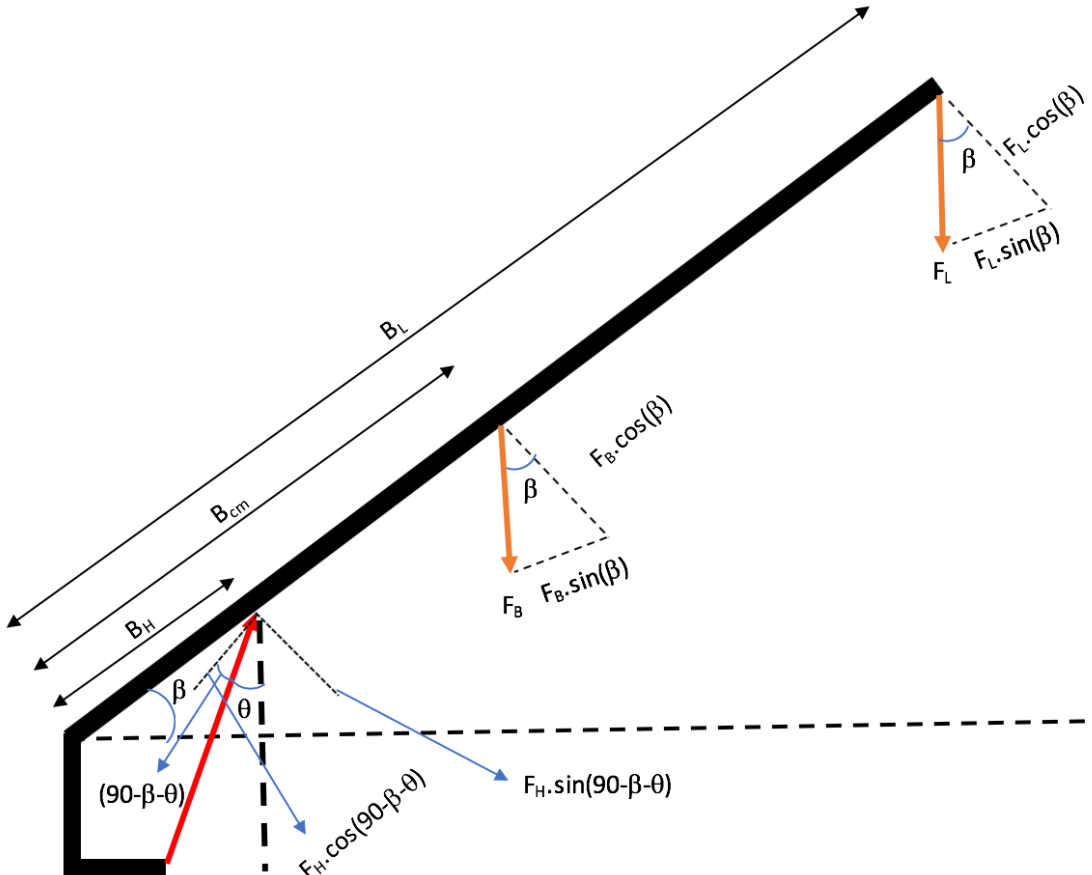


Figure 6: Schematic diagram of the forces acting on the boom

In Figure 6, the force F_L is due to the load acting at the end of the boom, F_B is the force due to the weight of the boom and F_H is the force of the hydraulic cylinder. B_H is the distance where the cylinder is attached to the manipulator. B_{cm} is the distance where the center of mass acts on the boom. B_L is the total length of the boom. The forces have been

resolved to horizontal and vertical components respectively. Therefore, to calculate the force required by the hydraulic cylinder, net torque acting on the boom must be equated to zero.

$$\Sigma T = 0 \quad (3.5)$$

Summing the torque to zero

$$-B_{cm} F_B \cos(\beta) - B_L F_L \cos(\beta) + F_H \sin(90 - \beta - \theta) B_H = 0 \quad (3.6)$$

Solving for F_H

$$F_H = \frac{B_{cm} F_B \cos(\beta) + B_L F_L \cos(\beta)}{\sin(90 - \beta - \theta) B_H} \quad (3.7)$$

The value of the parameter θ can be calculated from Equation 3.4. F_B is the force due to the weight acting at the center of the boom, it is assumed to be 50 kg. F_L is the load force acting at the end of the boom, a load of 30 kg is considered as per the considerations. B_L is the total length of the hydraulic arm; the arm length is about 5.8 meter. B_{cm} is the length at which the center of mass is acting, the length is about 2.9 meter. Now, consider the hydraulic boom is at 70° along the horizontal. The hydraulic force required from the cylinder can be calculated from Equation 3.7

Table 1: Parameter values to calculate F_H

$\theta(^{\circ})$	$\beta (^{\circ})$	$F_B (N)$	$F_L(N)$	$F_H (N)$
10.819	70	490	294.199	15955

3.4 Design of rack and pinion gear

Rack and pinion gear system are one of the widely used systems for the boom rotation. The linear motion of the hydraulic cylinder is converted to rotary motion using rack and pinion system. There are different types of rack and pinion gears, most commonly used are rack and pinion gear with straight tooth and helical tooth [17]. In this application, the rack is attached to the hydraulic cylinder and the pinion is attached to the base of the boom. Therefore, the hydraulic cylinder that is attached to the rack gear makes a linear movement and the pinion connected to the base makes a rotary motion. Straight tooth rack and pinion are used in this project work.

To initiate the gear design process, pinion with module 2mm, rack of length 300 mm and pinion of diameter 96 mm was selected. The design procedure for the spur gear is according to [18]. The rack and pinion system should carry a load of 150 kg.

The maximum torque (T_p) produced by the pinion is 2.7 Nm from the manufacturers catalogue [19].

The Power (P_p) generated by rack and pinion is calculated using speed (n_p) and torque (T_p) as seen in Equation 3.8:

Considering n_p as 30 rpm.

$$P_p = \frac{2 \pi n_p T_p}{60} \quad (3.8)$$

$$= 8.5 W$$

Circular pitch (p_c) is calculated using module (m_p). A 2mm module for the gear is considered for the application:

$$p_c = \pi \cdot m_p \quad (3.9)$$

$$= 6.28 mm$$

Pitch line velocity(v_p) is calculated at a speed (n_p) of 30 rpm and the gear consists of 48 teeth (T_n).

$$v_p = \frac{p_c T_n n_p}{60} \quad (3.10)$$

$$= 0.15 m/s$$

Tangential tooth load (W_T) is calculated with a service factor (C_s) of 1.54. When the gears are run for three hours a day and there is a heavy shock on gears, service factor of 1.54 is considered [18].

$$W_T = \frac{P_p \cdot C_s}{v_p} \quad (3.11)$$

$$= 87.27 N$$

Dynamic tooth load (W_D) can be calculated by considering the face width of the gear as three times the circular pitch (p_c). Deformation factor (C_D) is taken as 456 N/mm as the rack and pinion are made of steel. Therefore, using Buckingham equation, the dynamic tooth load is calculated [18].

$$W_D = W_T + \frac{21 \cdot v_p (3 \cdot p_c \cdot C_D + W_T)}{21 \cdot v_p + \sqrt{3 \cdot p_c \cdot C_D + W_T}} \quad (3.12)$$

$$= 109.28 N$$

Static tooth load (W_S) determines the strength of the tooth [18]. If the static tooth load (W_S) is 1.5 times the dynamic tooth load (W_D), then the gear tooth is strong enough. A

half thickness of the tooth at critical section is calculated (Y_T) Equation 3.13. Flexural endurance limit stress (σ_e) for the steel material is 1.75 times the Brinell hardness number (BHN) of steel. Further, the BHN is considered to be 300 and Flexural endurance limit stress is 525 MPa.

$$Y_T = 0.154 - \frac{0.912}{T_n} = 0.135 \quad (3.13)$$

Calculating static tooth load:

$$W_S = \sigma_e \cdot 3 \cdot p_c \cdot pi \cdot m_p \cdot Y_T = 8389.84 \text{ N} \quad (3.14)$$

As static tooth load (W_S) in Equation 3.14, is more than the dynamic tooth load (W_D), the rack and pinion system is strong enough to take any shock loads [18]. Hence, with a module 2mm, pinion of outer diameter of 100 mm, rack of length 300 mm and with steel being the material used, the rack and pinion system can carry 150 kg of load at 30 rpm with shocks. As $W_S > 1.5 W_D$, the rack and pinion design are considered to be safe. The Figure 7 and 8 below shows the rack and pinion gears designed by Mekanex Oy, Finland [20]. These are the selected gears used for the rack and pinion system.

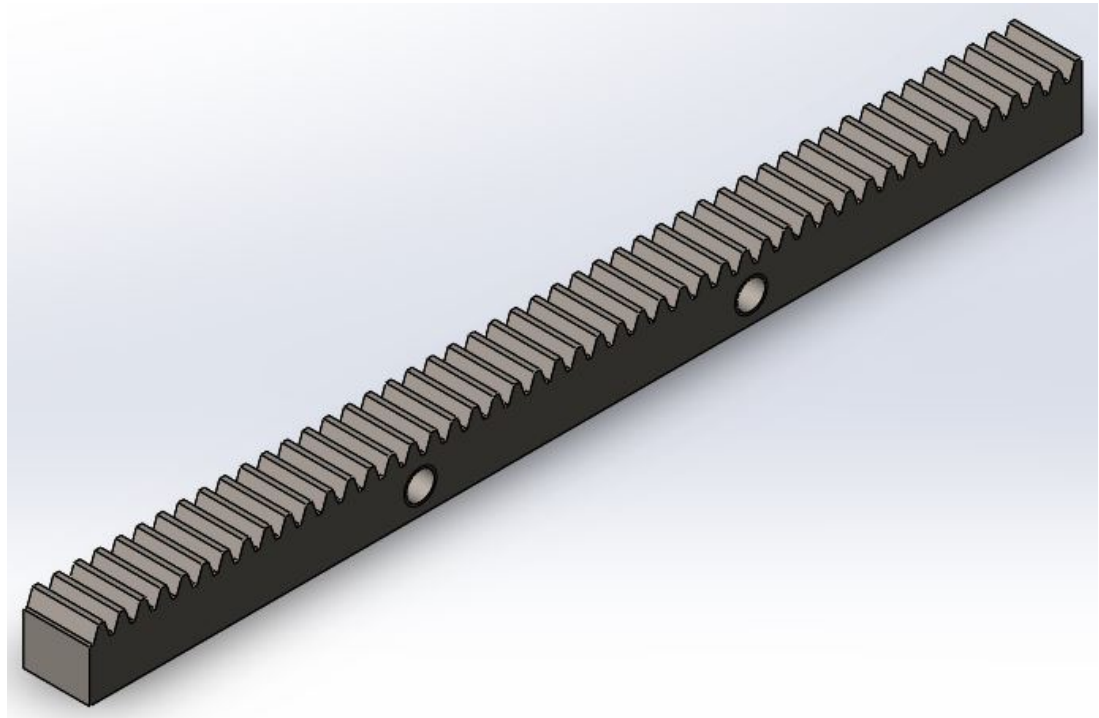


Figure 7: Rack gear[20]

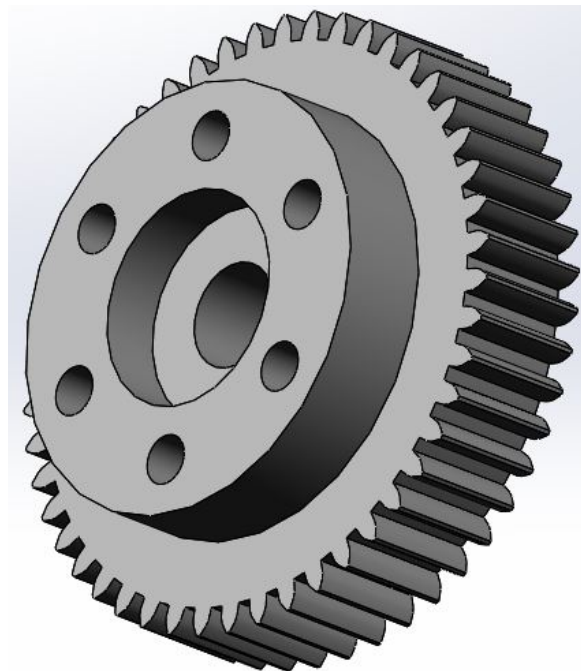


Figure 8: Pinion gear[20]

3.5 Sheet metal design of the manipulator components

Sheet metal is one of the most commonly used metal for manufacturing of components. Sheet metal consists of metal drawn into thin sheets. The thickness of the sheet metal is usually in the range of few millimeters. Sheet metal manufacturing is one of the cost-efficient process for manufacturing, as the manufacturing involves a simple machining process like bending, welding and drilling.

In the offshore conditions, the boom is prone to humid conditions where most of the metal corrode due to the humid atmosphere. The corrosion issue can be sorted if a corrosion resistant metal is used. Therefore, aluminium 5052 sheet metal of 10mm thickness is selected. Aluminium 5052, has good corrosion-resistance to the humid atmosphere, good weldability, good formability, lightweight and low maintenance. The strength of this alloy ranges from medium to high strength [21] [22]. Hence, the aluminium 5052 sheet metal is best suitable for manufacturing the arms of the boom in this project.

3.5.1 Sheet metal design of arms

Figure 9 below shows the potential area in front of the mast, where the hydraulic boom could be assembled. When the boom is in the transport position, the total length of the boom must not extend over 3500 mm. This is not a major problem as the first arm length of the boom is already constrained to be 3000mm. As the main purpose of this hydraulic boom is to launch and retrieve the UAV its span has to be considered. The span of the Albatross fixed-wing UAV is 3 meters [23]. The retrieval of the UAV happens through a skyhook process, wherein the UAV hooks itself at its center to the tip of the hydraulic manipulator. As the length of the second arm is 2.8 m and the combined length of both the arms when the boom is in working position is 5.8m. Hence, the boom does not collide with the UAV.

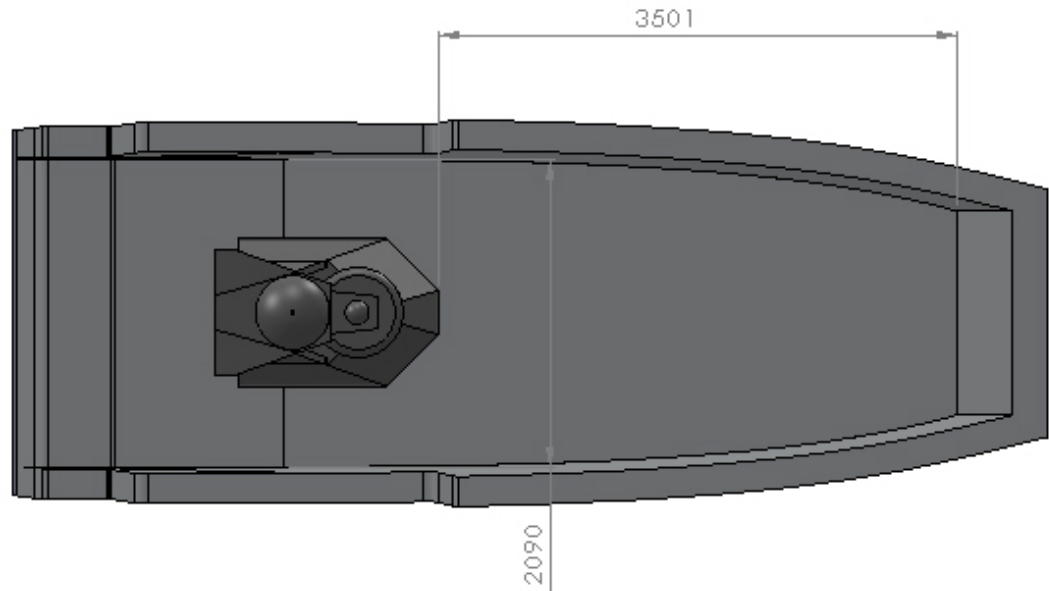


Figure 9: Top view of the aColor surface vehicle showing the area where the hydraulic boom can be assembled.

The below Figures 10, 11 shows the sheet metal design of the first arm and second arm respectively. The length of the second arm is considered as 2.8 meters as the hydraulic cylinder would collide with the second arm when the boom is in the transport position. The arms are made up of 10 mm thick aluminium sheet metal. SOLIDWORKS is the mechanical design tool used for designing the arms of the hydraulic manipulator.

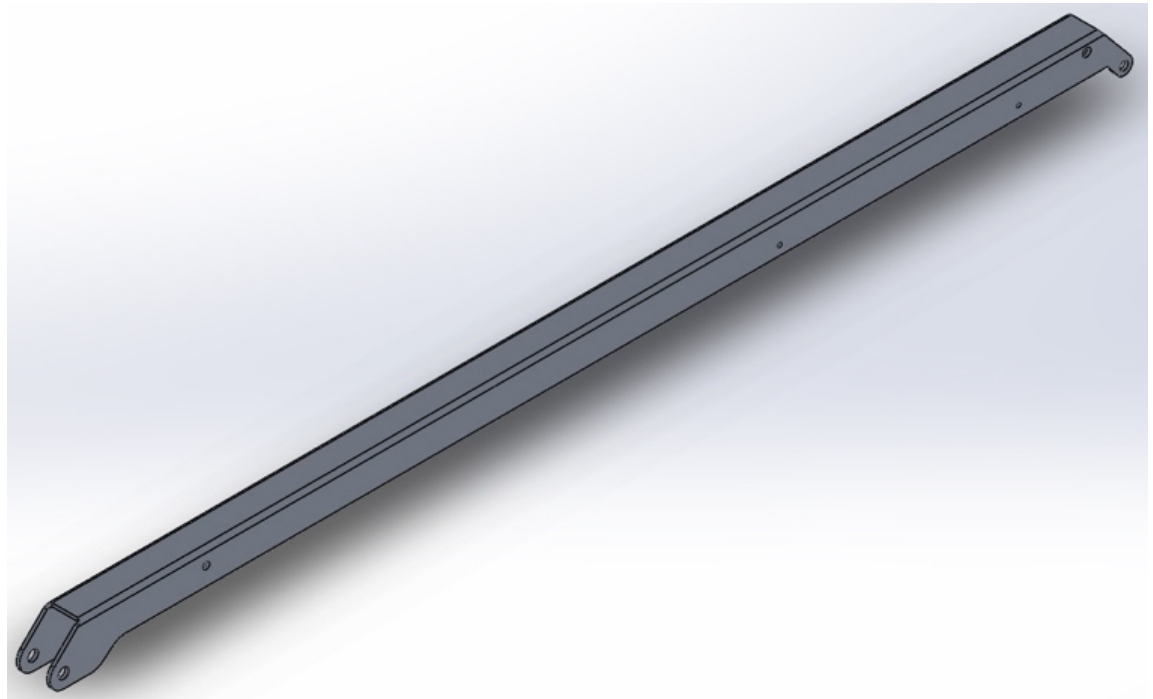


Figure 10: Sheetmetal design of first arm

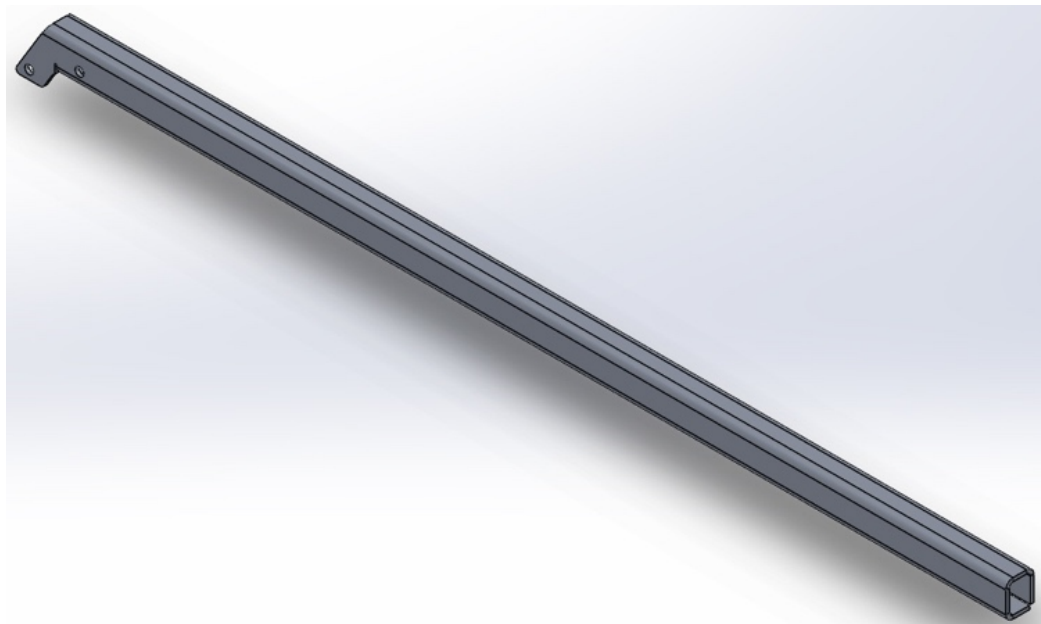


Figure 11: Sheetmetal design of second arm

3.5.2 Sheet metal design of base

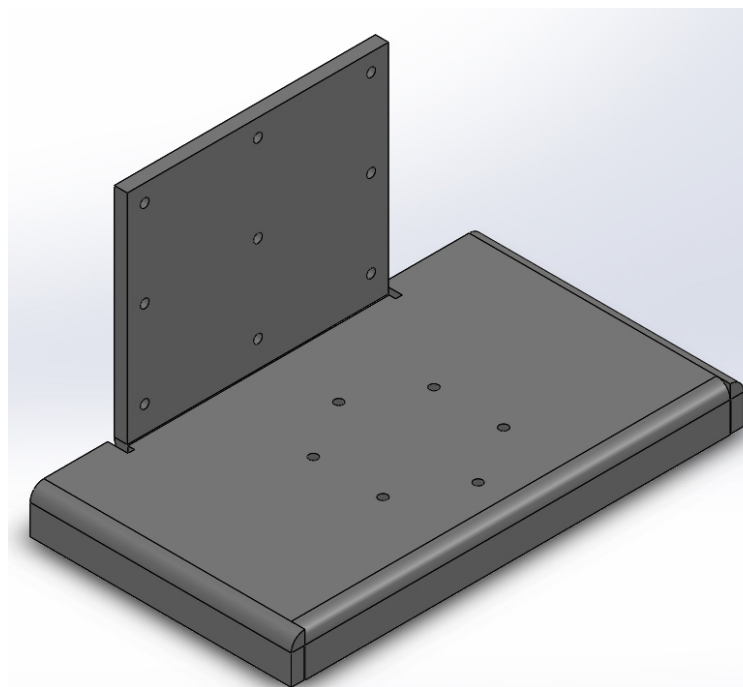


Figure 12: Sheetmetal design of the base

Figure 12 shows the base of the boom. The base is made up of 10mm thick aluminium sheet metal. Upon the base structure, the shaft driving the pinion is mounted. The pinion gear meshes with the rack gear and the hydraulic cylinder are attached to the rack gear via clamps. The flange of the base sheet metal is connected to the bottom part of the mast on the surface vessel.

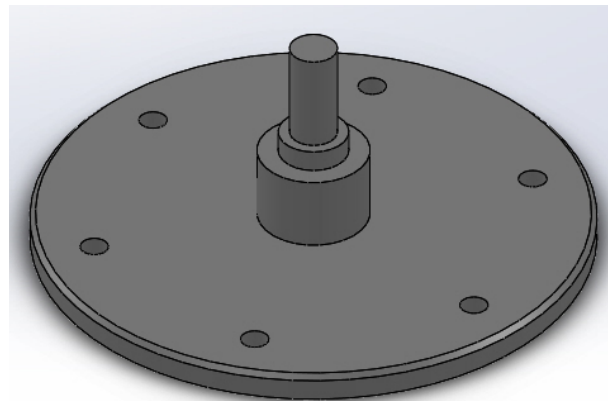


Figure 13: Shaft connecting the base part and pinion

Figure 13 shows the shaft attached to the base part of the boom. The pinion is connected to the shaft. Roller bearings and thrust bearings are used to connect the pinion gear with the shaft. This reduces the friction between the shaft and pinion gear, helps to withstand the shock loads and acts as an aid to balance the axial and radial loads [18]. Figure 14 below shows the assembly of the rack and pinion with the base sheet metal and shaft with bearings.

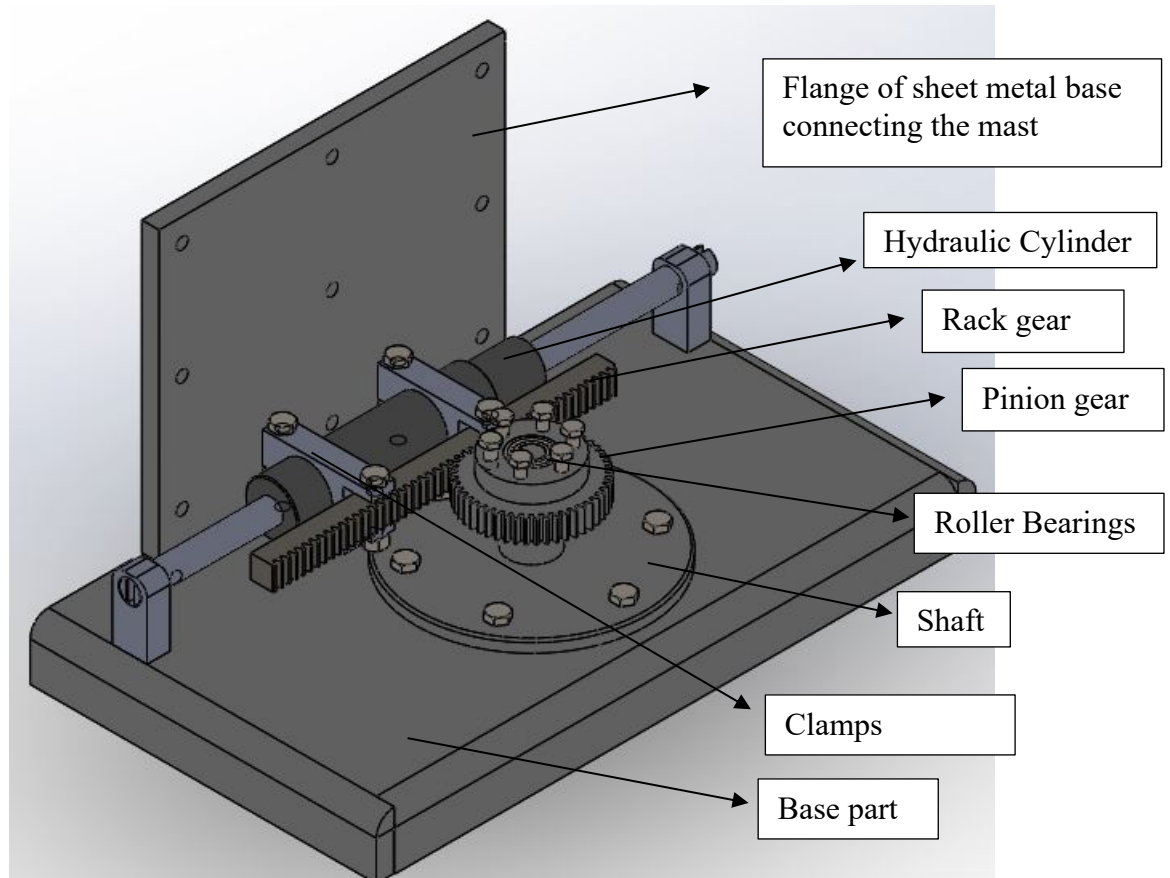


Figure 14: Assembly of rack and pinion system

3.6 Design of cylinder placements

As discussed in section 3.1, the cylinder has to be placed at an angle of 56.189° (Equation 3.2), when the boom angle is 8° . The boom is kept at 8° angle during the transport position. The hydraulic cylinder is attached to the boom and boom lift via clevis pins. In Figure 15, the cylinder placement angle is 59.97° which is close to the theoretical value from Equation 3.2, where the cylinder placement angle (θ) is about 56.189° . The boom lift houses the hydraulic cylinder connecting the first arm. The rotary motion of the pinion gear is transmitted to the boom lift. Figure 15 shows the placement of the lift cylinder in hydraulic boom.

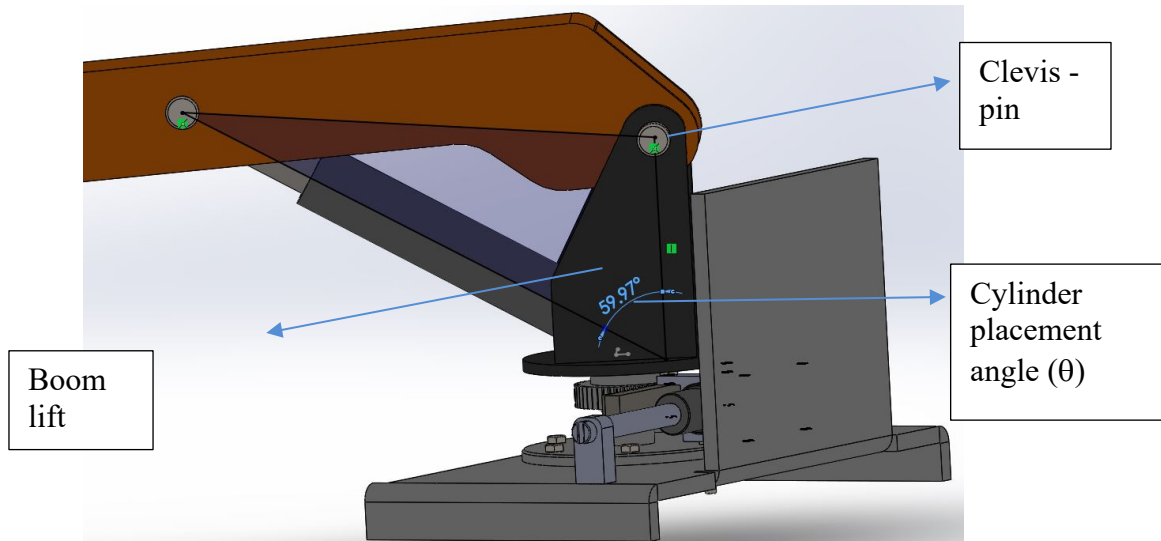


Figure 15: Placement of hydraulic cylinder for first arm

The cylinder placement for the second arm is horizontal, as the cylinder used is a double-sided piston cylinder. The connection of this cylinder for the second arm involves in the design of complex linkage mechanism, which is discussed in Section 3.7. Figure 16 shows the placement of a double-sided piston cylinder. The cylinder is placed inside the first arm. The first arm acts as a shield preventing the sea water to splash on the hydraulic piston and cylinder, thereby protecting the hydraulic cylinder from corrosion.

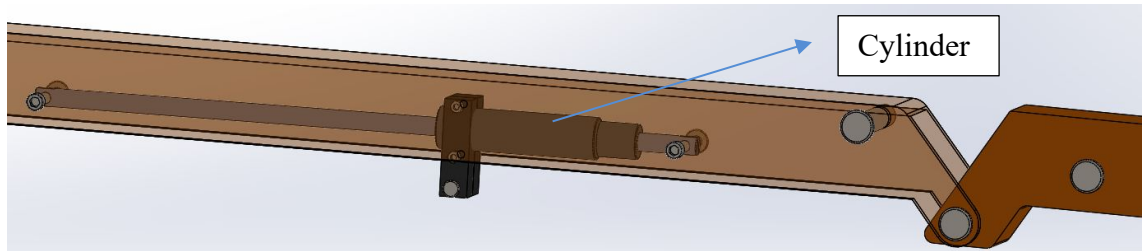


Figure 16: Cylinder placement for the second arm

3.7 Design of linkages

An indigenous linkage mechanism was developed to convert the translation motion of the hydraulic cylinder to the rotary motion of the second arm. This helps in moving the boom from the transport position to any working position within the working range. Initially, the boom was assembled with the hydraulic cylinder in a horizontal fashion. Then, the

clamp for the hydraulic cylinder was designed. A 4-bar linkage mechanism that is normally used in an articulated boom is designed. Further, a 2-bar linkage that connects the cylinder clamp to the 4-bar linkage is designed. This is a conceptual and indigenous 6 bar linkage design shown in Figure 17.

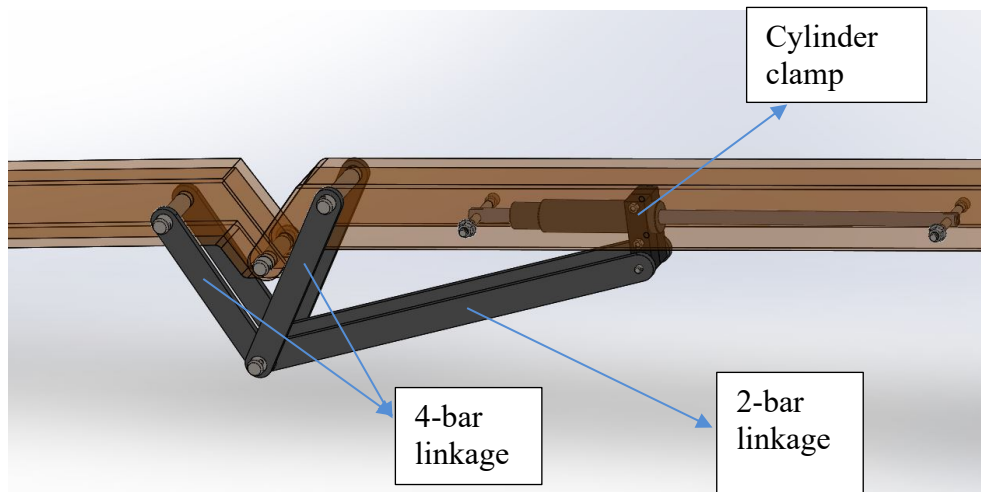


Figure 17: Linkage design for the rotary movement of second arm

3.8 Mechanical assembly of the boom

3D mechanical assemblies represent the final picture of any product or system. Mechanical assemblies allow the system to be built in a 3D environment, which can help in estimating the movement of parts with respect to each other and provides the final appearance of the system designed.

In this project, the main intent of creating a mechanical assembly is to estimate the movement of the parts with respect to each other. The end effector of the hydraulic arm is capable to move in X, Y and Z directions. These movements can be foreseen in the mechanical assembly. Figure 18 shows the mechanical assembly of the boom in the transport position.



Figure 18: Assembly of the hydraulic boom in transport position



Figure 19: Assembly of the boom when cylinder of first arm is at full stroke

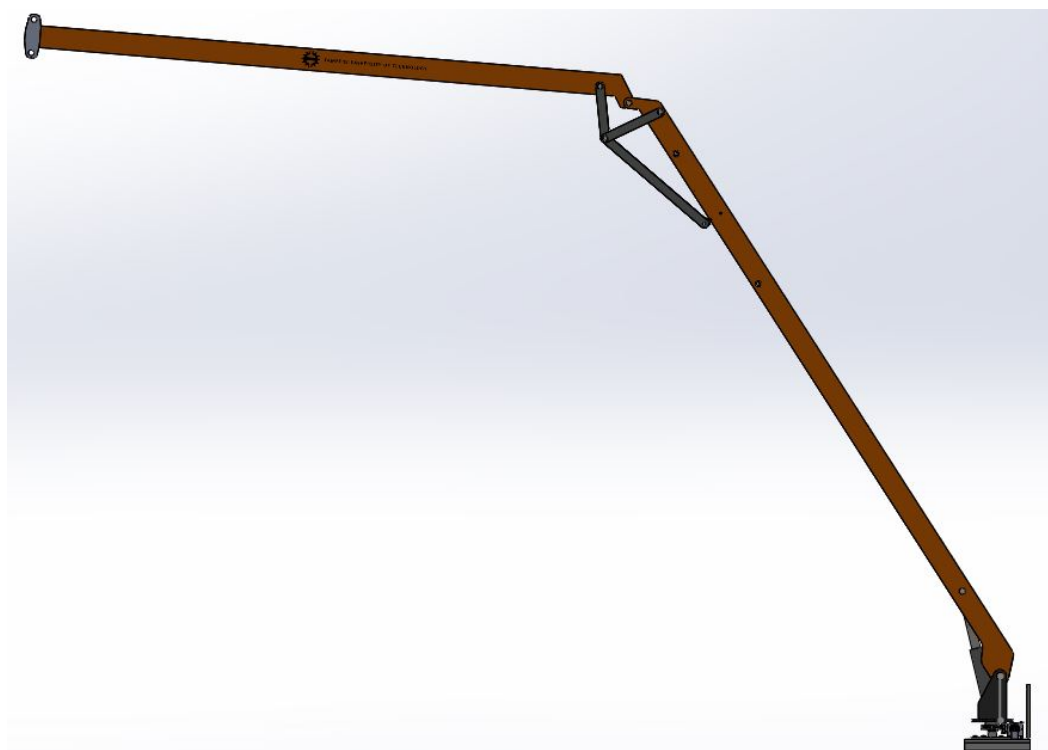


Figure 20: Working position of the boom

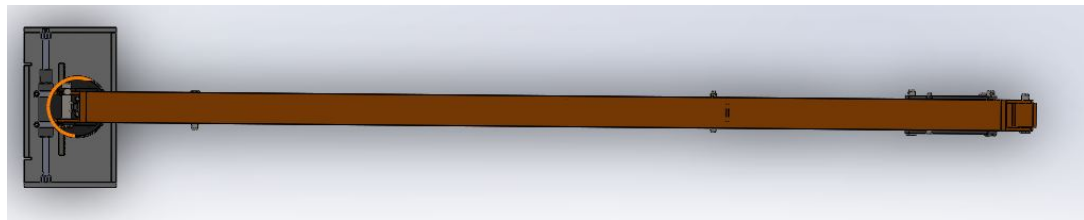


Figure 21: Top view of the boom



Figure 22: Isometric view of the hydraulic boom showing degrees of freedom (DOF)

The movement of the hydraulic boom in various positions is depicted in the Figures 19,20,21and 22. The movement of the arms with different stroke lengths can be inferred from this mechanical assembly. The assembly consists of 3 hydraulic cylinders, which provides 3 degrees of freedom (DOF) to the system. With the help of a mechanical assembly, some of the important quantities like weight, the center of mass and moment of inertia can be estimated. Table 2 below represents the values of certain quantities pertaining to the hydraulic boom. On this basis, it can be inferred that the mechanical assembly is a crucial step in the design process as the component design and movement of parts with respect to each other can be estimated.

Table 2: Some important quantities estimated by mechanical assembly

Quantities	Values
Mass	73.435 kg
Volume	0.03 cubic meters
Surface area	5.34 square meters
Center of mass at transport position	X = 1.76 m, Y = 1.46 m, Z = 0.37 m

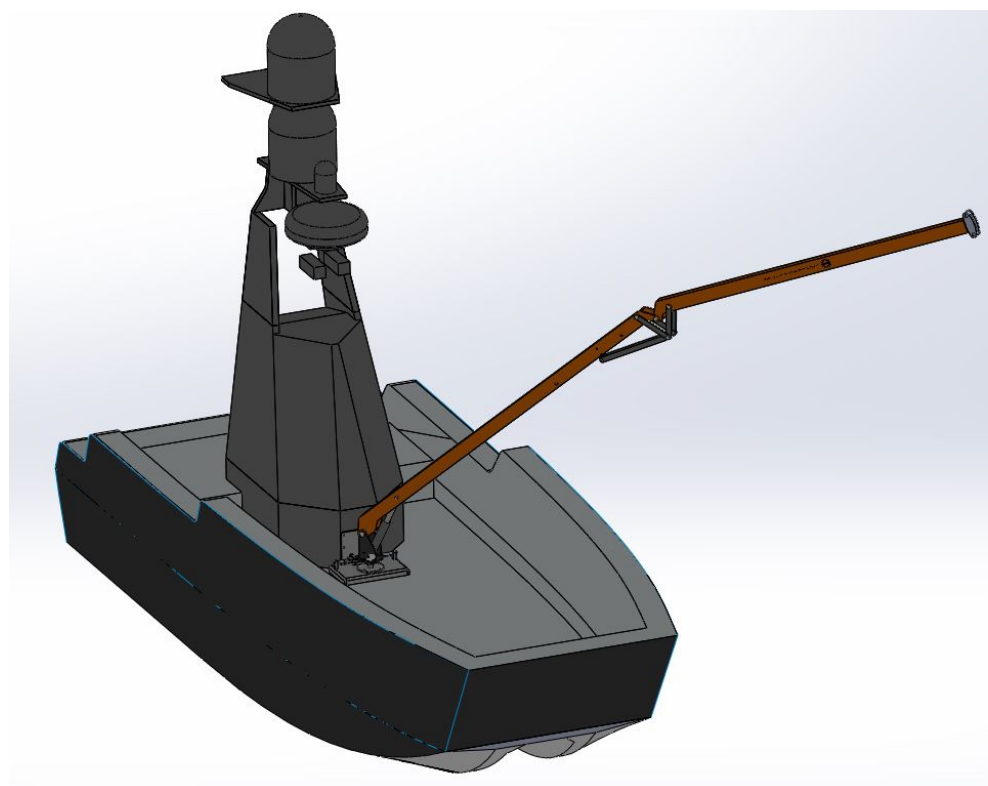


Figure 23: Assembly of boom in the surface vessel

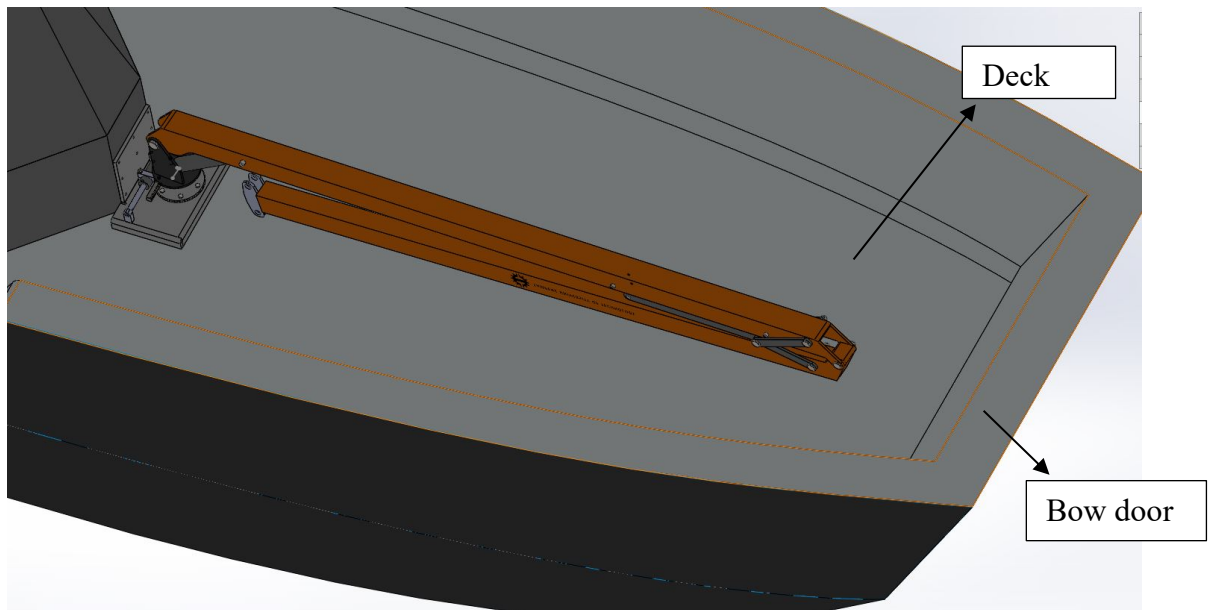


Figure 24: Assembly of boom and surface, when the boom is in transport position

The hydraulic boom is assembled in front of the surface vessel's mast as seen in Figure 23, 24. From the above images, it can be seen that the boom is not in contact with the bow door or colliding with the deck of the surface vessel.

4 MODELLING OF HYDRAULIC SYSTEM

A basic hydraulic system as shown in Figure 25 consists of a hydraulic power pack (motor + constant flow pump + filter + relief valve + tank), valve and an actuator. In this project, the block diagram of the cylinder, 4/3 valve, and hydraulic boom are modelled, and the hydraulic pump is assumed to be a constant displacement pump. Therefore, it produces a constant flow at a certain pressure.

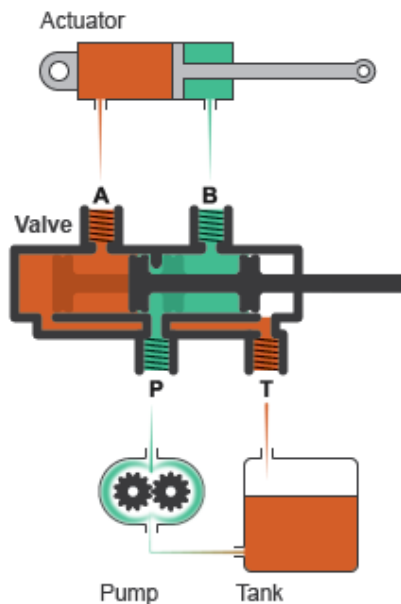


Figure 25: Basic layout of hydraulic system [24]

To get a clear picture, the equations governing these hydraulic components are studied, modelled and then implemented to the system. After modelling the hydraulic system, it is connected to the SOLIDWORKS assembly of the hydraulic boom through SIMSCAPE model. Then the behavior of the hydraulic system can be observed, this is also known as co-simulation process. The PID controller for each valve is designed and implemented. To design and stabilize the movement of the hydraulic boom, inverse kinematics of the hydraulic boom is calculated and implemented in the system. Further, this inverse kinematics model can be utilized for stabilization using heave compensation methods.

4.1 Modelling of 4/3 direction control valve

Most commonly used direction control valve (DCV) is usually spool type valves. Figure 26 describes the features of the DCV. It consists of the 4 ports namely P, T, A and B. In Figure 26 below, the P- port is connected to the B – port and A- Port is connected to the T – Port. Similarly, P- port can be connected to A port and B port can be connected to the T port. P-port is usually connected to the pump and T-port is usually connected to the tank. The ISO symbol of the 4/3 valve, Figure 26 shows that all the ports are closed and there is no flow happening. The opening and closing of the ports are determined by the movement of the spool. The term 4/3 indicates 4 ports and 3 directions of the valve. The

spool of the DCV can be controlled manually by hand lever or an electric solenoid with an amplifier [25].

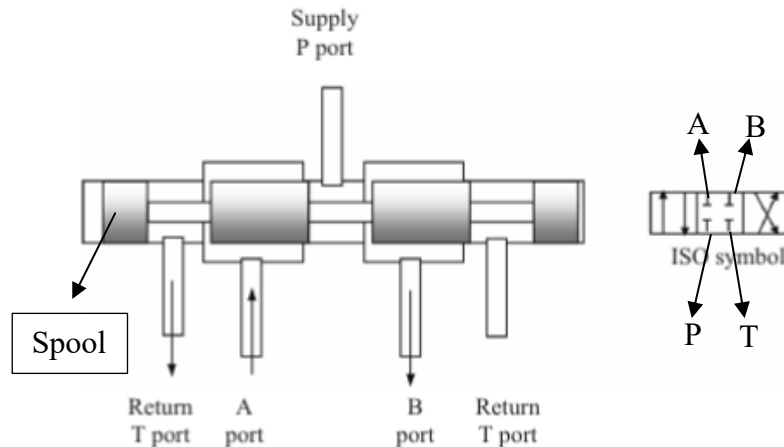


Figure 26: 4/3 direction control valve (DCV) [25]

Proportional electrohydraulic DCV produces an electric signal which helps in actuating the spool movement. The accuracy and resolution of the proportional valves are high and they can be used for a range of applications [25]. Figure 27 shows the electrically actuated proportional DCV.

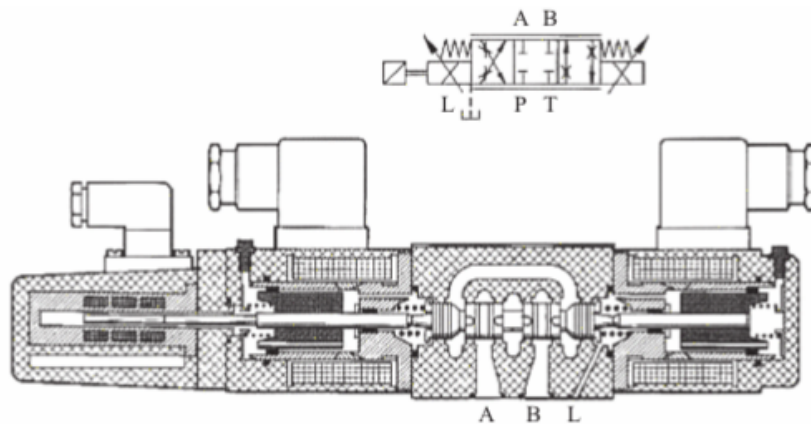


Figure 27: 4/3 proportional DCV [25]

The Simulink block diagram representation of the DCV in this project is according to [26], the following steps are involved in block diagram modelling 4/3 DCV:

1. Valve Dynamics: In the valve dynamics, the relative opening of the spool with respect to the control signal is defined.
2. Relative opening of valve flow area with respect to relative opening of the spool: In this part, the data of opening area of the valve with respect to relative position of the spool is defined.
3. Equations for volume flow rates of flow paths (modelling of orifice blocks): In this step the orifice equations are modelled using the Simulink blocks.
4. Summing up the orifice blocks: In this step, the modelled orifice blocks are connected together to form a 4/3 DCV.

4.1.1 Valve dynamics

Valve dynamics for proportional valves is one of the important characteristics of a closed-loop hydraulic system. Valve dynamics decides how fast the valve responds to the input signal. The frequency response of the valve is given by the manufacturer. A second-order transfer function is good enough for the valve model. The frequency response of valve changes with the amplitude of the input signal. The response time of the valve depends on the delay. Larger the delay slower is the response time. A saturation block is used in the model to restrict the system overshoot. Hysteresis is negligible with the servo valve [26] [27]. The values for second order delay, natural frequency and damping coefficient are taken from the manufacturer's catalogue. The block diagram representation of the valve dynamics is as seen Figure 28.

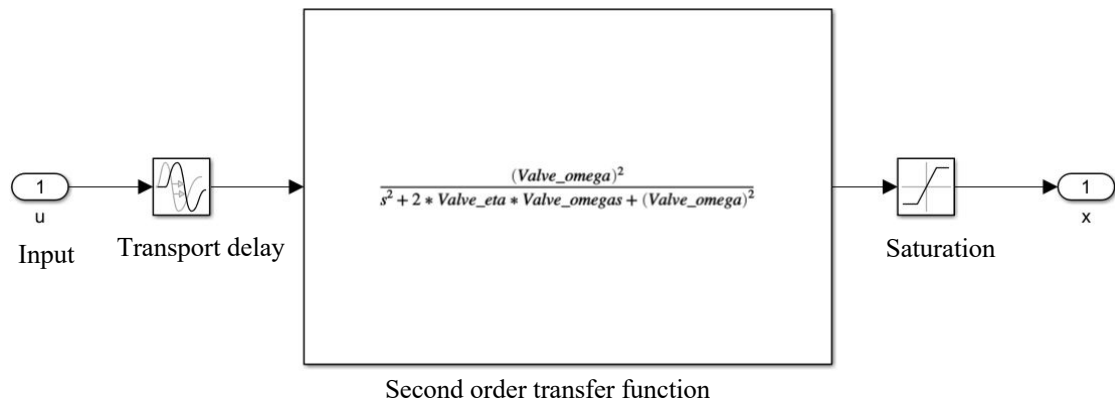


Figure 28: A Simulink block diagram of servo valve dynamics

4.1.2 Relative openings

The relative opening is a relation between the spool position and flow rate. The suppliers would normally provide the data which defines the relation between spool position and flow rate. Sometimes measurements are needed or some adjustments are done with respect to the behavior of the system [26].

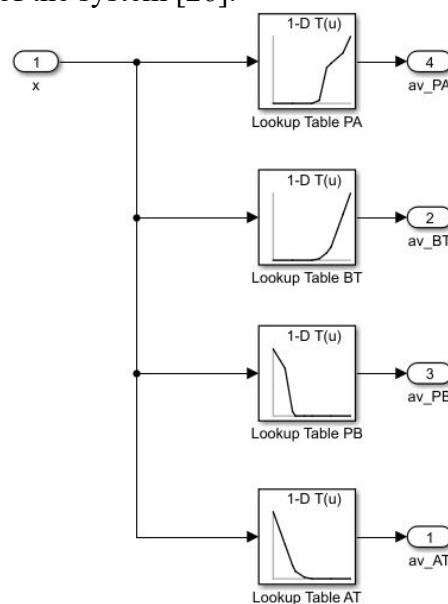


Figure 29: A Simulink block diagram of Relative openings of the valve

Figure 29 shows the relative opening of the proportional hydraulic valve. It is seen from Figure 29 that, PA and PB shows a gradually increasing exponential curve and BT and AT shows a gradually decreasing curve. The flow rate to the PA side is divided by the maximum flow of the PA side, thereby setting the maximum limit to unity. Similarly, this process is continued for BT, PB and AT.

In this project, the hydraulic valve is selected from Bosch Rexroth. The model of the valve selected is 4WRA series. The data of the flow rate and the spool position is obtained from Figure 30. The input signal U_s is divided by 10 V, to obtain a range from (-1 to 1).

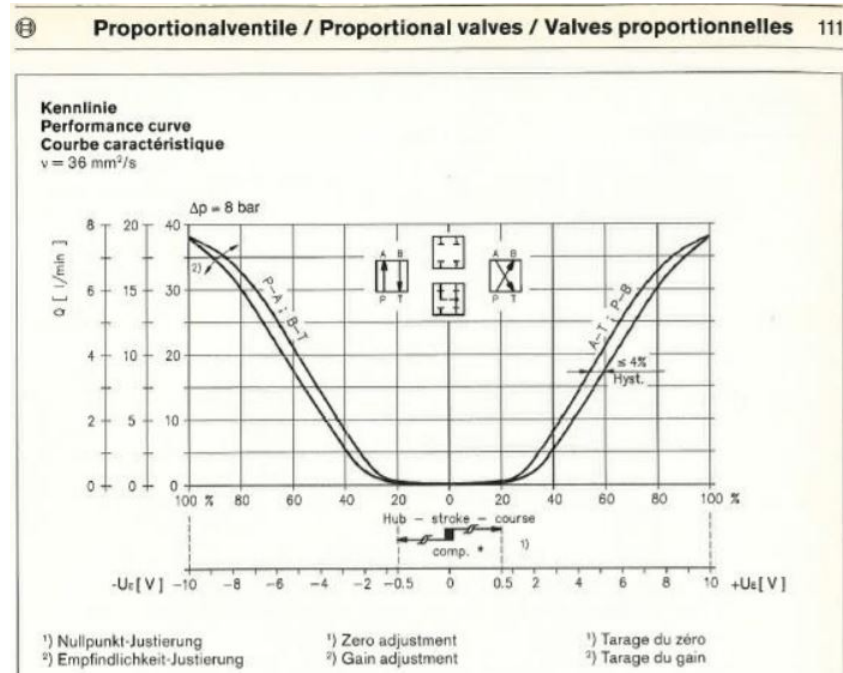


Figure 30: Flow vs Input signal (Bosch Rexroth 4WRA) [28].

4.1.3 Orifice modelling

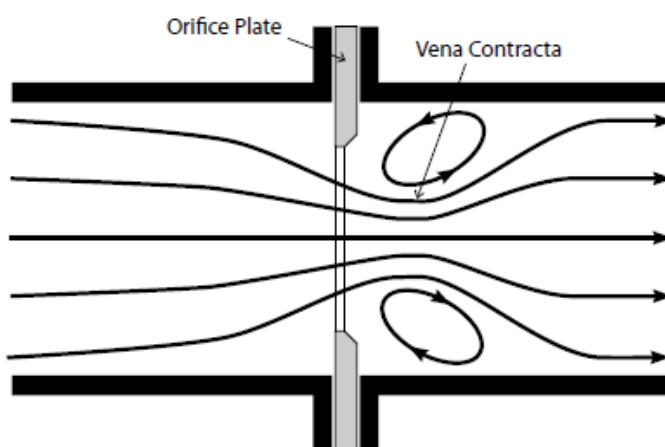


Figure 31: Layout of an orifice [29].

An orifice is a small section in a flow path of a fluid, wherein the cross-sectional area is smaller than the area of the cross-section of the path seen in Figure 31 [30]. For several geometries of the orifice, the empirical formula is derived according to [31] and [26], seen in Equation 4.1. Where, Q is the flow rate through the orifice, C_q is the flow coefficient, A is the area of the cross-section of an orifice, p_1 is the pressure before the orifice and p_2 is the pressure after the orifice and ρ is the fluid mass density.

$$Q = C_q A \sqrt{\frac{2(p_1 - p_2)}{\rho}} \quad (4.1)$$

In the modelling of an orifice, to enable the volume flow on both the directions Equation 4.2 is modified [31] [26].

$$Q = K_v \cdot \text{sgn}(p_1 - p_2) \cdot \sqrt{|p_1 - p_2|} \quad (4.2)$$

Where, $K_v = C_q \cdot A$

Equations 4.1 and 4.2 are not a good fit for the numerical simulations as the simulation program terminates when the pressure gets to zero value or the solver becomes stiff [31]. To solve this issue the square root equation is replaced in situations where the pressure differences become too small. The modified equations are as seen in Equation 4.3 [31] [26].

$$Q = \begin{cases} K_v \cdot \text{sgn}(p_1 - p_2) \cdot \sqrt{|p_1 - p_2|}, & |p_1 - p_2| > p_{tr} \\ \frac{K_v(p_1 - p_2)}{2\sqrt{p_{tr}}} \left(3 - \frac{|p_1 - p_2|}{p_{tr}} \right), & |p_1 - p_2| \leq p_{tr} \end{cases} \quad (4.3)$$

The transition pressure (p_{tr}) is selected on the basis of Reynold's number or it is assumed to be 0.5 % of the maximum pressure. If the value of the transition pressure is too small then the simulation slows down and if the value is too big the simulation generates error [26] [31]. In the simulation model, the inputs are pressure and the outputs are volume flow rates. Figure 32 shows the orifice model used for simulation and Figure 33 is the subsystem of the orifice block.

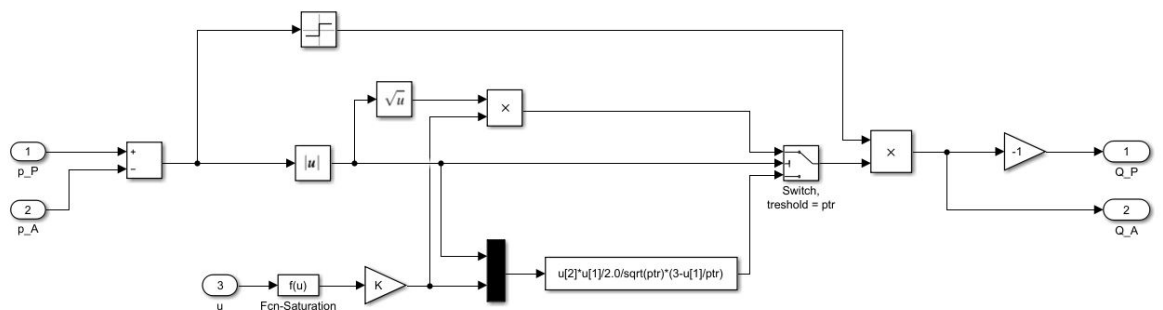


Figure 32: Simulink block diagram of an orifice

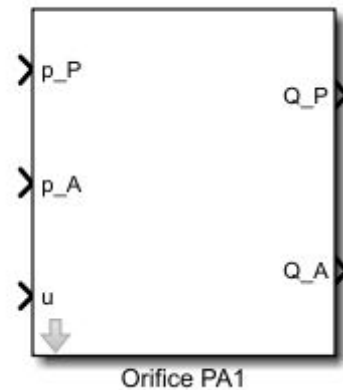


Figure 33: Subsystem of orifice block

4.1.4 Flow paths

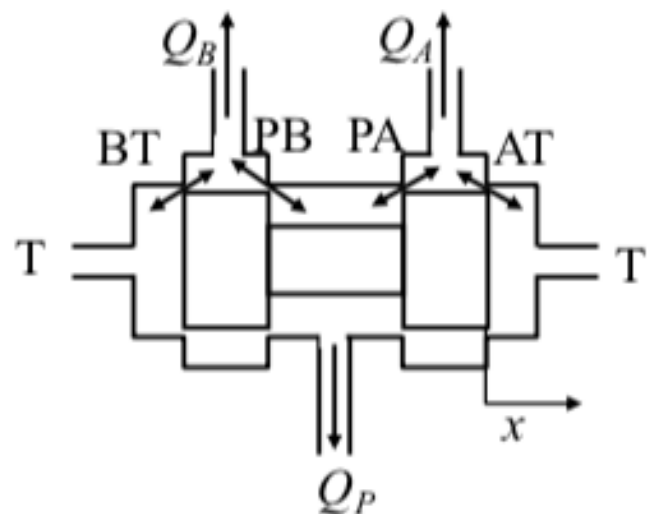


Figure 34: Flow paths in a 4/3 valve [26]

The flow paths in the 4/3 valve are PA, PB, BT and AT as seen in Figure 34. These flow paths are modeled by connecting four orifices together. An orifice is assigned to each path namely orifice PA, orifice BT, orifice PB and orifice AT. The inputs for these orifices are from the relative openings block. The supply line is connected to PA and PB side. The tank side is connected to paths AT and BT. In Figure 35, it can be seen that the signal to the orifice (u) is the derived output from the relative opening block. The output of the flow path is the volume flow rate. The flowrate on the A side of the valve is the sum of the flow from the PA and AT side. Similarly, for the B side, P side and T side of the valve. The flow paths are connected as seen in Figure 35 [26].

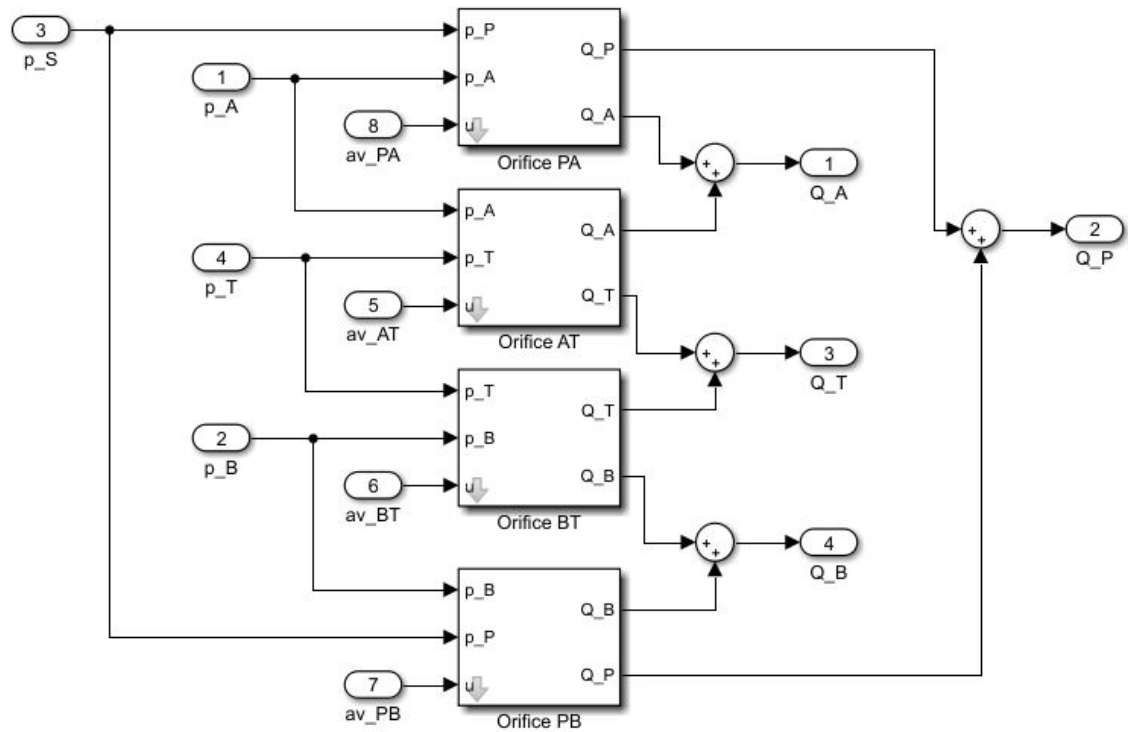


Figure 35: A Simulink block diagram representation of flow paths in 4/3 valve

4.1.5 Simulink block diagram representation of 4/3 valve

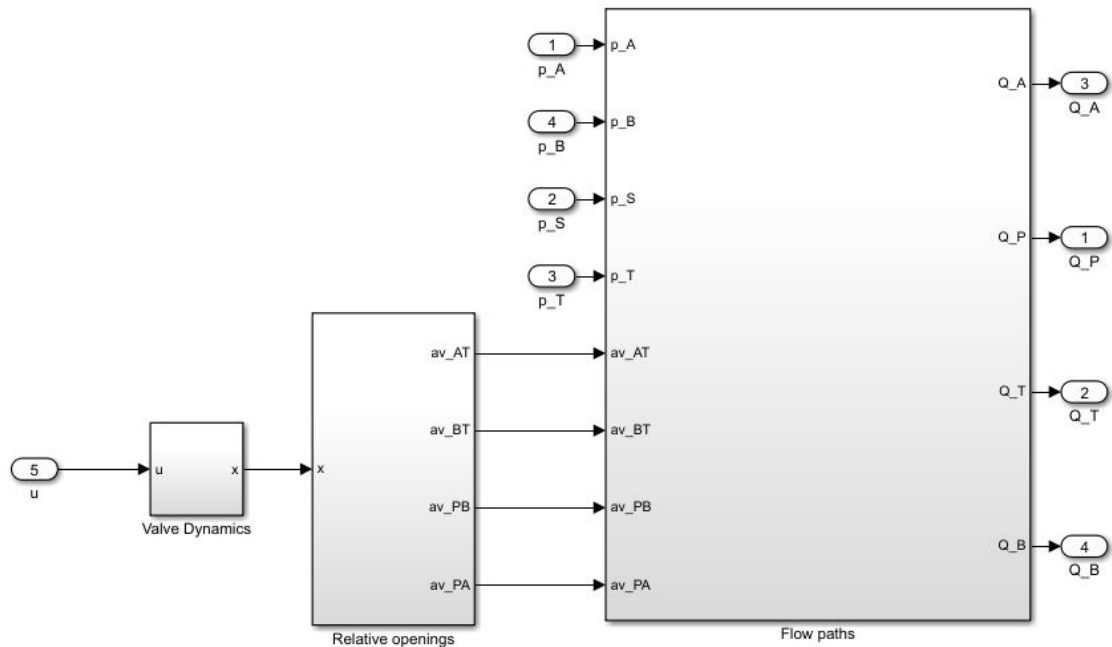


Figure 36: A Simulink block diagram representation 4/3 valve

Figure 36 shows the 4/3 valve's block diagram. It is the combination of valve dynamics, relative openings and flow paths models as seen in Figure 36. In brief, the valve dynamics takes the input from the system and generates corresponding value for the spool position.

For the obtained spool position value, the opening area is calculated. Then the relative opening values are the inputs to the flow path subsystem. In the flow path subsystem, the values for flowrate on A side and B side are calculated. Further, these flowrates are input to the cylinder model.

4.2 Modelling of hydraulic cylinder

Hydraulic cylinder works on the principle of Pascal's law, which states that pressure exerted at any point on an enclosed liquid is transmitted undiminished in all directions to the walls of the container [32]. Therefore, the pressurized liquid from the pump reaches the directional control valve and the valve routes the pressurized liquid to the cylinder chamber. As the pressurized fluid reaches the cylinder chamber it transmits the pressure on the walls of the piston which causes piston movement. The movement of the piston is guided through the directional control valve. This is the working principle of the hydraulic actuator.

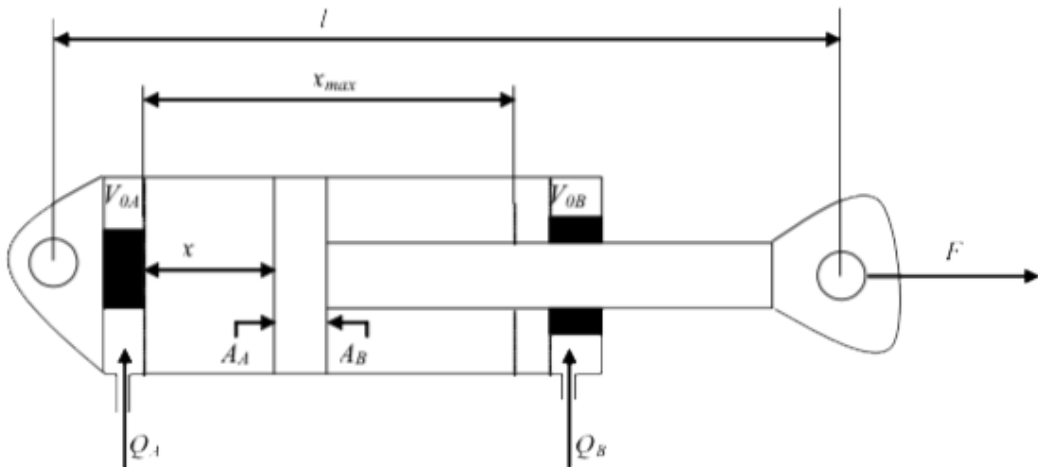


Figure 37: Schematic diagram of hydraulic cylinder [26]

The hydraulic actuator consists of 2 chambers namely A and B as shown in Figure 37. The Simulink block diagram of the hydraulic cylinder is modelled based on the following equations [26] :

To model the volume of chamber A. Following variables are assigned. V_A is the volume of chamber A, A_A is the area of chamber A, x is the piston position and V_{0A} is the dead volume of chamber A.

$$V_A = A_A \cdot x + V_{0A} \quad (4.4)$$

As the volume changes with respect to time, Equation 4.4 is differentiated with respect to time.

$$\frac{dV_A}{dt} = A_A \cdot \frac{dx}{dt} \quad (4.5)$$

Similarly, V_B is volume of chamber B, A_B is the area of chamber B, x is the piston position, x_{\max} is the maximum stroke and V_{0B} is the dead volume of chamber B.

Now calculating volume for chamber B:

$$V_B = A_B(x_{max} - x) + V_{0B} \quad (4.6)$$

As the volume changes with respect to time, Equation 4.6 is differentiated with respect to time.

$$\frac{dV_B}{dt} = -A_B \cdot \frac{dx}{dt} \quad (4.7)$$

Therefore, the force generated by the hydraulic cylinder is calculated as seen in Equation 4.8

$$F_{cyl} = A_A \cdot p_A - A_B \cdot p_B - F_\mu \quad (4.8)$$

Where F_{cyl} is the force generated by hydraulic cylinder, p_A and p_B is pressure in chamber A and B and F_μ is the viscous friction.

Viscous friction is calculated by:

$$F_\mu = b \cdot \frac{dx}{dt} \quad (4.9)$$

Where b is the viscous friction coefficient. The value of 'b' is taken as 2000 in the simulation.

In the hydraulic system, there are two double-sided piston cylinders. All the equations to model the double-sided piston cylinder remains to be the same, except for the equation to calculate the area of the chamber.

For a single-sided piston cylinder shown in Figure 38, the chamber area calculated is seen in Equation 4.10 and 4.11

$$A_A = \frac{\pi}{4} \cdot D^2 \quad (4.10)$$

$$A_B = \frac{\pi}{4} \cdot (D^2 - d^2) \quad (4.11)$$

The equation to calculate chamber area for the double-sided piston cylinder is:

$$A_A = \frac{\pi}{4} \cdot (D^2 - d^2) \quad (4.12)$$

$$A_B = \frac{\pi}{4} \cdot (D^2 - d^2) \quad (4.13)$$

Where 'D' is the piston diameter of A-side chamber and 'd' is the piston rod diameter of the B-side chamber. Figure 38 below shows the Simulink block diagram of a cylinder for simulation.

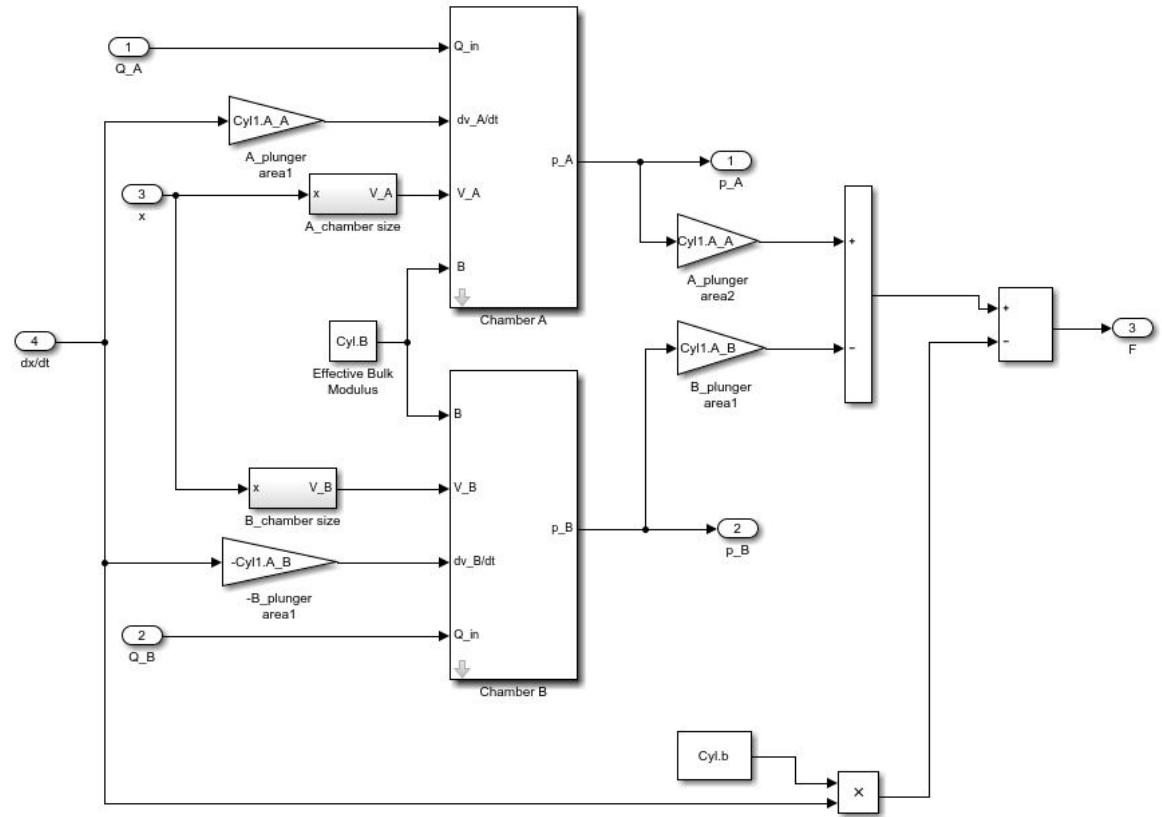


Figure 38: A Simulink block diagram representation of hydraulic cylinder

4.3 Integration of DCV and cylinder to the hydraulic system

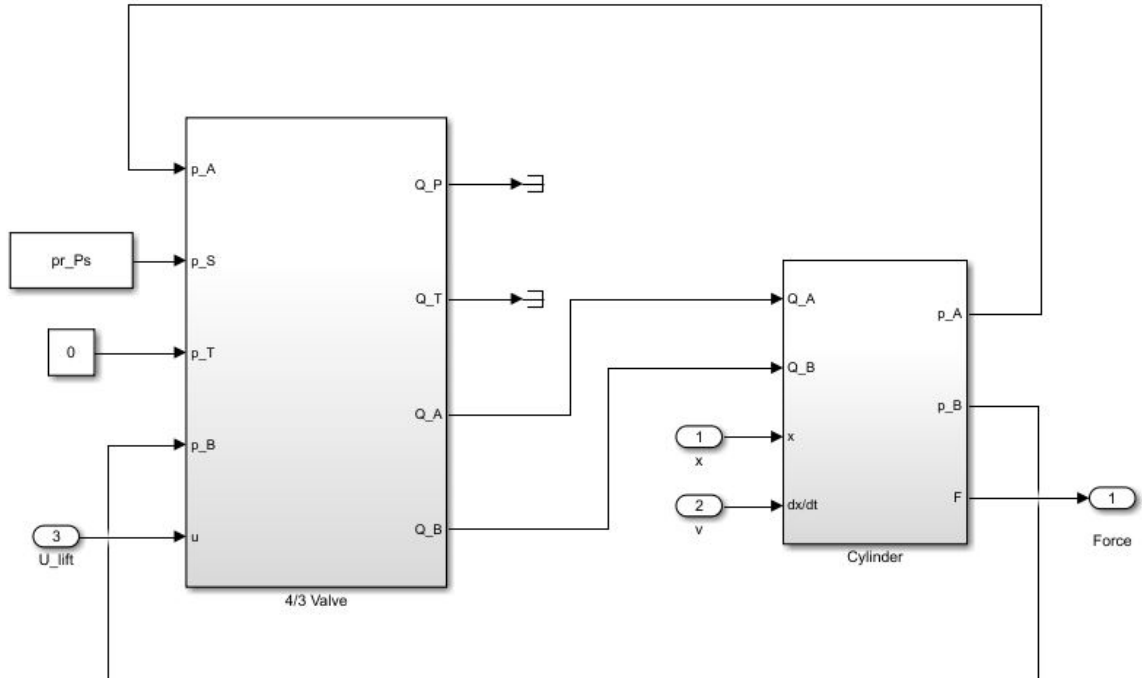


Figure 39: A Simulink block diagram representation of hydraulic system

The hydraulic system for the simulation as shown in Figure 39, is the combination of 4/3 valve and cylinder model. The hydraulic boom has three actuators. Hence, there are three 4/3 DCV's connected to three cylinders independent of each other. In Figure 40, it can be seen that three cylinders and the respective DCV's are connected independently of each other. The output of the hydraulic system is the force, this hydraulic force is input to the SIMSCAPE mechanism in the simulation.

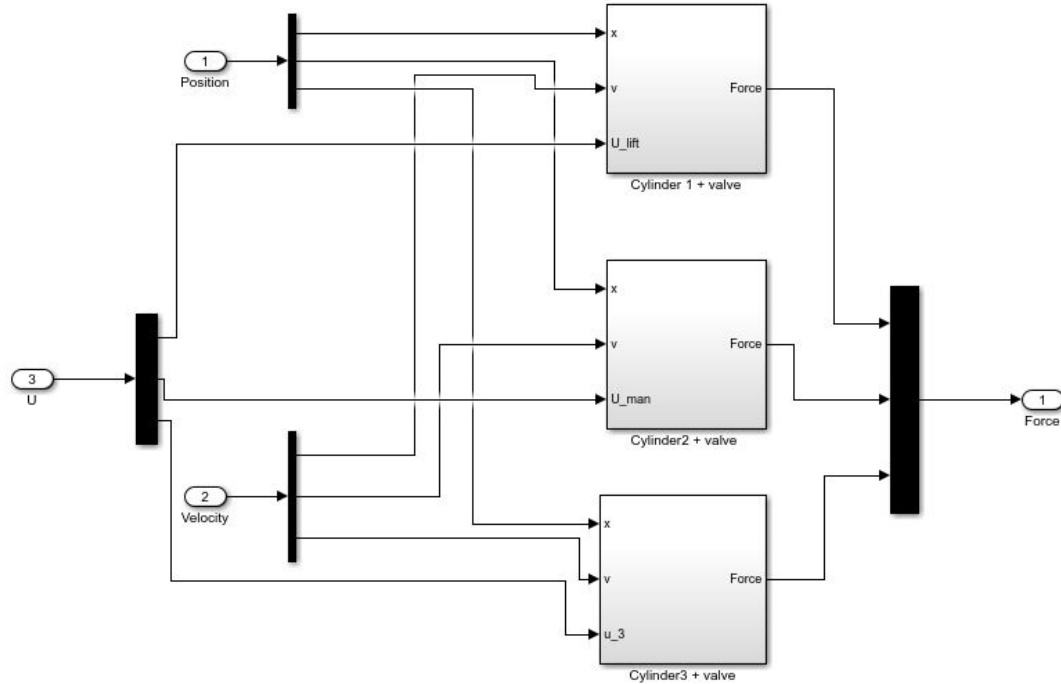


Figure 40: A Simulink block diagram representation of 3 cylinders and 3 DCV's connected

4.4 Modelling and Simulation of a physical system of hydraulic boom

SIMSCAPE is tool which provides multibody simulation in a 3D environment. A multi-body assembly can be built by assembling the blocks representing sensors, joints, constraints and force elements. The equations of motion of a system can be formulated and solved using this tool. In addition, the CAD assemblies can be imported including all the design parameters like mass, inertia and joint constraints. Using SIMSCAPE, the dynamic behavior of the system can be visualized which helps in development of the control system [33].

In this project, the preliminary mechanical assembly of the hydraulic boom is converted to the SIMSCAPE model using a plug-in from SOLIDWORKS software. SIMSCAPE model consists of cylinder joints to which force is an input. The dynamic behavior of the system can be visualized in 3D environment. Another added advantage is the use of SIMSCAPE sensors for obtaining the feedback to the control system. Angular feedback from the revolute joints and linear piston displacement feedback is used in this project.

Figure 41 shows a subsystem which involves in modelling of rack and pinion system using SIMSCAPE. To build a multibody assembly, reference frames need to be assigned for the rigid bodies. The position of these bodies in the 3D environment are defined by their reference frames. The movement of the rigid bodies are defined through the type of joints. For an instance, a revolute joint is used to connect the pinion and the base pillar of the boom. Further, the constraints like rack and pinion constraint can be defined between two rigid bodies for rack and pinion action. The geometry and other mechanical properties of the rigid body are defined using solid blocks in SIMSCAPE. Similarly, the entire boom mechanism can be defined in SIMSCAPE. In Figure 42, the 3D visualization of the hydraulic boom in SIMSCAPE model explorer can be seen. The hydraulic system is connected to the SIMSCAPE model as in Figure 43.

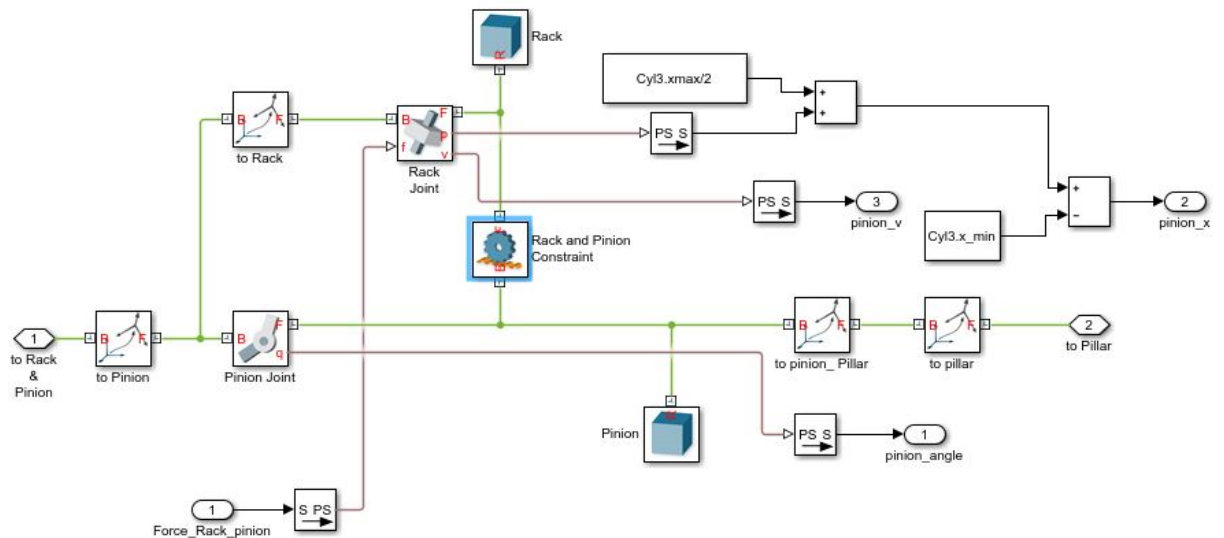


Figure 41: SIMSCAPE block diagram of Rack and Pinion

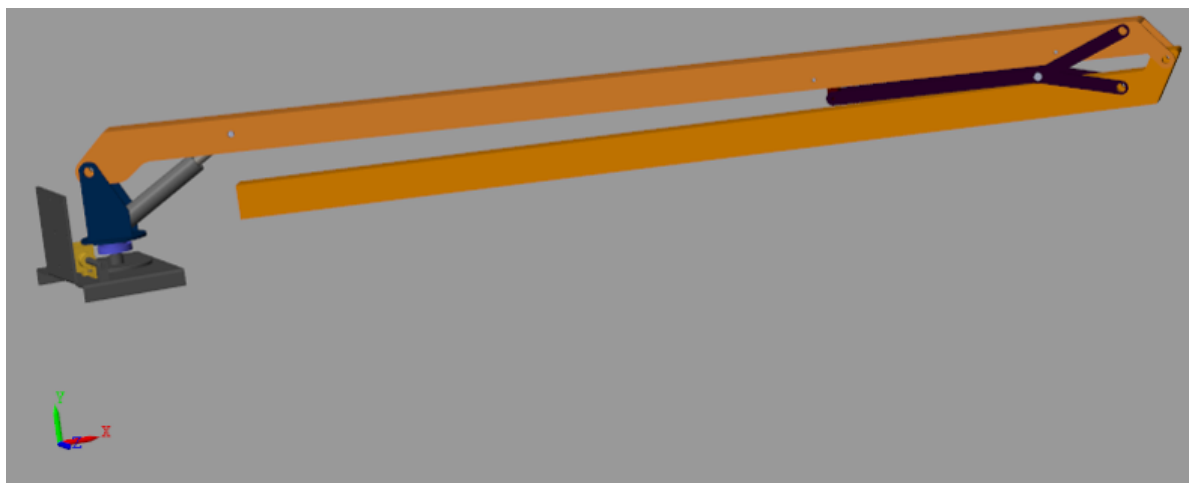


Figure 42: SIMSCAPE visualization of the boom

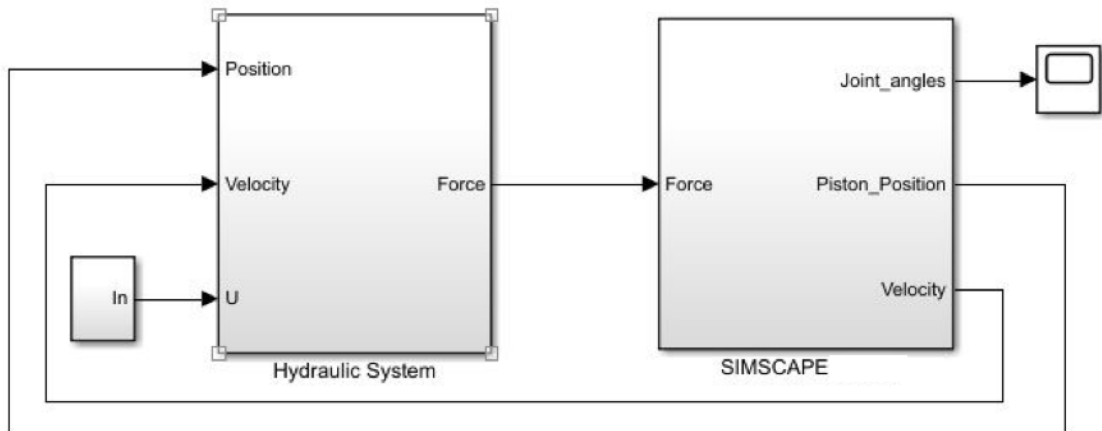


Figure 43: A Simulink block diagram representation of hydraulic system connect to SIMSCAPE block

4.5 Control System

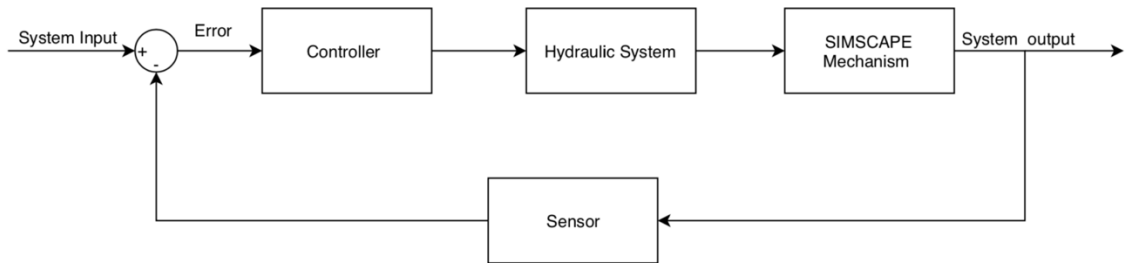


Figure 44: Initial control system scheme

A simple control scheme is implemented initially followed by the implementation of joint space control scheme. The Joint space control consists of an inverse kinematics program, which takes the input X and Y coordinates and gives an output joint angle.

After modelling the hydraulic system and SIMSCAPE blocks of the hydraulic boom, a controller and feedback system had to be implemented. Figure 44 above, shows a schematic diagram of a closed-loop control system, which is implemented in the project. In the closed loop control system, the output signal is measured by a sensor, also known as ‘feedback signal’. Closed loop control system is designed such that the desired output is maintained in comparison to the actual condition of the system. The error signal is generated by the difference between the output and the input signal [34].

In the simulation, a step input is provided as an input reference. PID (Proportional Integral Derivative) controller is used as it is robust in nature. The controller is connected to the proportional hydraulic valve in the hydraulic system. The hydraulic valve decides the amount of flowrate and direction of the flow into the hydraulic actuator. The hydraulic actuator transmits the force to the mechanism or the model. In this project, two types of feedback systems are used namely hydraulic cylinder position feedback and boom angle feedback. The feedback systems implemented will be studied in detail in Chapter 5. SIMSCAPE multibody program provides a tool wherein the linear displacement feedback of hydraulic cylinder and angular feedback of the boom can be estimated.

4.5.1 PID Controller

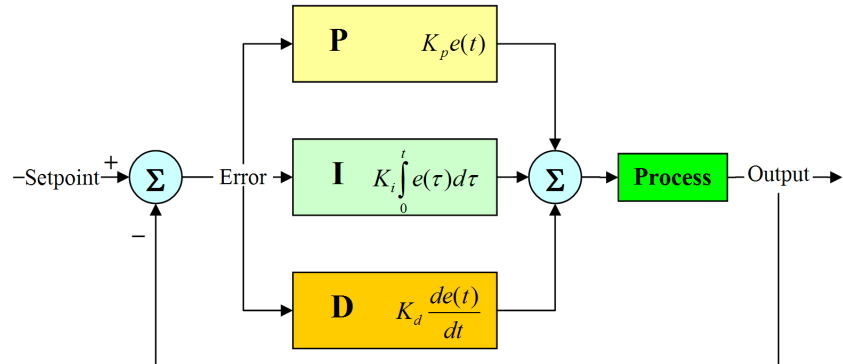


Figure 45: PID control [35]

PID controller one of the versatile controllers used for real-world applications. The control error signal (e) is generated by the difference of the output and input reference as seen in Figure 45. PID controller involves three parameters namely Proportional, Integral, and Derivative. The proportional parameter produces a signal which is proportional to the control error, the integral parameter produces a signal using a low-frequency compensation technique through an integrator which reduces the steady state errors and derivative parameter produces a signal using a high-frequency compensation technique through a differentiator and improves the transient response of the system [9]. The output of the PID controller can be calculated as follows [36]:

$$u(t) = K_p e(t) + K_i \int e(t) dt + K_d \frac{de}{dt} \quad (4.14)$$

Where $u(t)$ is the output from the PID controller, K_p is proportional gain, K_i is integral gain and K_d is the derivative gain. These gain values are tuned by trial and error method. Initially, proportional gain is increased such that there is a small overshoot in the system, then other gains (K_i & K_d) are tuned to make the system work with less oscillations. Figure 46 below shows the PID controller used in the simulation. There are three 4/3 direction control valves used in the project. Therefore, there are three PID controllers for three 4/3 DCV's respectively. The gain values for the PID controller are shown in Table 3. Figure 47 shows the Simulink block diagram of the boom with PID controller and cylinder stroke as the feedback.

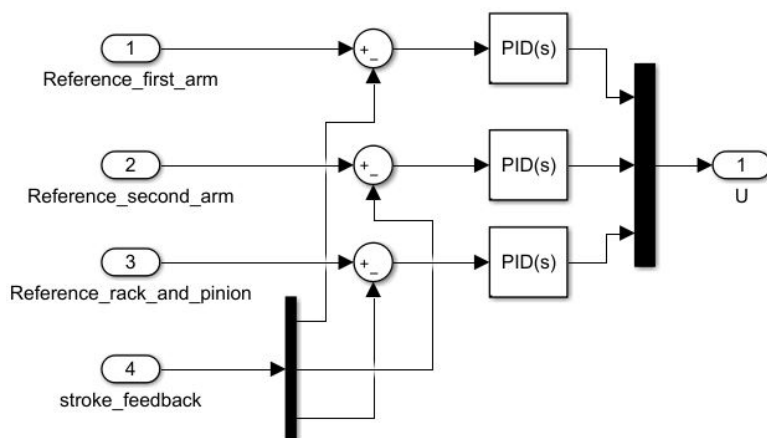


Figure 46: PID controller used in simulation

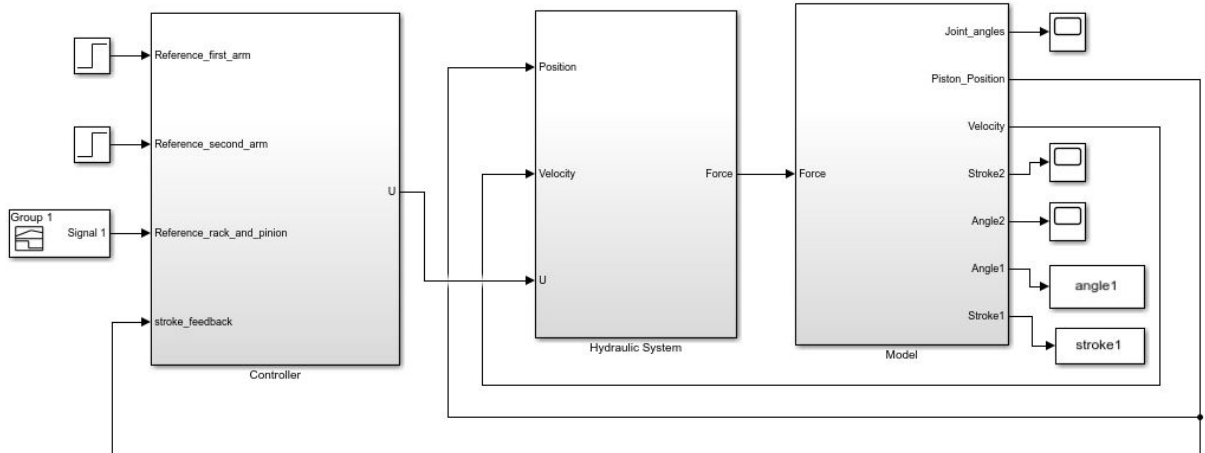


Figure 47: A Simulink block diagram of the hydraulic system with controller.

4.5.2 Cylinder stroke feedback

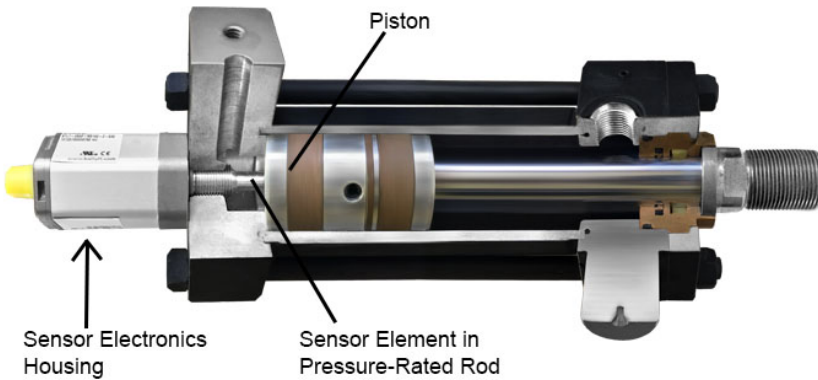


Figure 48: Hydraulic cylinder assembled with sensor [37]

Position sensors are used in the hydraulic cylinders for stroke feedback as seen in Figure 48. These sensors provide a feedback signal to the controller. These sensors can be internally or externally mounted in hydraulic cylinders. Nowadays, the hydraulic cylinders are usually assembled with the position sensors. Linear Variable-Displacement Transformer (LVDT) is most commonly used in the fluid power industry. LVDT is the most accurate position sensor. The linear displacement of the piston is converted to analog electrical output [38]. The idea of cylinder stroke feedback was according to the work done in [39].

The advantages of using a position feedback for the system:

- Responses from the controller are good.
- Cost effective method
- It is compact, as some hydraulic cylinders are assembled with linear displacement sensors
- It is rugged and can be used in harsh environments as the sensor element is protected inside the cylinder.

The disadvantages of using position feedback system:

- The relation between cylinder stroke and boom angle had to be formulated when the joint control scheme was implemented. This involved in finding complex geometrical equations. Due to these geometrical relations the simulation model becomes stiff. Further, there is error in position of end effector as the frames of defining the SIMSCAPE model are not accurately defined.
- Execution time is slow compared to boom angle feedback.
- It is complex to mount the sensors in the hydraulic cylinder.

4.5.3 Boom angle feedback



Figure 49: Incremental encoder from BEI sensors [40]

Incremental encoders are usually used as angular sensors in the hydraulic boom [41] [42]. These encoders can be used for sensing the position of the arms with respect to each other. Incremental encoders generate electrical pulses when the encoder shaft is rotating. The angular position of the boom is proportional to the electrical pulses emitted by the encoder. Incremental rotary encoders use a disc which consists of transparent and opaque sections which are equally spaced. A light emitting diode is used to pass the light through the disc and the light is detected by photo detector. Therefore, this detector generates a sequence of electrical pulses. The position can be measured by the number of pulses per revolution [43]. To acquire the data from the encoder, a dSPACE system with circuit boards DS1103, DS2001 and DS2004 can be utilized [41]. Encoders with water resistant rating of IP69K are available in the market. One of such encoders is BEI sensors DXM5s as seen in Figure 49 [40].

The advantages of boom angle feedback:

- The inverse kinematics program can be directly linked as input reference to the system. When the stroke feedback was used complex geometrical relations between the boom angle and stroke had to be formulated.
- Easy to mount in the hydraulic boom.

The disadvantages of using boom angle feedback

- Water resistant encoder has to be used. The encoders are subjected to marine time environment. In the stroke feedback, the sensors are usually assembled inside the cylinder therefore, there would not be any damage to the sensor.

4.6 Controller testing

In the offshore conditions, there are several disturbances like ocean waves and wind which are main factors for the inaccuracy for the end effector positioning. To overcome this issue, the controller has to be tuned in such a way that, it is capable to take those disturbances into account.

In the offshore there are several kinds of offshore waves namely, ripples, sea waves, swell and tsunamis. The time period of ripples is less than 0.2 seconds, for sea waves it ranges from 0.2 to 9 seconds and for swell it ranges from 9 to 30 seconds time period [44]. Therefore, in the simulation, the disturbance of a sine wave with the frequency in the range of 0.2 to 31 rad/s is added to the system. Further, the noise in the feedback is also considered. Figure 50 shows the control closed loop system with the addition of disturbance and noise.

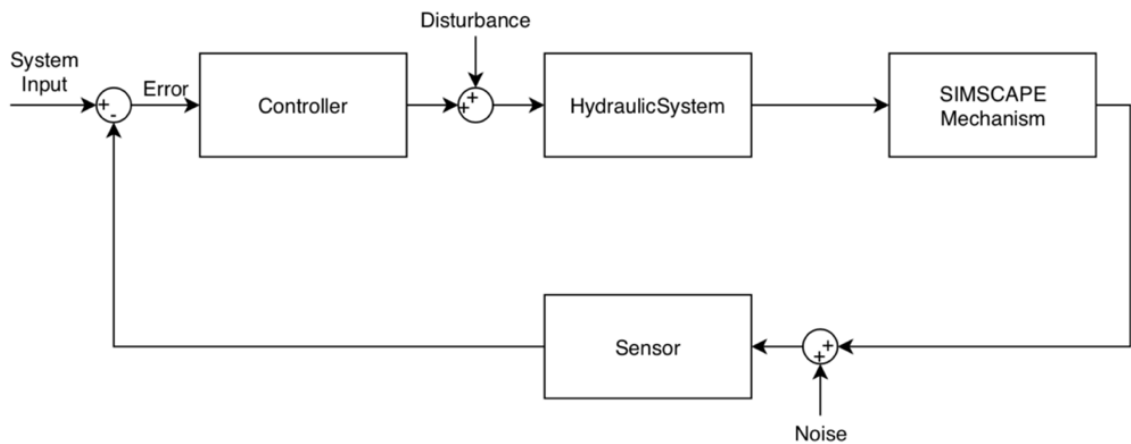


Figure 50: Closed loop system with disturbance and noise

5 DYNAMIC BEHAVIOUR ANALYSIS OF THE HYDRAULIC BOOM

Simulation is nothing but an imitation of a real-world system or virtual representation of a real-world system behavior. By performing the simulations, the system behavior under various conditions can be estimated without actually building a prototype thereby saving the cost of building a prototype.

In this project, MATLAB/SIMULINK/SIMSCAPE is used for the simulation. The hydraulic system is modelled using SIMULINK and the mechanical assembly of the manipulator is built in SIMSCAPE. A variable step simulation is conducted in this project and ode45 (Dormand-Prince) is used as a solver. The system is tested with various feedback namely cylinder stroke feedback and boom angle feedback. PID controller is tested along with the disturbance from sea waves and noise in the sensor. This simulation can be used to program the hydraulic system in real-time.

5.1 Cylinder stroke feedback

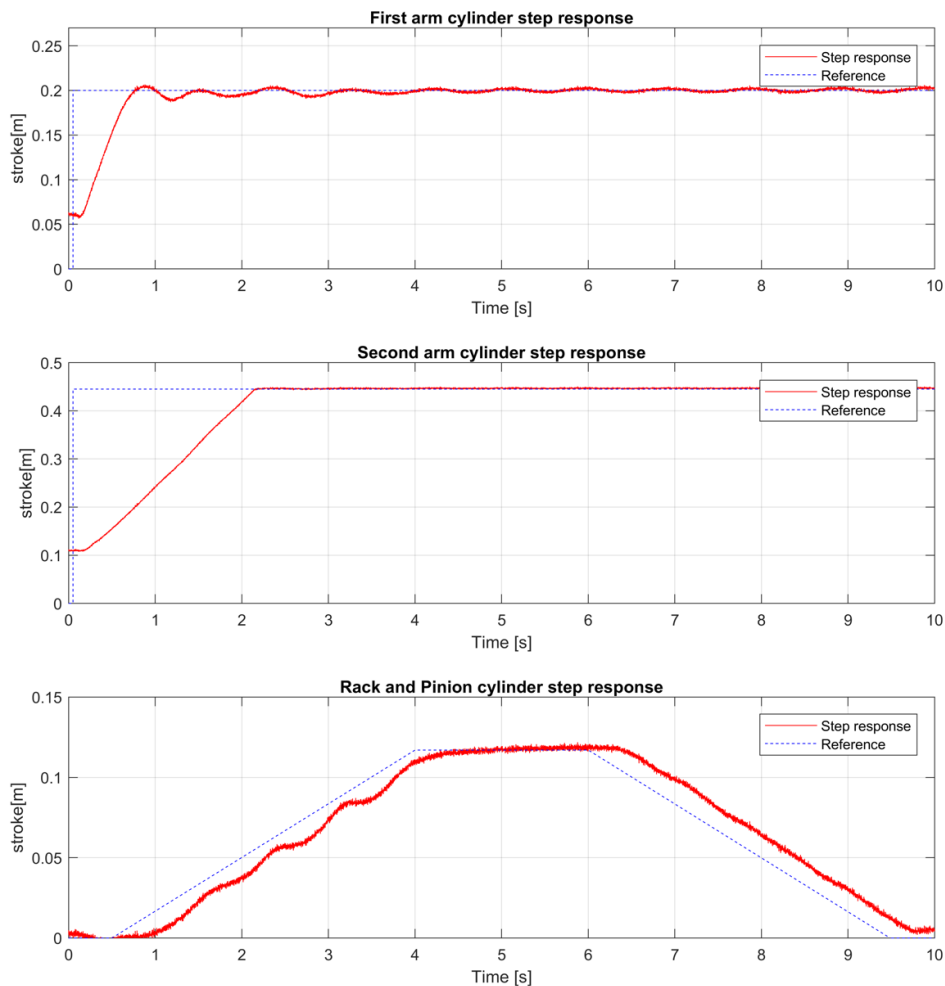


Figure 51: Step response of cylinder 1,2 and 3 with cylinder stroke as feedback and disturbance (sine wave of 31rad/s frequency)

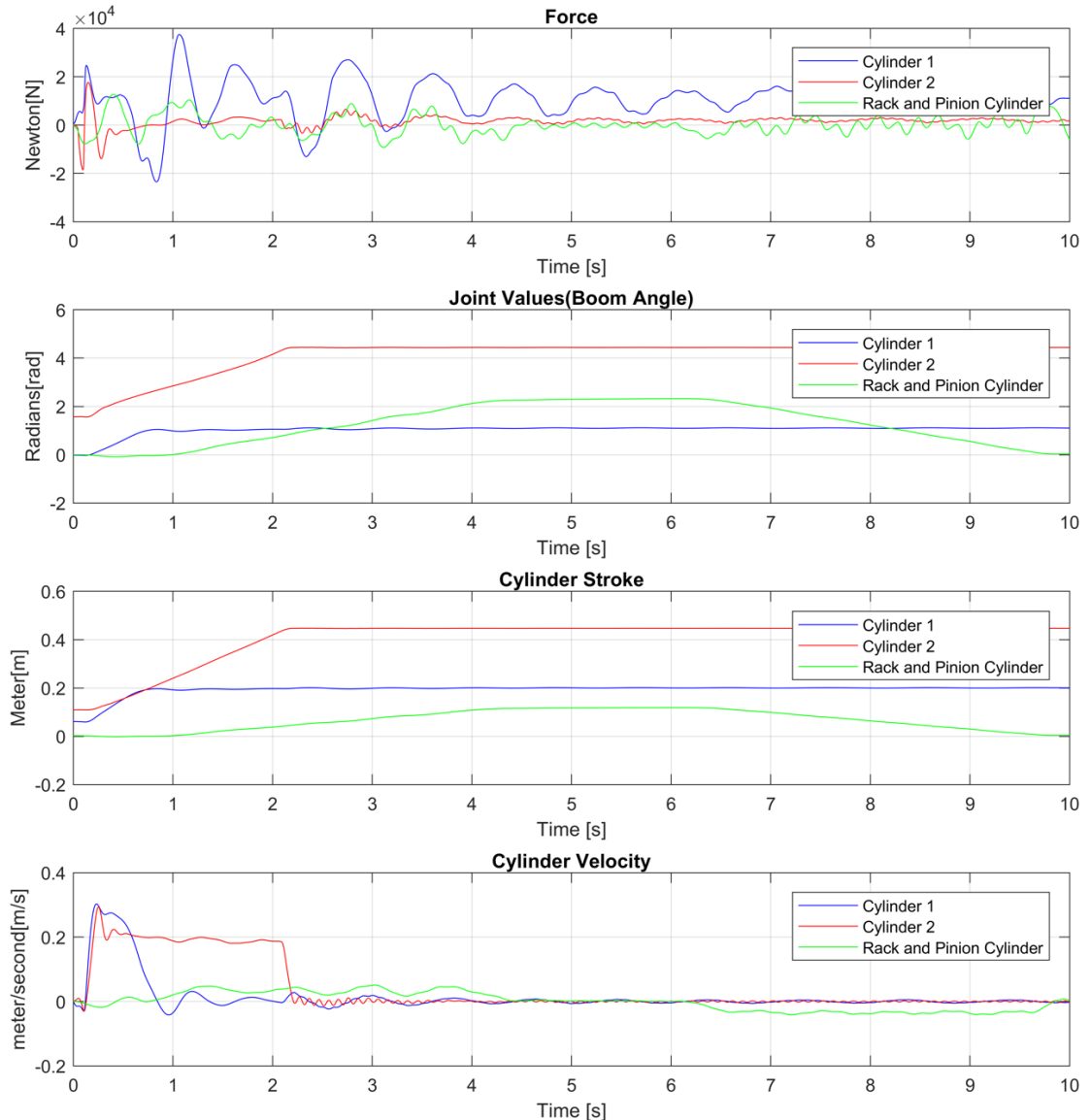


Figure 52: Force, Boom angle, Cylinder stroke and Piston Velocity vs Simulation time (10 seconds) for stroke feedback

The simulation is performed under conditions where the hydraulic boom is subjected to disturbances, payload, and noise in the feedback line. As discussed in Section 4.6, the system is subjected to different types of waves in the offshore. Therefore, to imitate this real-world condition, a sine wave is added as a disturbance to the system and the system behavior is predicted in the range of 0.7 rad/s and 31 rad/s frequency. The total weight of the hydraulic boom is 73.44 kg, then a payload of 100 kg at a span of 3 m and 30 kg and at the end of the boom is accounted in the simulation. For generating the noise in the feedback line, a SIMULINK block of Band-Limited White Noise is used with a sample time of 0.001 seconds. SIMSCAPE model is acting under earth gravity of 9.81 m/s in negative Y-direction.

The feedback used here is stroke feedback therefore, the input reference has to be cylinder stroke. The input reference for each of the hydraulic cylinders is a step input with an initial value as minimum stroke and final value as maximum stroke of the cylinder. The

step time is 0.05 seconds. In Figure 51, the step response of all the cylinders are seen. A sine wave disturbance of 31 rad/s frequency is used. It can be noticed that the controller is tracking the input reference quite good. But there are some oscillations observed in the first cylinder's step response as the proportional gain (K_p) is increased so that the system can have better response time. The response from the first cylinder can be made better if the proportional gain is reduced and system is underdamped. In this application, the response time is given more preference over oscillations in the system as the boom has to reach the required position in a very quick time for immediate retrieval of UAV or AUV. In Figure 52, the force generated by each of cylinder, joint values of the boom, stroke of cylinder and piston velocity is plotted over the simulation time. This can represent the behavior of each subsystem of the hydraulic boom.

Figure 53 shows the response of the system when it is subjected to a huge ocean wave of time period 9 seconds. As the time period of the ocean wave is high and frequency is less, it can be noticed that after 6th second of simulation time the oscillations are high, and controller deviates a little bit from the reference and again it tracks the reference immediately. As the error is not substantially high, it can be concluded that the controller is good.

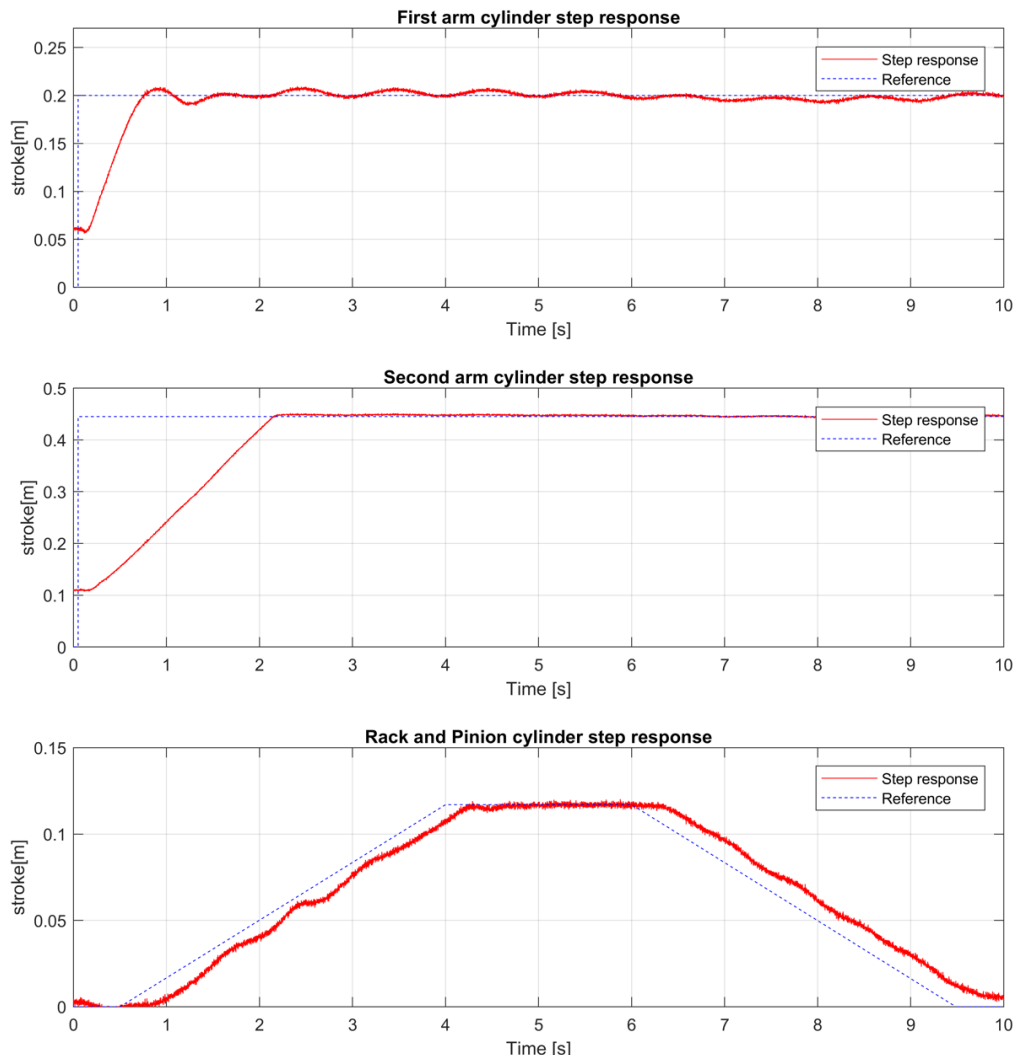


Figure 53: Step response of cylinder 1,2 and 3 with cylinder stroke as feedback and disturbance (sine wave of 0.7 rad/s frequency)

5.2 Boom angle feedback

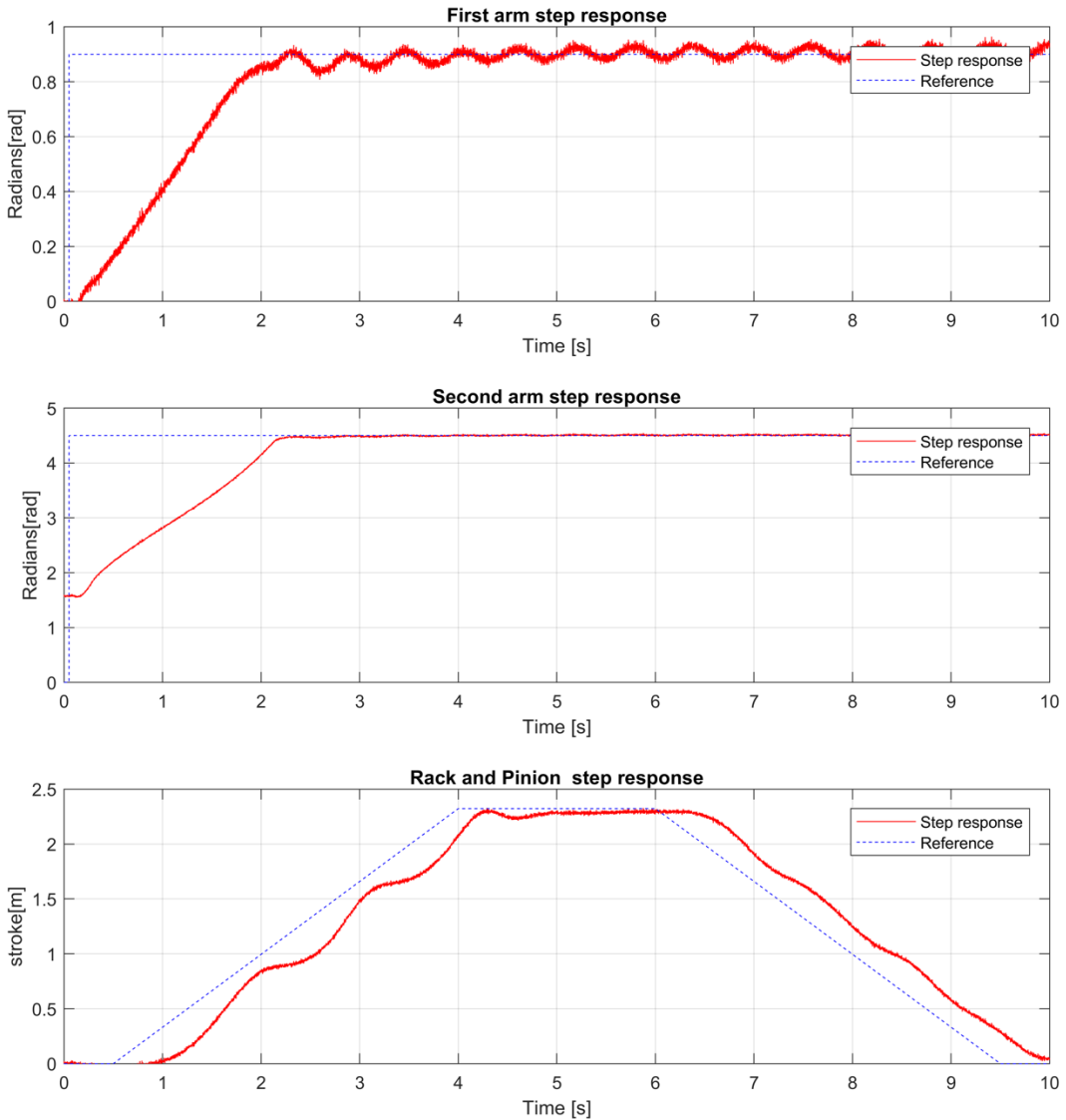


Figure 54: Step response of cylinder 1,2 and 3 with cylinder boom angle as feedback and disturbance (sine wave of 31rad/s frequency)

This simulation is performed under conditions where the hydraulic boom is subjected to disturbances, payload, and noise in the feedback line. The system is subjected to different types of waves in the offshore. Now to imitate this condition, a sine wave is added as a disturbance to the system and the system behavior predicted in the range of 0.7 rad/s and 31 rad/s frequency. The total weight of the hydraulic boom is 73.44 kg. A payload of 100 kg at a span of 3 m and 30 kg and at the end of the boom is accounted in the simulation. SIMSCAPE model is acting under earth gravity of 9.81 m/s in negative Y-direction.

Boom angle (Joint Values) are used as a feedback therefore, the input reference to this system is joint values. In this simulation, the joints are moved from the transport position of the boom to the position where the cylinder stroke is maximum or the highest joint value the arms can reach. Therefore, the input reference to this system is a step input of initial value as the joint value in transport position and the final value is the maximum joint value of the arm with a step time of 0.05 seconds. In addition, the noise is generated in the feedback line with a SIMULINK block of Band-Limited White Noise with a sample

time of 0.001 seconds. Further, a sine wave of frequency 31 rad/s is added as a disturbance to the system. Usually, the surface vehicle is set to move on the water surface where ripples are more. In Chapter 4.6, the time period for ripples are less than 0.2 seconds, therefore, the frequency of waves is high. In Figure 54, the step response of the system under a sine wave of disturbance with a frequency of 31 rad/s is noticed. Further, there are oscillations observed in the step response for the first arm, this is due to an increase in proportional gain (K_p). The proportional gain is increased to increase the response time of the system. The response from the first arm can be made better if the proportional gain is reduced and the system is underdamped. In this application, the response time is given more preference over oscillations in the system as the boom has to reach the required position in a very quick time for immediate retrieval of UAV or AUV. As the step responses in Figure 54 appears to be good, the PID controller seems to work well.

In the Figure 55, the force generated by each of cylinders, joint values of the boom, stroke of cylinder and piston velocity is plotted over simulation time. This can represent the behavior of each subsystem of the hydraulic boom.

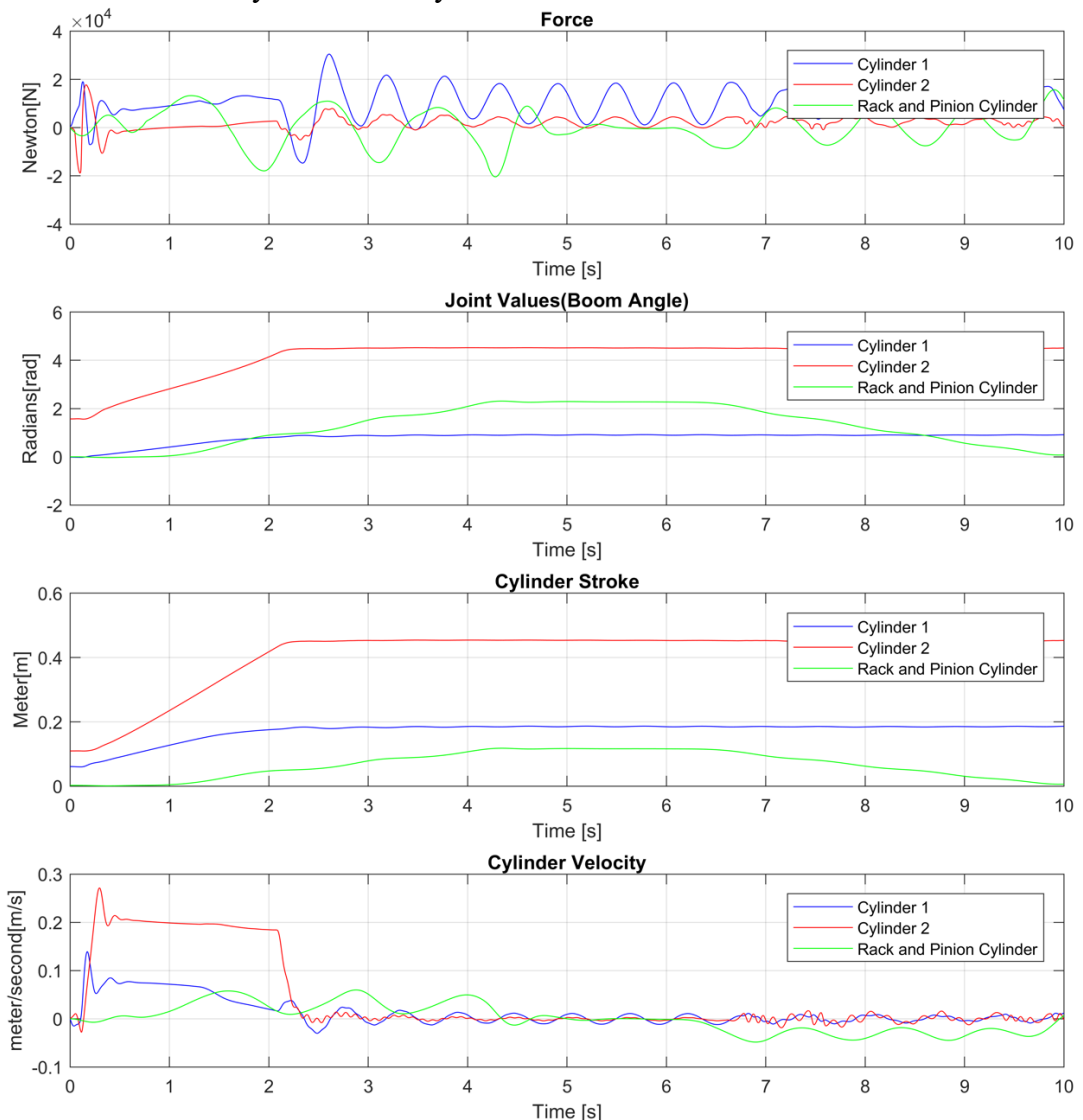


Figure 55: Force, Boom angle, Cylinder stroke and Piston Velocity vs Simulation time (10 seconds) for boom angle feedback

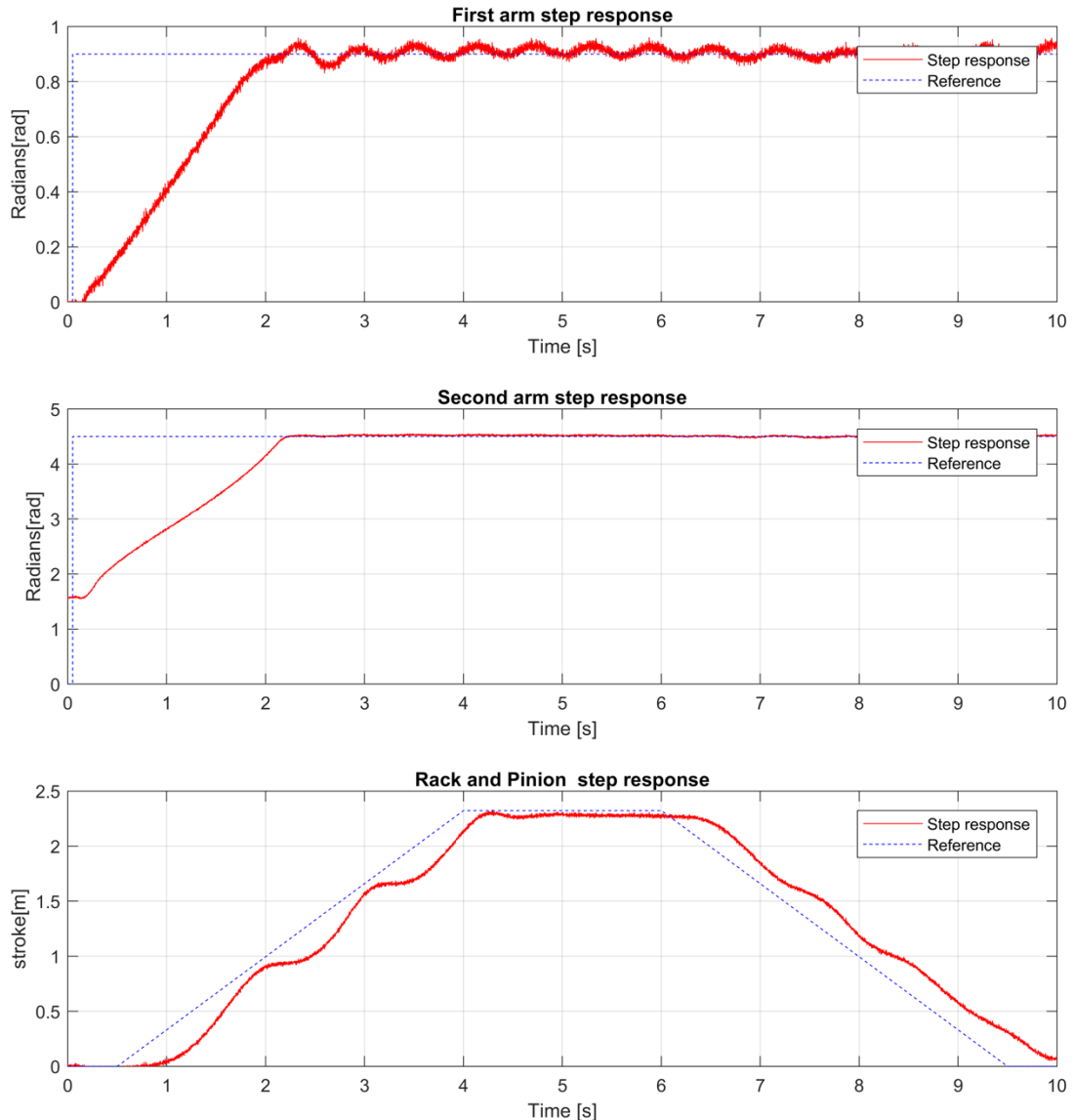


Figure 56: Step response of cylinder 1,2 and 3 with boom angle as feedback and disturbance (sine wave of 0.7 rad/s frequency)

Similar to the conditions in the stroke feedback, the system with the boom angle feedback is also subjected to a huge ocean wave of time period 9 seconds. In Figure 56, the response of the system is seen, when it is subjected to a huge ocean wave of time period 9 seconds. Comparing to the step responses in Figure 56 and 54, it can be noticed that the step responses remain to be the same. It can be concluded that the controller is working really well, and it is robust to the high or low ocean waves.

5.3 Comparison of stroke feedback and boom angle feedback

The simulations were performed for different feedback systems, these results play an important role in selecting what sensor should be used in the system. The linear displacement sensor is used when the cylinder stroke is used as feedback. An incremental encoder is used when the boom angle is feedback.

While comparing the step responses of stroke feedback and boom angle feedback, it is noticed that the step responses of stroke feedback are quite good, as the oscillations are

less. When the joint space control scheme is implemented, the stroke feedback becomes very complex as the system has to compute the cylinder stroke from the joint values given by the inverse kinematics program. This involves a lot of computational difficulties, thereby making the solver stiff. Further, if the relations between the joint values and stroke is not formulated properly, it could lead to position errors. The computational time taken to solve these geometrical relations between the boom angle and stroke is high. In future, this project aims to design an autonomous control of the hydraulic manipulator wherein kinematics of the manipulator plays an important role. Therefore, stroke feedback is not a feasible option when joint space control and autonomous control are implemented.

In the boom angle feedback, the step responses are good but, the response time to meet the setpoint is more compared to the stroke feedback. The oscillations in the responses are more compared to stroke feedback. Response time is an important factor in this project. If the proportional gain is increased further the system becomes unstable. With the boom angle feedback, the implementation of joint space control or autonomous control becomes easier and when the frequency of the disturbance is low or high the responses remains to be almost the same. With these two advantages, the boom angle feedback definitely has an edge over the stroke feedback. Hence, with this simulation study, it can be concluded that boom angle reference would be the feasible option in this project. The disadvantages of using stroke feedback when it is implemented with the joint space control scheme is discussed in Section 6.4.

Table 3: Gain values used in the project

Gains	Valve 1 (Cylinder 1)	Valve 2 (Cylinder 2)	Valve 3 (Cylinder 3)
K_p (Boom angle feedback) (rad)	4	3	1.5
K_i (Boom angle feedback) (rad)	0.05	0.0000000001	0.000001
K_d (Boom angle feedback) (rad)	0.01	-0.000001	0.0000001
K_p (Stroke feed-back) (m)	17	40	31.5
K_i (Stroke feed-back) (m)	0.005	0.1	2.5
K_d (Stroke feed-back) (m)	-1.1	0.01	1.9

6 KINEMATICS OF THE HYDRAULIC BOOM

A schematic representation of the hydraulic boom consists of rigid bodies or links which are connected through prismatic or revolute joints. One end of these links is connected to a fixed point known as a base. The end effector is fixed at the end of the last link. The end effector can move about (x, y, z) directions. The kinematics is the study of the motion of each link with respect to the previous ones. Every joint in the hydraulic arm is represented through a frame. With the help of the kinematics equations, some aspects of motion like acceleration, velocity, and position can be studied. Kinematics is an integral part of joint space control of hydraulic boom [12]. In this chapter, the inverse kinematics and forward kinematics of the manipulator are studied. The forward kinematics deals with the formulation of kinematic equations to determine the position of the end effector when the joint values (boom angle) are known. Inverse kinematics deals with the study of the kinematic equations when the position of the end effector in a space is known and the joint values to reach the position has to be computed [12] [11]. The main intention of using inverse kinematic equations is to develop active heave compensation and joint space control programs.

6.1 Forward kinematics of the hydraulic boom

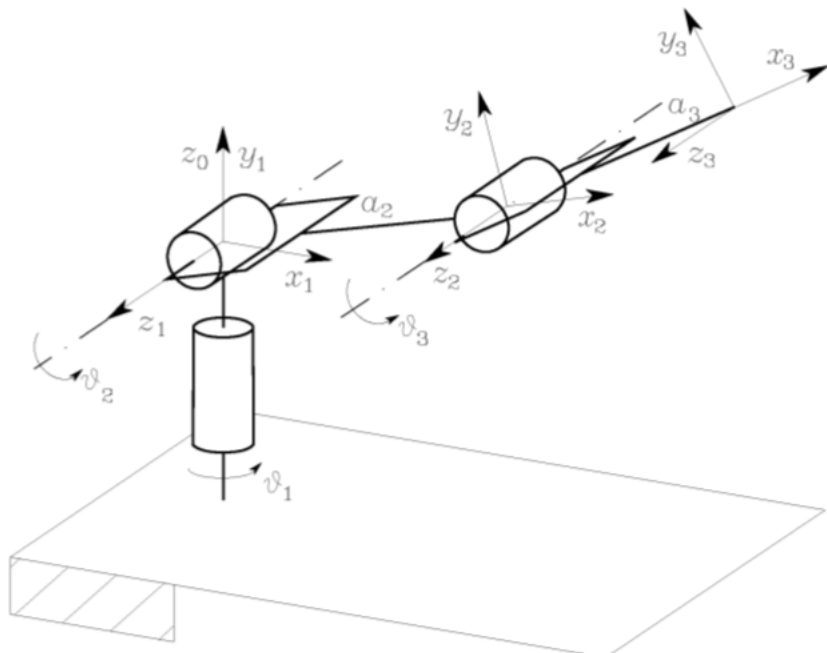


Figure 57: Schematic representation of hydraulic boom [12]

The schematic representation of hydraulic boom is as shown in Figure 57. There are three rigid links and each of the links is assigned with a frame. The world frame is denoted by x_0 , y_0 and z_0 . The world frame is also known as frame 0. The other frames are assigned to the links as shown in Figure 57. To find the forward kinematics of the hydraulic boom, the initial step is to determine the DH (Denavit-Hartenberg) parameters.

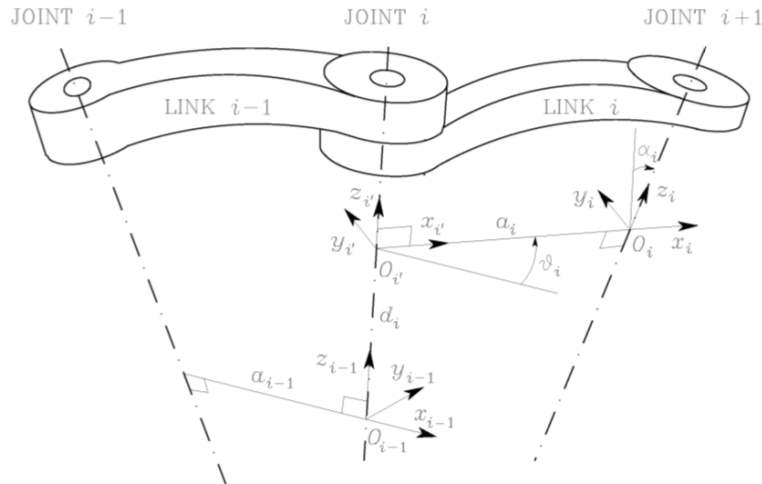


Figure 58: DH parameters general representation [12]

DH parameters standardize a set of rules to attach the frames for each of the links in a kinematic chain. Therefore, with this systematic approach, the relative position and orientation of the two-consecutive links in a kinematic chain can be determined. The four parameters associated with DH notations are: number of joints(i), distance between O_i and O_i' or the length of the link (a_i), length of the coordinate O_i' along Z_{i-1} axis (d_i), the angle between Z_{i-1} and Z_i along X_i axis (α_i) and angle between X_{i-1} and X_i about Z_{i-1} axis (v_i). The set of rules to form the DH parameters are according to [12]. Table 4 below shows DH parameters of the hydraulic boom configuration as shown in Figure 58.

Table 4: DH parameter for the hydraulic boom

Link	a_i	α_i	d_i	v_i
1	0	$\pi/2$	0	v_1
2	a_2	0	0	v_2
3	a_3	0	0	v_3

The transformation between the joint frame (i) and joint frame (i-1) is denoted by the transformation matrix. The reference frame to formulate the transformation matrix is frame 0. The transformation matrix from frame 0 to frame 1 is shown in Equation 6.1 below [12]:

$$T_1^0 = \begin{bmatrix} C_1 & 0 & S_1 & 0 \\ S_1 & 0 & -C_1 & 0 \\ 0 & 1 & 0 & 0 \\ 0 & 0 & 0 & 1 \end{bmatrix} \quad (6.1)$$

Similarly, for joint 2 and 3:

$$T_2^1 = \begin{bmatrix} C_2 & -S_2 & 0 & a_2 C_2 \\ S_2 & C_2 & 0 & a_2 S_2 \\ 0 & 0 & 1 & 0 \\ 0 & 0 & 0 & 1 \end{bmatrix} \quad (6.2)$$

$$T_3^2 = \begin{bmatrix} C_3 & -S_3 & 0 & a_3 C_3 \\ S_3 & C_3 & 0 & a_3 S_3 \\ 0 & 0 & 1 & 0 \\ 0 & 0 & 0 & 1 \end{bmatrix} \quad (6.3)$$

Now, the matrix product of Equations 6.1, 6.2 and 6.3 gives the transformation from frame 0 to 6.

$$T_3^0 = T_1^0 T_2^1 T_3^2 = \begin{bmatrix} C_1 C_{23} & -C_1 S_{23} & S_1 & C_1(a_2 C_2 + a_3 C_{23}) \\ S_1 C_{23} & -S_1 S_{23} & -C_1 & S_1(a_2 C_2 + a_3 C_{23}) \\ S_{23} & C_{23} & 0 & a_2 S_2 + a_3 S_{23} \\ 0 & 0 & 0 & 1 \end{bmatrix} \quad (6.4)$$

Where $C_1 = \cos(\nu_1), S_1 = \sin(\nu_1)$
 $C_{23} = \cos(\nu_2 + \nu_3), S_{23} = \sin(\nu_2 + \nu_3)$

The forward kinematics can be calculated from the Equation 6.4

6.2 Inverse kinematics of hydraulic boom

Inverse kinematics plays an important role in joint space control of the manipulator. It is involved in solving complicated mathematical equations which are computationally expansive, the execution time is very long in the real-time applications. In a Cartesian space, the tasks of the manipulator are performed. In joint space, the manipulators actually work in real-time. The Cartesian space is represented by position vector and orientation matrix whereas, the joint space is defined with joint values (boom angle). Therefore, the inverse kinematics involves in the conversion of Cartesian space coordinates to the joint space coordinates [45]. Inverse kinematics of the manipulator can be determined by geometric and algebraic methods. In this chapter, inverse kinematics equations are derived for 3-DOF and 2-DOF manipulator.

6.2.1 Inverse kinematics of 3-DOF manipulator

The 3-DOF manipulator is as shown in Figure 57. The main objective of developing these equations is to find the desired joint variables according to the end effector position (pw). The orientation of the end effector position is given by pw_x, pw_y and pw_z . The mathematical calculations are according to [12].

The angle ν_1 is shown in Figure 57. Calculating the angle ν_1 :

$$\nu_1 = \text{Atan2}(pw_y, pw_x) \quad (6.5)$$

Now, calculating ν_2 and ν_3 :

$$c_3 = \frac{pw_x^2 + pw_y^2 + pw_z^2 - a_2^2 - a_3^2}{2a_2a_3} \quad (6.6)$$

$$s_3 = \pm\sqrt{1 - c_3^2} \quad (6.7)$$

Therefore, ν_3 is given by:

$$\nu_3 = \text{Atan2}(s_3, c_3) \quad (6.8)$$

When s_3 is positive the elbow movement is upwards and when the s_3 is negative the elbow movement is downwards from Equation 6.7.

ν_2 is given by:

$$\nu_2 = \text{Atan2}(s_2, c_2) \quad (6.9)$$

Where

$$s_2 = \frac{(a_2 + a_3c_3)pw_z - a_3s_3\sqrt{pw_x^2 + pw_y^2}}{pw_x^2 + pw_y^2 + pw_z^2} \quad (6.10)$$

$$c_2 = \frac{(a_2 + a_3c_3)\sqrt{pw_x^2 + pw_y^2} - a_3s_3pw_z}{pw_x^2 + pw_y^2 + pw_z^2} \quad (6.11)$$

Where

a_2 is the length of link 1.

a_3 is the length of link 2.

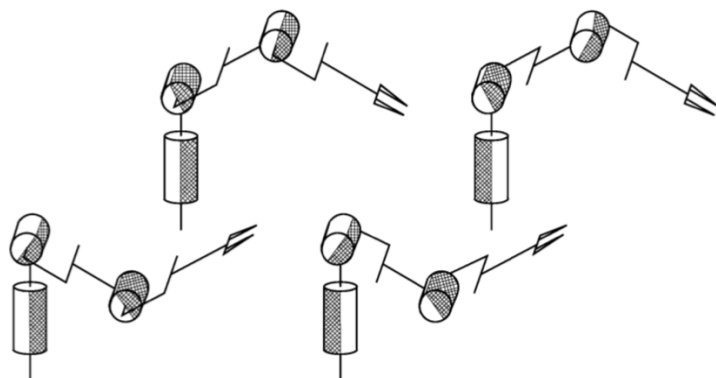


Figure 59: Configurations of the manipulator [12]

The above equations can be used to solve the configurations shown in Figure 59. Therefore, when the end effector position in Cartesian space pw (pw_x , pw_y , pw_z) is known, the joint values (ν_1 , ν_2 , ν_3) can be calculated. This solution can be used in the real-time system and in Section 6.3 it will be tested using a robotics toolbox in MATLAB.

6.2.2 Inverse kinematics of 2-DOF manipulator

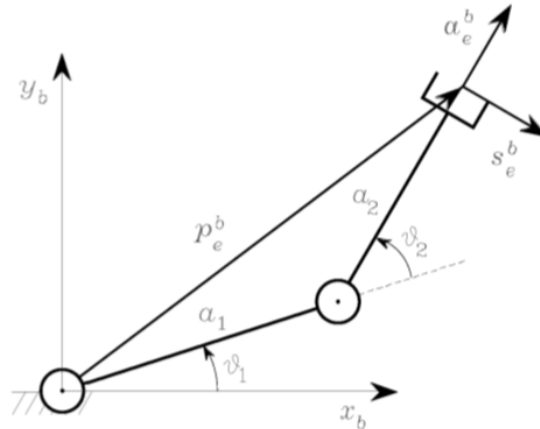


Figure 60: 2-DOF Manipulator [12]

The 2-DOF manipulator is as shown in Figure 60. The arm can move in X and Y direction only. The base rotation is not considered. The SIMSCAPE model of the project is directly converted from the SOLIDWORKS assembly of the hydraulic boom. In this process, the joint frames are misaligned. This causes errors in computing the joint values in SIMSCAPE model. Further, the complexity of the simulation increases when 3-DOF Inverse kinematics is used. Therefore, to avoid the complexity in the simulation the hydraulic boom is considered to have only two degrees of freedom. Hence, 2-DOF inverse kinematics equations are formulated to be implemented in the simulation. When the system is working in the real-time, 3-DOF inverse kinematics program can be utilized.

The inverse kinematics equations for 2-DOF manipulator are formulated according to [11]. Algebraic solutions provide the most accurate results when implemented in the simulation. Therefore, algebraic methods are used to formulate inverse kinematic equations. Let us consider that the end effector in Cartesian space is at position (pw). The joint values (\$\vartheta_1, \vartheta_2\$) has to be calculated.

For a 2-DOF arm the transformation matrix is as follows

$$T_3^0 = T_1^0 T_2^1 T_3^2 = \begin{bmatrix} C_{123} & -S_{123} & S_1 & a_1 C_1 + a_2 C_{12} \\ S_{123} & C_{123} & -C_1 & a_1 S_1 + a_2 S_{12} \\ 0 & 0 & 1 & 0 \\ 0 & 0 & 0 & 1 \end{bmatrix} \quad (6.12)$$

According to direct kinematics of 2-DOF arm:

$$pw_x = a_1 C_1 + a_2 C_{12} \quad (6.13)$$

$$pw_y = a_1 S_1 + a_2 S_{12} \quad (6.14)$$

Squaring and adding Equations 6.13 and 6.14

$$pw_x^2 + pw_y^2 = a_1^2 + a_2^2 + 2a_1 a_2 C_2 \quad (6.15)$$

$$C_2 = \frac{pw_x^2 + pw_y^2 - a_1^2 - a_2^2}{2a_1a_2} \quad (6.16)$$

$$S_2 = \pm \sqrt{1 - C_2^2} \quad (6.17)$$

Therefore, computing the joint value v_2 by arc tangent:

$$v_2 = \text{Atan2}(S_2, C_2) \quad (6.18)$$

For computing joint value v_1 , the Equations 6.13 and 6.14 are written as seen below:

$$pw_x = k_1C_1 - k_2S_1 \quad (6.19)$$

$$pw_y = k_1S_1 + k_2C_1 \quad (6.20)$$

Where

$$k_1 = a_1 + a_2C_2$$

$$k_2 = l_2S_2$$

Therefore, the v_1 is formulated as shown in Equation 6.21

$$v_1 = \text{Atan2}(pw_y, pw_x) - \text{Atan2}(k_2, k_1) \quad (6.21)$$

These are the equations implemented in the simulation for joint space control.

6.3 Testing the inverse kinematics program

The inverse kinematics program can be tested through a tool known as Robotics Toolbox. This library consists of various functions, which computes accurate joint values. It is a freeware built for MATLAB. Some of the inverse kinematics, forward kinematics, and trajectory generations functions can be built easily with the inbuilt libraries. Further, the manipulator developed can be visualized schematically using this robotics toolbox [46].

The 3-DOF manipulator is built according to the DH parameters seen in Table 4. With the help of the toolbox, the manipulator workspace visualization is possible. The movement of the arm with different joint values (q_1, q_2, q_3) can be observed with toolbox visualization and the end effector position (x, y, z) with different joint values can be observed as in Figure 62. Figure 61 shows the schematic representation of boom in the transport position.

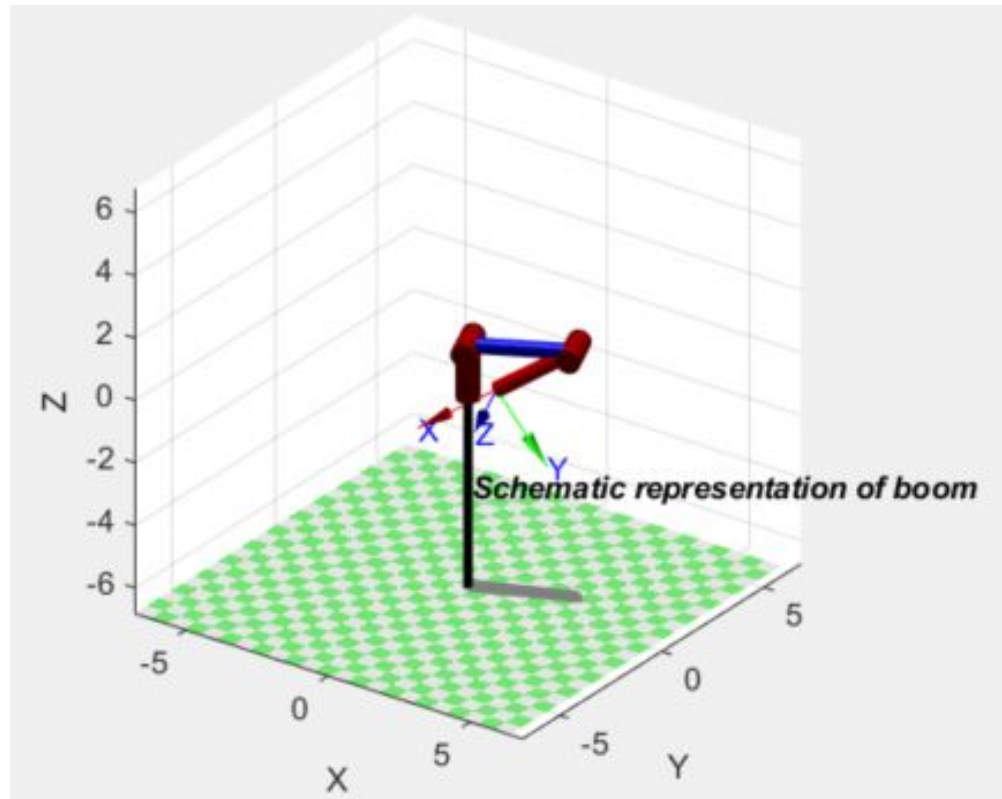


Figure 61: Schematic representation of manipulator in robotics toolbox

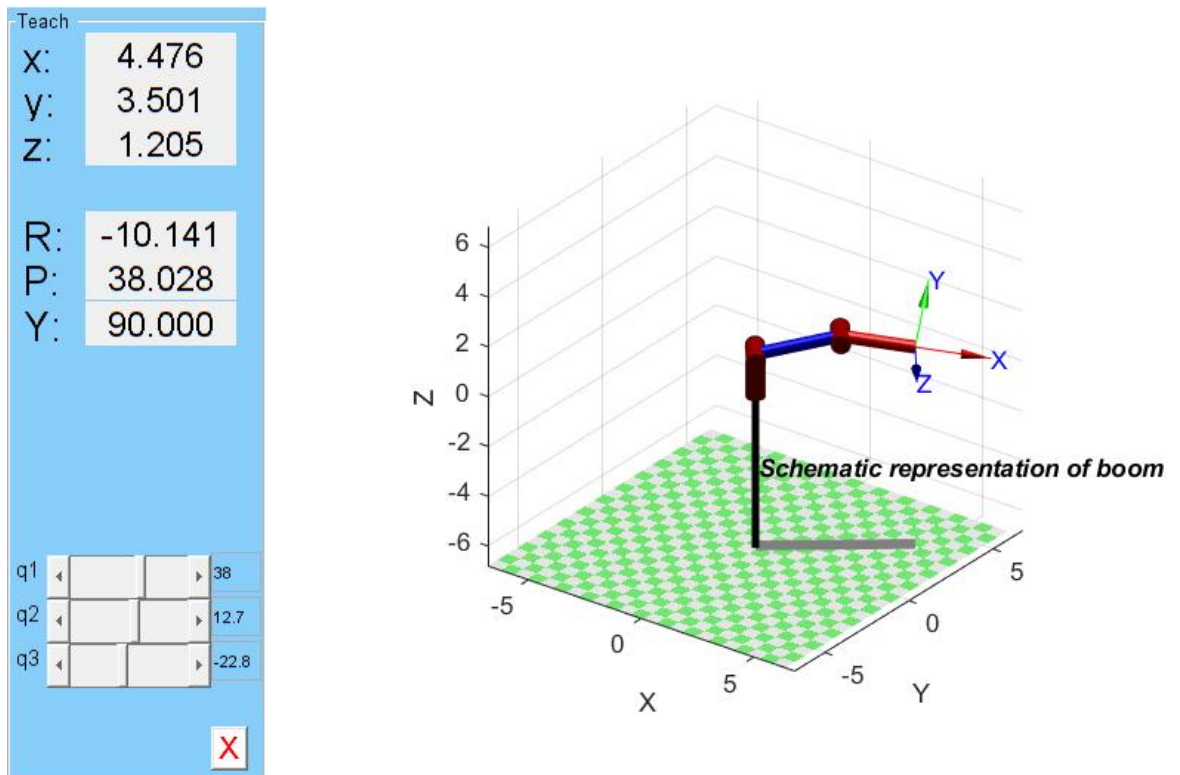


Figure 62: Teaching the movements of the manipulator using the toolbox

6.4 Joint space control

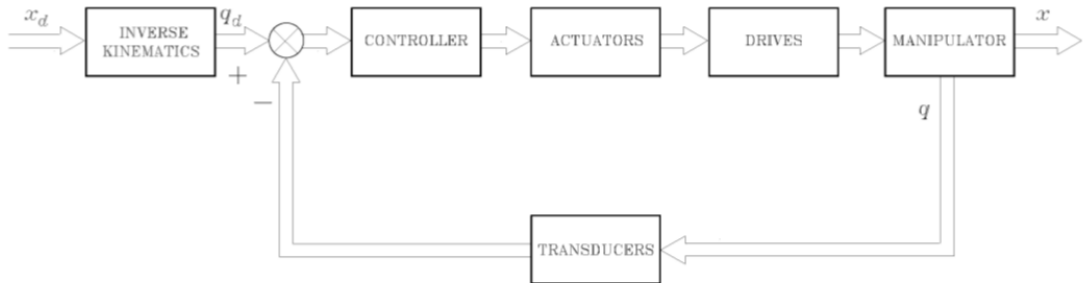


Figure 63: General scheme of joint space control [12]

As seen in the earlier chapters, the input reference for the system was usually a step input. But in the joint space control, inverse kinematics program is used as an input reference to the system. Figure 63 shows the general scheme of joint space control. The joint space control is divided into two stages. In the first stage, the inverse kinematics equations are solved to transform the motion from Cartesian space to joint space of the manipulator, as in Section 6.2. In the next stage, the joint control scheme is designed to track the reference input for the system [12]. Therefore, the inverse kinematics function is used as a reference input, wherein the end effector position is defined, and the inverse kinematics program generates the joint values. These joint values act as an input reference for the PID controller. This control scheme is an initial step for the active heave compensation and the autonomous movement of the boom.

Figure 64 shows the joint space control scheme with stroke feedback system. Piston stroke is used as feedback in this system. An additional block representing the relation between the boom angle and piston stroke is modelled. The complex geometrical equations between the stroke and boom angle are formulated, using these equations the simulation model was getting stiff. To solve this issue, look-up tables block was used, and the data of piston stroke vs boom angle was plotted using look-up tables block in Simulink. The data of stroke vs boom angle is obtained through the previous simulation with step input as an input reference seen in Section 4.5. The inverse kinematics block takes in the joint space position as an input and returns boom angle as an output. This boom angle is an input to ‘relation between stroke and joint angle’ block and this block generates the corresponding piston stroke as an output to the system. Further, this piston stroke is used as an input reference to the system. Linear displacement sensor is used as feedback in this system.

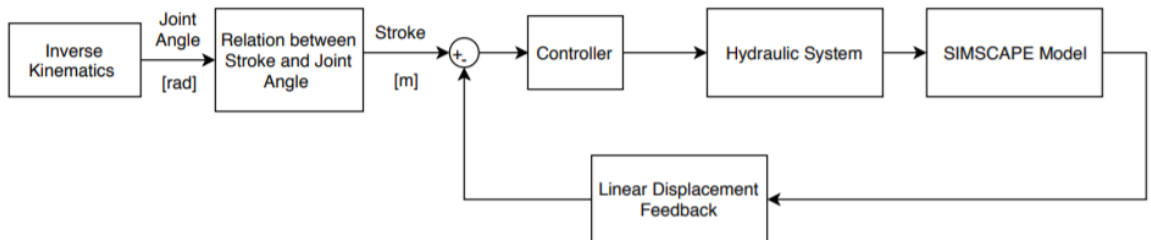


Figure 64: Joint control scheme with cylinder stroke feedback

Figure 65 shows the joint space control scheme with boom angle feedback. In this system, the inverse kinematics model takes a joint space position as an input and then generates

boom angle as an output. This output from the inverse kinematics block is the direct input reference to the system. Incremental encoder is used a feedback sensor in this system.

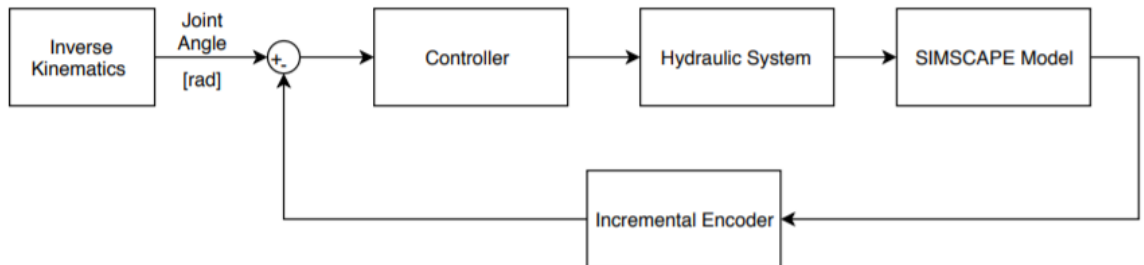


Figure 65: Joint space control scheme with boom angle feedback

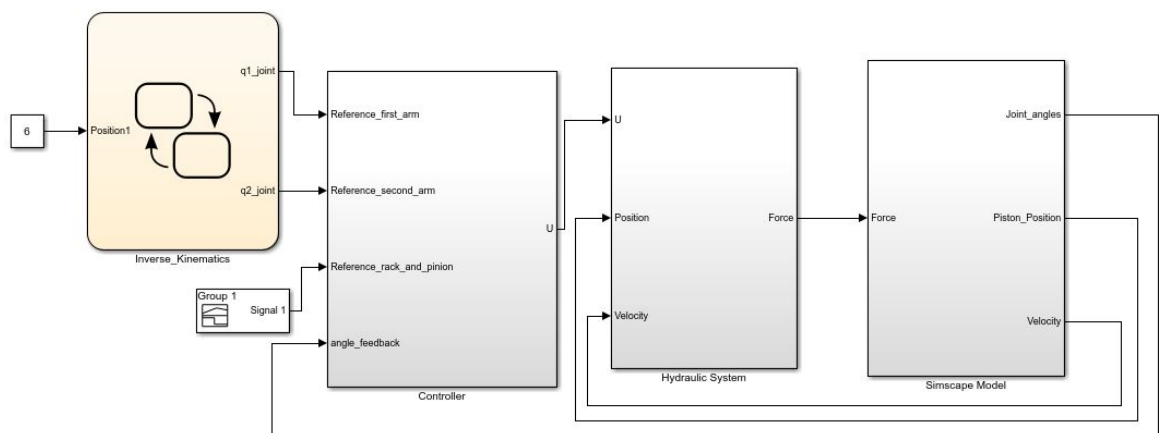


Figure 66: Joint control scheme implemented in the simulation

Figure 66 shows the inverse kinematics program implemented in the boom feedback system. The joint values (q_1, q_2) are the reference to the PID controller. In the system shown in Figure 66, joint values are used as feedback. The simulation execution time is faster when the joint values are used as feedback. When the cylinder stroke is used as a feedback, an extra program which defines the relation between joint angle and stroke has to be formulated, this requires extra execution time. The usage of stroke feedback system leads to end-effector position errors in simulation, this problem arises as some of the frames are not aligned perfectly in the SIMSCAPE model and inaccuracy in formulating geometrical relations between boom angle and cylinder stroke. Therefore, using boom angle feedback would make the system simple and work efficiently. Most of the industries use joint angle as feedback due to the simplicity in working, minimal errors and the model can be further developed for autonomous control and active heave compensation.

The inverse kinematics program is implemented in the state-chart as seen in Figure 66. There are 6 modes defined using state-charts. Each mode corresponds to a particular position in joint space. Figures 67, 68 and 69 shows the various modes defined in the state-chart. Alternatively, these modes can be named as loading position, launching position and extreme working position.

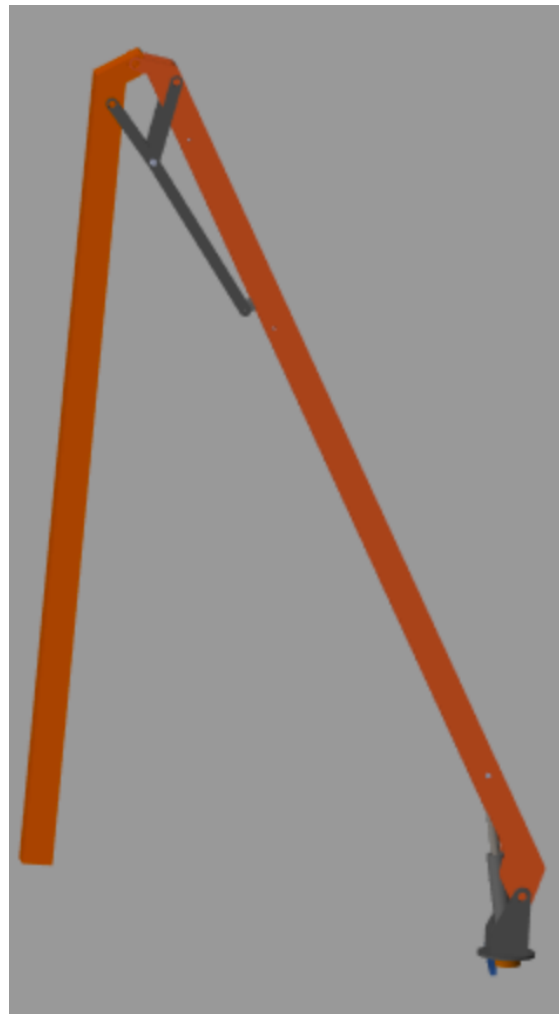


Figure 67: Loading position $(x, y) = (4, 3)$ (mode 6)

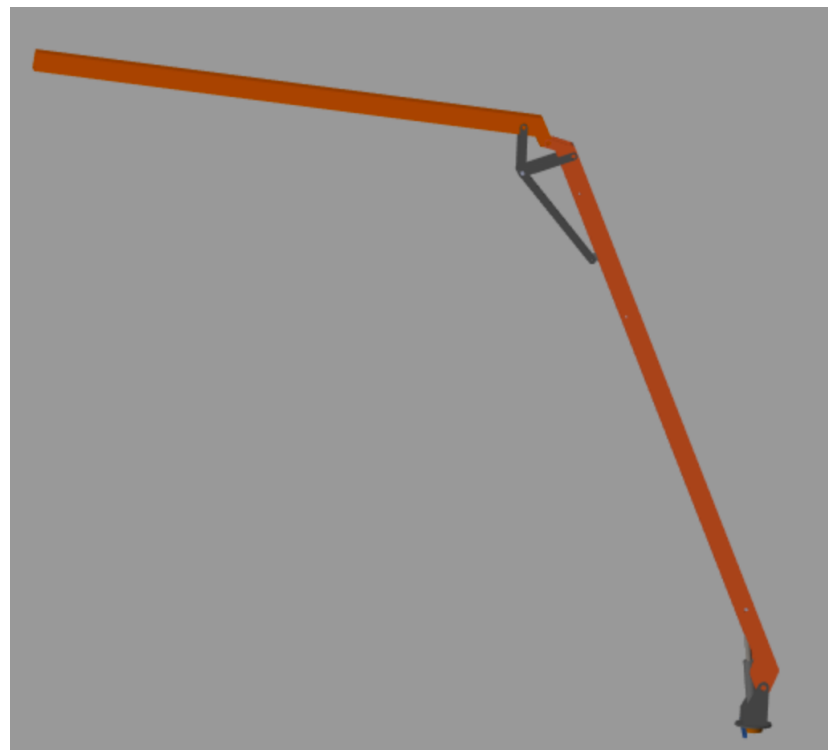


Figure 68: Launching position $(x, y) = (4, 5.8)$ (mode 5)

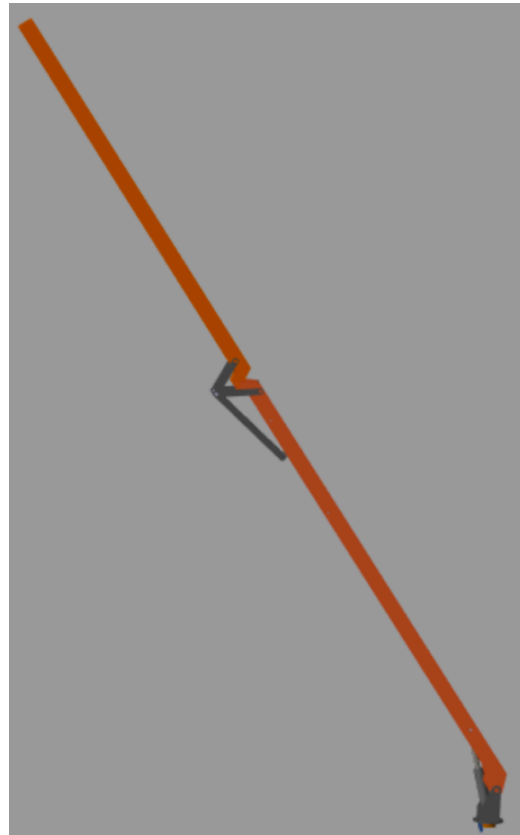


Figure 69: Extreme position (x, y) = (5.8, 5.8) (mode 4)

6.5 Active heave compensation (Stabilization)

Offshore involves very high disturbances and uncertainties, the hydraulic boom must be robust enough to withstand these disturbances and uncertainties. Many research and investigations have been performed to reduce the disturbances, uncertainties, and risks in the offshore. Heave compensation is one such technology which can stabilize the tooltip of the hydraulic boom thereby causing less position error. There is a need for heave compensation in the project as the hydraulic boom is designed to retrieve the UAV with the help of a skyhook. If there are a lot of waves in the offshore and if the tooltip of the hydraulic boom is not stabilized, then due to the position error the boom might not be able to retrieve the UAV. Figure 70 shows the location of the MRU and the movements of the vessel in X, Y, Z directions.

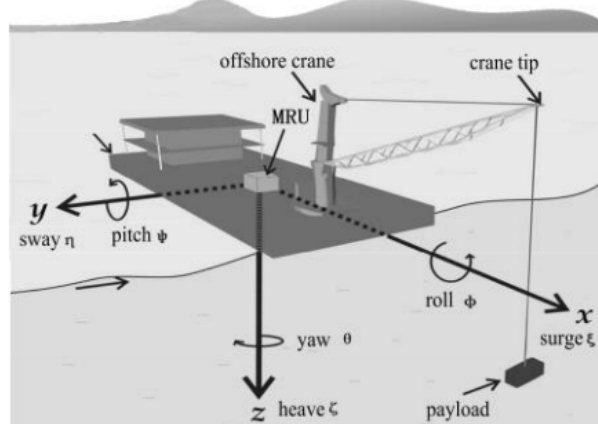


Figure 70: Location of MRU and movements of the vessel [47]

The heave compensation has two main approaches namely Passive Heave Compensation (PHC) and Active Heave Compensation (AHC). PHC system is modelled as a spring damping system with hydraulic cylinders and compressors. AHC system actively compensates the heave movements by controlling the actuator. To sense, the movement of the surface vessel an Inertial Measurement Unit (IMU) or Motion Reference Unit (MRU) is used. The signal sent by IMU or MRU is used to compensate the movement of the hydraulic actuator by the controller in accordance to the heave generation recorded by IMU [2]. The MRU or IMU is usually fixed on the deck or parallel to the deck, along with the vertical axis of the surface vessel [47]. The active heave compensation is usually performed on the hydraulic winch. There is no existing literature wherein the active heave compensation is used for a specific application like skyhook.

There are many strategies to perform the heave compensation. The traditional way is to perform the passive heave compensation. With the implementation of modern-day technologies like IMU or MRU, the heave compensation problem can be solved. In this active heave compensation, the kinematics of the entire boom is considered. Therefore, one of the best and easy approaches to solve the heave compensation was in [2] and the implementation is according to [13]. From Equation 6.4, the direct kinematics can be formulated.

From Equation 6.4, direct kinematics:

$$\begin{bmatrix} x \\ y \\ z \end{bmatrix} = \begin{bmatrix} C_1(a_2C_2 + a_3C_{23}) \\ S_1(a_2C_2 + a_3C_{23}) \\ a_2S_2 + a_3S_{23} \end{bmatrix} \quad (6.22)$$

In differential kinematics, jacobians are used to relate the cartesian velocities to angular velocities as seen in Equation 6.23.

$$\dot{V} = J(q)\dot{q} \quad (6.23)$$

Where

\dot{V} is cartesian velocity

\dot{q} is angular velocity

Therefore, the jacobian matrix can be written as follows [12]:

$$J(q) = \begin{bmatrix} -S_1(a_2C_2 + a_3C_{23}) & -C_1(a_2S_2 + a_3S_{23}) & -a_3C_1S_{23} \\ C_1(a_2C_2 + a_3C_{23}) & -S_1(a_2S_2 + a_3S_{23}) & -a_3S_1S_{23} \\ 0 & a_2C_2 + a_3C_{23} & a_3C_{23} \end{bmatrix} \quad (6.24)$$

By calculating the jacobian inverse the joint angular velocity can be formulated as seen in Equation 6.25.

$$\dot{q} = J(q)^{-1}\dot{V} \quad (6.25)$$

Based on these equations the boom tip can be controlled in all directions. Now to compensate the heave motion of the wave or to keep the end effector of the boom in a steady position the angular velocity is calculated as follows:

$$\dot{q} = J(q)^{-1} \begin{bmatrix} 0 \\ 0 \\ -V_{heave} \end{bmatrix} \quad (6.26)$$

If there are any singularity issues while calculating the inverse matrix, the Damped Least Squares Method (DLS) method is used to find the inverse Jacobian matrix [2]. The cartesian velocity of the heave (V_{heave}) can be obtained through MRU or IMU. For replicating the offshore conditions the Marine System Simulator can be used [48].

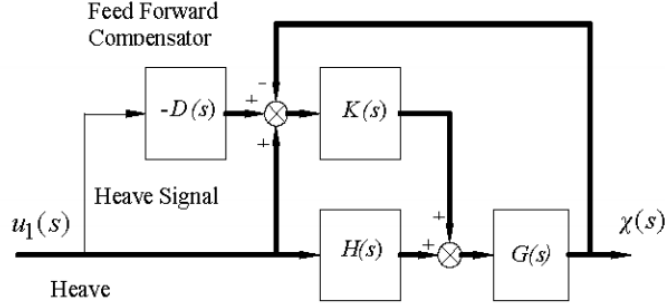


Figure 71: Implementation of AHC in the system [13]

Active heave compensation can be implemented in the system through a feedforward approach. This method is illustrated in Figure 71. Feedforward compensation depends upon the accuracy of the sensor and response time of the hydraulic system. Closed loop hydraulic systems are more preferred for this approach [13].

7 CONCLUSION AND FUTURE WORK

The main objective of this thesis was to create a mechanical design, joint space control, stabilization and simulation of the hydraulic boom. The hydraulic boom must have the capabilities to work in the offshore environment as there are several disturbances like winds and sea waves. Due to these disturbances, the uncertainties are more in the offshore conditions. The hydraulic boom has to overcome all these difficulties to work in an efficient way. In this section, the results of this thesis work are discussed. Additionally, this section presents a view on the future work of this project.

While initiating the design process, several design considerations were taken in to account. The hydraulic boom has to work under offshore conditions therefore, the material with which the boom is designed must be corrosion resistant and must be strong enough to lift 150 kg of payload. Aluminium 5052 is corrosion resistant, light weight and has an ultimate tensile strength of 228 MPa [22] which is the best match for this project. Initially, the totally span of the boom had to be 6 m but due to the restriction of the space on the deck of the surface vehicle, the total span had to be reduced to 5.8 m.

The movement of the arms in the hydraulic boom is through hydraulic cylinders. The placement of these cylinders was the most important aspect of the design. The existing hydraulic cylinders at the lab had to be employed for the design process. Two of the hydraulic cylinders were double sided piston cylinders and one cylinder was single sided piston cylinder. An indigenous design had to be made such that the double-sided piston cylinder had to be used to actuate the second arm. A six-link mechanism was designed which could connect the hydraulic cylinder and the second arm. The mechanical sub assembly of the hydraulic boom was created using SOLIDWORKS. Further, this sub assembly was assembled on the surface vehicle to check the feasibility and workability of design with respect to the surface vehicle's dimensions. Thus, it could be concluded that the preliminary mechanical design created in this project is according to the design considerations, the material of the boom can be used in offshore conditions, the feasibility of the design to work on the surface vehicle is checked and the boom is designed according to the available resources.

A block diagram of hydraulic system was modelled using numerical equations to perform simulations and check the behavior of the system under various conditions. The numerical equations of hydraulic components are modelled using SIMULINK, the parameters to run the simulation is created in a MATLAB script and the SIMSCAPE multibody is used to build, simulate the physical model of the hydraulic boom. The Simulink block diagram of the hydraulic valve can be implemented on different valves with the incorporation of minor changes in the data related to the opening area and spool position as it differs from valve to valve. This system demanded for a robust controller, therefore a PID controller is implemented in the simulation as it is generally known to be robust in nature. A closed-loop control system was employed in this project. The controller is tuned in such a way that the response time to reach the setpoint is less and when the disturbances and noise are acting on the system the controller must be robust enough to follow the reference. There are two types of feedback mechanism studied in the thesis. These two feedback systems are implemented, and the results are discussed in Chapter 5. In addition, a joint

control scheme is implemented wherein the inverse kinematics program generates the joint values according to the end effector position. The end effector position error caused due to the offshore waves can be compensated through an Active Heave Compensation (AHC) technique.

To enhance the output response of the system, having a feedback is crucial in a system. The two types of feedback systems namely, boom angle feedback and piston stroke feedback are studied. This study benefits and validates in finding the right kind of sensor to the system. Boom angle feedback approach is the most feasible in this system as it does not involve in computational complexities, there is no uncertainty in the end effector position and acts as an aid for joint space control, AHC and future developments like autonomous control.

Kinematics is an essential study in this project work as it comprises of the study of the motion of the arms with respect to each other. The DH parameters for the hydraulic boom is defined and then the inverse kinematics and forward kinematics equations are formulated. These equations are further verified using an inbuilt robotics library. Formulating the kinematics equations initiates a way for further developments on joint space control and AHC technique. In addition, the kinematics equations can be used in the autonomous control of the hydraulic boom.

This thesis “Modelling and simulation of hydraulic boom for offshore purposes” involves in a preliminary mechanical design and assembly of the hydraulic boom, formulation of kinematics equations of the manipulator, Simulink block diagram representation of hydraulic system, modelling SIMSCAPE block diagram of the hydraulic boom, implementation of different feedback systems, joint space control implementation and study of Active Heave Compensation (AHC) for stability. The improvisation of the mechanical design of the hydraulic boom is discussed in Section 7.1. The block diagram of the controller and hydraulic system can be implemented in a real-time system. This work on offshore hydraulic boom proves as a substantial initial step in manufacturing, developing real-time control and autonomous control. Therefore, all the evidence and results in this thesis study provide a profound insight into mechanical design, control, stabilization and simulation of an offshore hydraulic boom.

7.1 Future work

The technological advancements, developments, and implementations strengthen the results of a system. In this project, some of the developments are on mechanical design, structural analysis, implementation of the AHC and autonomous control. Preliminary design of the hydraulic boom was created, the design needs to have more details in terms of integrating the electronics and hydraulic pipelines. Structural analysis like the torsional bending of the boom must be determined and transient structural analysis would provide an insight of the deformation when the boom is in motion. The control system along active heave compensation must be implemented in a real-time system. Manufacturing of this manipulator and autonomous control system implementation of this hydraulic boom is a prospective future for this project.

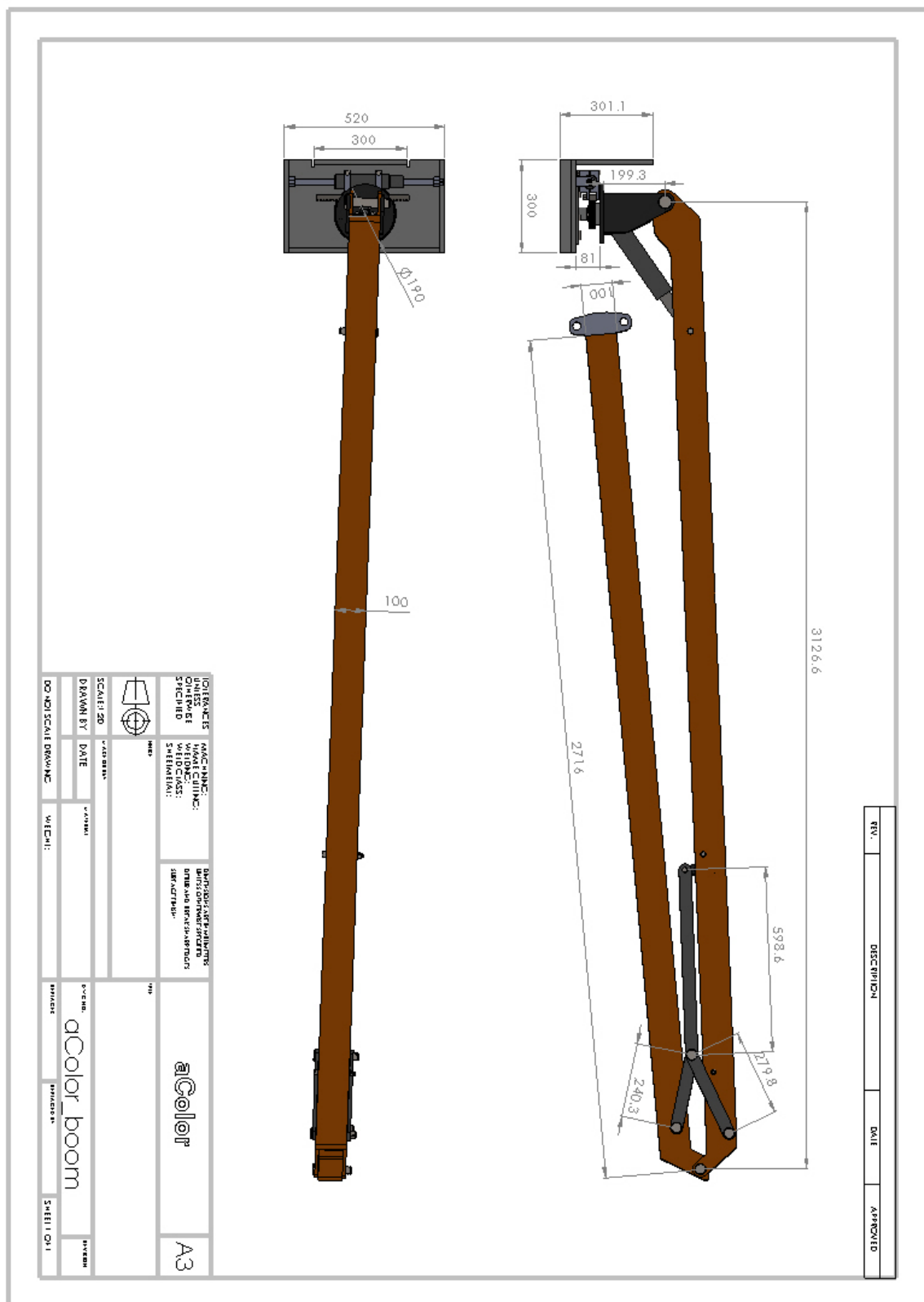
REFERENCES

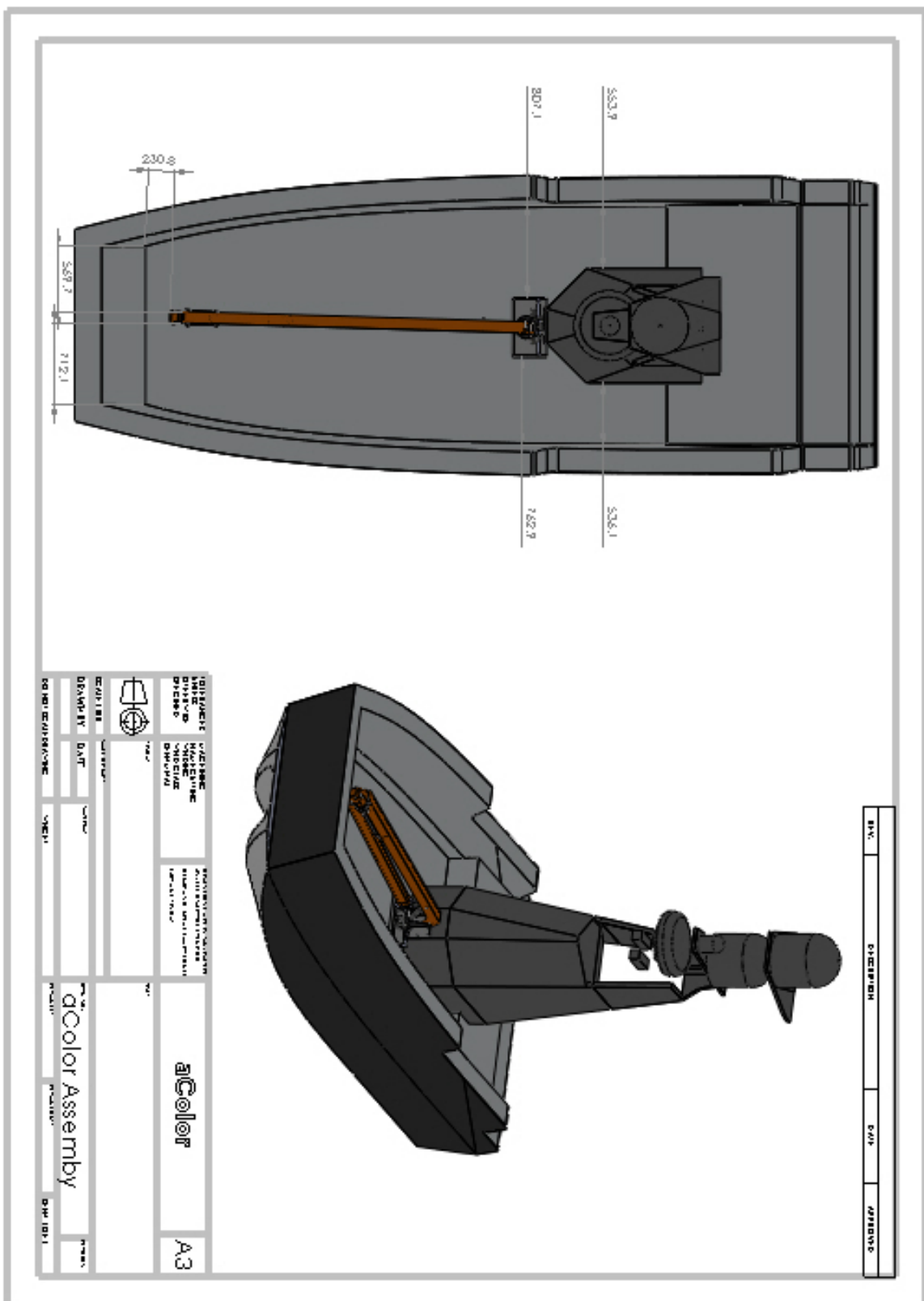
- [1] “Finnish Offshore Industry Report 2016-2017_EN Final.pdf.” .
- [2] Y. Chu, F. Sanfilippo, V. Asoy, and H. Zhang, “An effective heave compensation and anti-sway control approach for offshore hydraulic crane operations,” in *2014 IEEE International Conference on Mechatronics and Automation*, Tianjin, 2014, pp. 1282–1287.
- [3] “Autonomous and Collaborative Offshore Robotics (aCOLOR),” *Teknologiateollisuuden 100-vuotissäätiö*. .
- [4] “BlueROV2 Heavy Configuration Retrofit Kit | Blue Robotics.” [Online]. Available: <https://www.bluerobotics.com/store/rov/brov2-heavy-retrofit-r1-rp/>. [Accessed: 27-Sep-2018].
- [5] “Long Range Fixed Wing Drone & UAV For Sale, Best Commercial Drones.” [Online]. Available: <https://www.appliedaeronautics.com/>. [Accessed: 27-Sep-2018].
- [6] Y. Fang, P. Wang, N. Sun, and Y. Zhang, “Dynamics Analysis and Nonlinear Control of an Offshore Boom Crane,” *IEEE Transactions on Industrial Electronics*, vol. 61, no. 1, pp. 414–427, Jan. 2014.
- [7] “5 Benefits to Using Design Simulation.” [Online]. Available: <https://www.concurrent-engineering.co.uk/blog/5-benefits-to-using-design-simulation>. [Accessed: 24-Oct-2018].
- [8] D. J. Carrejo and J. Marshall, “What is mathematical modelling? Exploring prospective teachers’ use of experiments to connect mathematics to the study of motion,” *Mathematics Education Research Journal*, vol. 19, no. 1, pp. 45–76, Jun. 2007.
- [9] Kiam Heong Ang, G. Chong, and Yun Li, “PID control system analysis, design, and technology,” *IEEE Transactions on Control Systems Technology*, vol. 13, no. 4, pp. 559–576, Jul. 2005.
- [10] C. Systems and B. Boulet, “Introduction to feedback control systems,” p. 60.
- [11] J. J. Craig, “Mechanics and Control Third Edition,” *Pearson Education International*, p. 408.
- [12] L. Sciavicco and B. Siciliano, *Modelling and control of robot manipulators*. London ; New York: Springer, 2000.
- [13] J. T. Hatleskog and M. W. Dunnigan, “Active Heave Crown Compensation Sub-System,” in *OCEANS 2007 - Europe*, Aberdeen, Scotland, UK, 2007, pp. 1–6.
- [14] “Aluminium - Advantages and Properties of Aluminium,” *AZoM.com*, 04-Jun-2002. [Online]. Available: <https://www.azom.com/article.aspx?ArticleID=1446>. [Accessed: 23-Sep-2018].
- [15] P. Ghavami, “Force Systems on Structures,” in *Mechanics of Materials*, Cham: Springer International Publishing, 2015, pp. 17–50.
- [16] “Torque and Rotational Equilibrium.” [Online]. Available: http://spiff.rit.edu/classes/phys211/lectures/torq/torq_all.html. [Accessed: 25-Sep-2018].
- [17] “Rack and Pinion Gears Information | Engineering360.” [Online]. Available: https://www.globalspec.com/learnmore/motion_controls/power_transmission/gears/rack_pinion_gears. [Accessed: 26-Sep-2018].
- [18] R. . Khurmi and J. . Gupta, *A Textbook of Machine Design*, vol. 14 th edition. Ram Nagar, New Delhi -110 055: Eurasia Publishing House (PVT) LTD, 2005.
- [19] “Lieriöhammaspyörät,” *OY Mekanex AB*. .

- [20] "Lieriöhammaspyörät | OY Mekanex AB." [Online]. Available: <https://www.mekanex.fi/tuotteet/komponentit/hammaspyorat/lieriohammaspyorat/>. [Accessed: 26-Sep-2018].
- [21] L. Gillberg and C. Sandberg, "Developing design guidelines for load carrying sheet metal components with regards to manufacturing method," p. 59.
- [22] "ASM Material Data Sheet." [Online]. Available: <http://asm.mat-web.com/search/SpecificMaterial.asp?bass-num=ma5052h32&fbclid=IwAR2Ptn8F1v2jHTwWT2gs8pdm-lou2WCCvBd8RsLTFe8e0j6HOa6jWqhJceJk>. [Accessed: 21-Oct-2018].
- [23] "Technology." [Online]. Available: <https://www.appliedaeronautics.com/technology/>. [Accessed: 27-Sep-2018].
- [24] "Four-port three-position directional control valve - MATLAB." [Online]. Available: <https://www.mathworks.com/help/physmod/hydro/ref/4waydirectionalvalve.html>. [Accessed: 30-Sep-2018].
- [25] P. Chapple, *Principles of Hydraulic Systems Design, Second Edition*. New York, UNITED STATES: Momentum Press, 2014.
- [26] M. Hyvönen, *Lecture notes on "IHA-2609" 'Modelling of Fluid Power Components'*.
- [27] K.-E. Rydberg, "Hydraulic Servo Systems : Dynamic Properties and Control," *Hydraulic Servo Systems*, p. 111.
- [28] Bosch Robert(GmbH), *Characteristics of 4WRA/4WRAE*. 2018.
- [29] "NRPD and Meter dP - Engineered Software Knowledge Base - Global Site." [Online]. Available: <http://kb.eng-software.com/display/ESKB/NRPD+and+Meter+dP>. [Accessed: 03-Oct-2018].
- [30] "Flow Through an Orifice." [Online]. Available: <https://farside.ph.utexas.edu/teaching/336L/Fluid/node55.html>. [Accessed: 03-Oct-2018].
- [31] A. Ellman and R. Piche, "A Modified Orifice Flow Formula for Numerical Simulation of Fluid Power Systems," *Fluid Power Systems and Technology*, vol. Vol. 3, 1996.
- [32] "Basic Hydraulic Theory | Cross Mfg." [Online]. Available: <https://cross-mfg.com/resources/technical-and-terminology/basic-hydraulic-theory>. [Accessed: 03-Oct-2018].
- [33] "Simscape Multibody - MATLAB & Simulink." [Online]. Available: <https://www.mathworks.com/products/simmechanics.html>. [Accessed: 04-Oct-2018].
- [34] "Closed-loop System and Closed-loop Control Systems." [Online]. Available: <https://www.electronics-tutorials.ws/systems/closed-loop-system.html>. [Accessed: 14-Oct-2018].
- [35] "Proportional-Integral-Derivative (PID) Controller | Mr. Digital." [Online]. Available: <https://nicisdigital.wordpress.com/2011/06/27/proportional-integral-derivative-pid-controller/>. [Accessed: 22-Oct-2018].
- [36] "Control Tutorials for MATLAB and Simulink - Introduction: PID Controller Design." [Online]. Available: <http://ctms.engin.umich.edu/CTMS/index.php?example=Introduction§ion=ControlPID>. [Accessed: 14-Oct-2018].
- [37] "External Position Feedback for Hydraulic Cylinders – AUTOMATION INSIGHTS." [Online]. Available: <https://automation-insights.blog/2017/07/19/external-position-feedback-for-hydraulic-cylinders-2/>. [Accessed: 14-Oct-2018].
- [38] "Electro-Hydraulic Feedback Cylinders | Flodraulic Group." [Online]. Available: <https://www.flodraulic.com/tech-tips/electro-hydraulic-feedback-cylinders-0>. [Accessed: 14-Oct-2018].

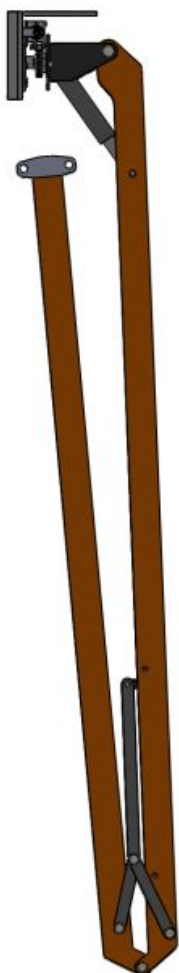
- [39] J. E. V. Escusol, “Computer simulation and modelling for intelligent control systems in small forestry machines,” p. 69.
- [40] “Encoder Sensor Model Quick Find Data Sheet | BEI Sensors.” [Online]. Available: <http://www.beisensors.com/encoder-sensor-model-find.html#D>. [Accessed: 01-Nov-2018].
- [41] M. Heikkilä, “Energy Efficient Boom Actuation Using a Digital Hydraulic Power Management System,” p. 116.
- [42] W. Armieński and A. Jungst, “SEMI-AUTOMATED FORWARDER CRANE CONTROL,” p. 104.
- [43] I. I. Incze, A. Negrea, M. Imecs, and C. Szabó, “Incremental Encoder Based Position and Speed Identification: Modeling and Simulation,” p. 13.
- [44] “Exploring Florida: A social studies resource for students and teachers.” Florida Center for Instructional Technology, 2005.
- [45] S. Kucuk and Z. Bingul, “Robot Kinematics: Forward and Inverse Kinematics,” in *Industrial Robotics: Theory, Modelling and Control*, S. Cubero, Ed. Pro Literatur Verlag, Germany / ARS, Austria, 2006.
- [46] P. I. Corke, *Robotics, vision and control: fundamental algorithms in MATLAB*. Berlin: Springer, 2011.
- [47] B. Shi, L. Xian, Q. Wu, and Y. Zhang, “Active heave compensation prediction research for deep sea homework crane based on KPSO - SVR,” in *Proceedings of the 33rd Chinese Control Conference*, Nanjing, China, 2014, pp. 7637–7642.
- [48] “Marine Systems Simulator - MSS.” [Online]. Available: <http://www.marine-control.org/>. [Accessed: 18-Oct-2018].

APPENDIX A: ASSEMBLY DRAWINGS





APPENDIX B: BILL OF MATERIALS OF HYDRAULIC BOOM



ITEM NO.	PART NUMBER	QTY.	ITEM NO.	PART NUMBER	QTY.
1	Mast1_no_boom_flange	1	14	ISO 4742 M12x 120 - 3A5	2
2	2004B-S20_Mekanex_pinion2	1	15	ISO - 4161 - M12 - N	2
3	Part13	2	16	ISO 2341 - B - 30 x 140 x 8 - S1	1
4	Alamain_piston_rod_jackpinion	1	17	LINK_1	2
5	alamain_cyl	1	18	LINK_2	2
6	Clamp for cylinder body	2	19	ISO 2341 - B - 24 x 120 x 6.3 - S1	2
7	K200500-S20_Mekanex_raci2	1	20	ISO 2341 - B - 24 x 140 x 6.3 - S1	2
8	Clamp for cylinder body_2	2	21	alamain_cyl_for_manipulator	1
9	ISO 15 RBS - 1017 - 12.DE.AC.12.68	2	22	Alamain_piston_rod_2	1
10	Rack and pinion_base	1	23	Cylinder_clamp2	2
11	base_1	1	24	ISO - 4034 - MB - N	3
12	Manipulator_part1	1	25	ISO 4762 M8 x 65 - 2B/N	2
13	Manipulator_part2	1	26	Link_1_cylinder_1	2
			27	ISO 2341 - B - 10 x 90 x 3.2 - S1	1
			28	ISO 8765 - M10x1.0 x 45 x 26-N	6

ITEM NO.	PART NUMBER	QTY.	ITEM NO.	PART NUMBER	QTY.
14	ISO 4742 M12x 120 - 3A5	2	15	ISO - 4161 - M12 - N	2
16	ISO 2341 - B - 30 x 140 x 8 - S1	1	17	LINK_1	2
18	LINK_2	2	19	ISO 2341 - B - 24 x 120 x 6.3 - S1	2
20	ISO 2341 - B - 24 x 140 x 6.3 - S1	2	21	alamain_cyl_for_manipulator	1
22	Alamain_piston_rod_2	1	23	Cylinder_clamp2	2
24	ISO - 4034 - MB - N	3	25	ISO 4762 M8 x 65 - 2B/N	2
26	Link_1_cylinder_1	2	27	ISO 2341 - B - 10 x 90 x 3.2 - S1	1
28	ISO 8765 - M10x1.0 x 45 x 26-N	6			

APPENDIX C: MATLAB CODE FOR HYDRAULIC PARAMETERS

```
%_____Hydraulic system parameters_____
%4/3 valve
%2nd order transfer function
Valve.secondorder_delay = 0.03;
Valve_omega = 40.5;
Valve_eta = 0.989;

%Look-up Tabel PA
Valve3.lookupopenPA = [5.33e-4 5.33e-4 6.33e-4 4.93e-2
5.23e-1 5.93e-1 7.43e-1 1];
Valve3.lookupspoolPA = [-1 -0.5 0 0.2 0.4 0.5 0.8 1];

%Look-up Tabel PB
Valve3.lookupopenPB = [1 6.13e-1 4.03e-1 3.23e-1
2.93e-1 4.33e-2 4.33e-2 4.33e-2];
Valve3.lookupspoolPB = [-1 -0.7 -0.5 -0.4 -0.2 0 0.5
1];

%Look-up Tabel BT
Valve3.lookupopenBT = [0 0.00115 0.00115 0.0347 0.1102
0.2088 0.6821 1];
Valve3.lookupspoolBT = [-1 -0.5 0 0.2 0.4 0.5 0.8 1];

%Look-up Tabel AT
Valve3.lookupopenAT = [1 0.5189 0.1990 0.1118 0.0343
0.00115 0.00115 0];
Valve3.lookupspoolAT = [-1 -0.7 -0.5 -0.4 -0.2 0 0.5
1];

%%%%%%%%%%%%%
%Look-up Tabel PA
Valve.lookupopenPA = [5.33e-4 5.33e-4 5.33e-4 4.93e-2
5.23e-1 5.93e-1 7.43e-1 1];
Valve.lookupspoolPA = [-1 -0.5 0 0.2 0.4 0.5 0.8 1];

%Look-up Tabel PB
Valve.lookupopenPB = [1 7.13e-1 6.03e-2 5.23e-3 3.93e-
4 3.33e-5 3.33e-5 3.33e-5];
Valve.lookupspoolPB = [-1 -0.7 -0.5 -0.4 -0.2 0 0.5
1];

%Look-up Tabel BT
```

```

Valve.lookupopenBT = [0 0.00115 0.00115 0.0347 0.1102
0.2088 0.6821 1];
Valve.lookupspoolBT = [-1 -0.5 0 0.2 0.4 0.5 0.8 1];

%Look-up Tabel AT
Valve.lookupopenAT = [1 0.5189 0.1990 0.1118 0.0343
0.00115 0.00115 0];
Valve.lookupspoolAT = [-1 -0.7 -0.5 -0.4 -0.2 0 0.5
1];

%Orifice/Flowpath Parameters

Valve1.QN.PA = 2e-5; % Nominal flow rate [m3/s]
Valve1.QN.BT = 2e-5;
Valve1.QN.PB = 2e-5;
Valve1.QN.AT = 2e-5;
Valve1.dpN = 0.5e6; % Nominal pressure difference [Pa]
Valve1.ptr = 0.1e6; % Transition pressure [Pa]

Valve2.QN.PA = 4.33e-5; % Nominal flow rate [m3/s]
Valve2.QN.BT = 4.33e-5;
Valve2.QN.PB = 4.33e-5;
Valve2.QN.AT = 4.33e-5;
Valve2.dpN = 0.5e6; % Nominal pressure difference [Pa]
Valve2.ptr = 0.1e6; % Transition pressure [Pa]

Valve3.QN.PA = 8.33e-5; % Nominal flow rate [m3/s]
Valve3.QN.BT = 8.33e-5;
Valve3.QN.PB = 8.33e-5;
Valve3.QN.AT = 8.33e-5;
Valve3.dpN = 0.5e6; % Nominal pressure difference [Pa]
Valve3.ptr = 0.1e6; % Transition pressure [Pa]

%Supply Pressure
pr_Ps = 200e5; % Pressure [Pa]

% Actuator

%Cylinder Parameters
Cyl.V0A = 0.2e-3; % Dead volume at A-side [m3]
Cyl.V0B = 0.2e-3; % Dead volume at B-side [m3]
Cyl.B = 1323e6; % Effective bulk modulus [Pa]

Cyl1.pa_init = 1e6; %Cylinder initial pressure [Pa]
Cyl1.pb_init = 1e6;
Cyl2.pa_init = 1e6;

```

```

Cyl2.pb_init = 1e6;
Cyl3.pa_init = 1e6;
Cyl3.pb_init = 1e6;

% Cylinder1
Cyl1.D = 40e-3; % Piston diameter A-side [m]
Cyl1.d = 25e-3; % Piston diameter B-side [m]
Cyl1.A_A = pi*(Cyl1.D)^2/4; % Piston area A-side [m2]
Cyl1.A_B = pi*((Cyl1.D)^2-(Cyl1.d)^2)/4; % Piston
area B-side area [m2]
Cyl1.xmax = 0.2; % Stroke Length [m]
v1=0.001;
Cyl1.m = 23.3+23.4+1.4+0.5+0.650+100; % Mass [Kg]
Cyl1.x_min = 0.4;

%Cylinder 1 Control (gains)
Kp.cyl1 = 4;
Ki.cyl1 = 0.05;
kd.cyl1 = 0.01;
Fil.cyl1 = 100;

%Cylinder2
Cyl2.D = 43e-3; % Piston diameter A-side [m]
Cyl2.d = 25e-3; % Piston diameter B-side [m]
Cyl2.A_A = pi*((Cyl2.D)^2-(Cyl2.d)^2)/4; % Piston area
A-side [m2]
Cyl2.A_B = pi*((Cyl2.D)^2-(Cyl2.d)^2)/4; % Piston area
B-side area [m2]
Cyl2.xmax = 0.455; % Maximum Stroke Length [m]
Cyl2.m = 23.4+30; % Mass [Kg]
v2=0.001; %delta Xmax maxdisplacement plunger
can go over natural movement range
Cyl2.x_min = 0;

%Cylinder 2 Control (gains)
Kp.cyl2 = 3;
Ki.cyl2 = 0.0000000001;
kd.cyl2 = -0.000001;
Fil.cyl2 = 100;

%Cylinder3
Cyl3.D = 43e-3; % Piston diameter A-side [m]
Cyl3.d = 25e-3; % Piston diameter B-side [m]
Cyl3.A_A = pi*((Cyl2.D)^2-(Cyl2.d)^2)/4; % Piston area
A-side [m2]

```

```
Cyl3.A_B = pi*((Cyl2.D)^2-(Cyl2.d)^2)/4; % Piston area  
B-side area [m2]  
Cyl3.xmax = 0.115; % Maximum Stroke Length [m]  
Cyl3.m = 23.3+23.4+1.4+0.5+0.650+120+10; % Mass acting  
on cylinder[Kg]  
Cyl3.x_min = 0.055; % Minimum Stroke Length [m]  
  
%Friction Model  
Cyl.b = 2000; % Viscous friction coefficient  
Cyl.b2 = 2000;  
Cyl.b3 = 2000;
```

APPENDIX D: MATLAB CODE FOR INVERSE KINEMATICS

-----Inverse Kinematics for 3DOF manipulator-----

```

function [q1,q2,q3] = IK(Px,Py,Pz)

a2 = 3.103337;
a3 = 2.706429;

c3 = (Px^2+Py^2+Pz^2-a2^2-a3^2)/2*a2*a3;
s3 = sqrt(complex(1-c3^2));
s2 = ((a2+(a3*c3))*Pz - a3*s3*sqrt(complex(Px^2+Py^2)))/(Px^2+Py^2+Pz^2);
c2 = ((a2+(a3*c3))*sqrt(complex(Px^2+Py^2))+a3*s3*Pz)/(Px^2+Py^2+Pz^2);
q3_3 = atan2(real(s3),real(c3))
q2_2 = atan2(real(s2),real(c2))
q1_1 = atan2(Py,Px)

q3 = q3_3(1);
q2 = pi+q2_2(1);
q1 = q1_1(1);

end

```